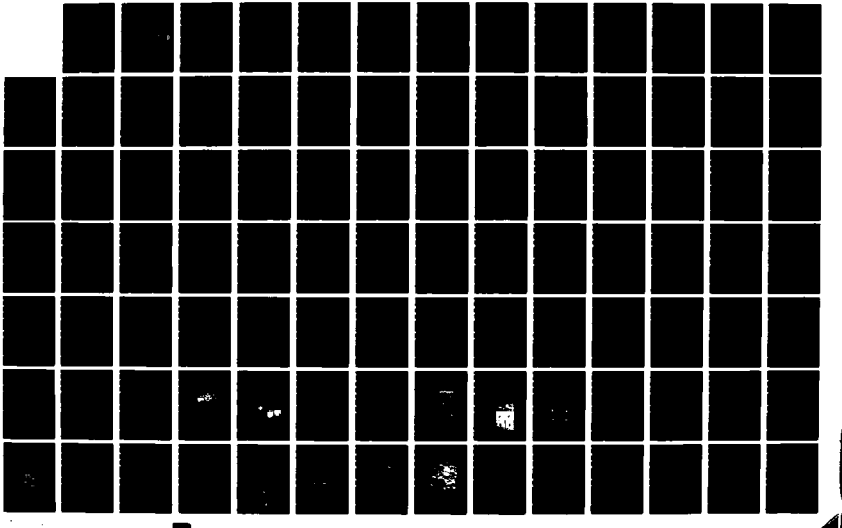

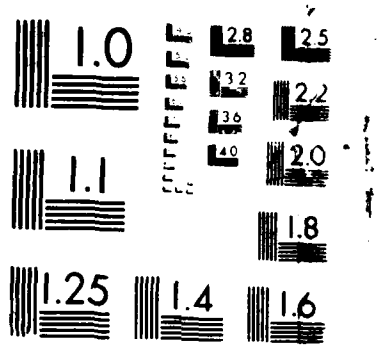

MICROCOPY RESOLUTION TEST CHA
NATIONAL BUREAU OF STANDARDS 1963

AD-A187 704

REPORT DOCUMENTATION PAGE

READ INSTRUCTIONS BEFORE COMPLETING FORM

DTIC FILE COPY

1. REPORT NUMBER

2. GOVT ACCESSION NO.

3. RECIPIENT'S CATALOG NUMBER

4. TITLE (and Subtitle)

ACETYLCHOLINE RECEPTORS IN MODEL MEMBRANES: STRUCTURE/FUNCTION CORRELATES

5. TYPE OF REPORT & PERIOD COVERED
Annual/Final
9/1/82 - 12/31/85*

6. PERFORMING ORG. REPORT NUMBER

7. AUTHOR(s)

Mauricio Montal, M.D., Ph.D.

8. CONTRACT OR GRANT NUMBER(s)

DAMD17-82-C-2221

9. PERFORMING ORGANIZATION NAME AND ADDRESS
The Regents of the University of California
The University of California, San Diego, B-019
La Jolla, CA 92093

10. PROGRAM ELEMENT, PROJECT, TASK AREA & WORK UNIT NUMBERS

61102A.3M161102BS10.EF.419

11. CONTROLLING OFFICE NAME AND ADDRESS
US Army Medical Research and Development Command
Fort Detrick
Frederick, MD 21701-5012

12. REPORT DATE
December 1985

13. NUMBER OF PAGES
102

14. MONITORING AGENCY NAME & ADDRESS (if different from Controlling Office)

15. SECURITY CLASS. (of this report)
Unclassified

15a. DECLASSIFICATION/DOWNGRADING SCHEDULE

16. DISTRIBUTION STATEMENT (of this Report)

Approved for public release; distribution unlimited

DTIC ELECTE DEC 0 2 1987 S D

17. DISTRIBUTION STATEMENT (of the abstract entered in Block 20, if different from Report)

18. SUPPLEMENTARY NOTES

*Annual report for the period: 1 Sept. 84-31 - Dec. 85
Final report for the period: 1 Sept. 82-31 - Dec. 85

19. KEY WORDS (Continue on reverse side if necessary and identify by block number)

NICOTINIC ACETYLCHOLINE RECEPTOR/ION CHANNELS/MEMBRANE RECONSTITUTION/ VOLTAGE SENSITIVE CHANNELS/ION SELECTIVITY/CHANNEL GATING/MONOCLONAL ANTIBODIES

20. ABSTRACT (Continue on reverse side if necessary and identify by block number)

The nicotinic cholinergic receptor (AChR*) from *Torpedo californica* electric organ and the voltage sensitive sodium channel from rat brain were purified and thereafter reconstituted into lipid vesicles as well as into planar lipid bilayers. The reconstituted membrane displayed the biophysical, pharmacological and immunochemical properties characteristic of these channel proteins *in vivo*. Specifically, the single channel conductance (γ) of the reconstituted AChR was 45 pS in 0.5 M NaCl. γ was ohmic and

DD FORM 1 JAN 73 1473 EDITION OF 1 NOV 65 IS OBSOLETE

SECURITY CLASSIFICATION OF THIS PAGE (When Data Entered)

Abstract (continued)

independent of the agonist. Single channel currents increased with Na^+ concentration to a maximum of 95 pS with half saturation at 395 mM. The apparent ionic selectivity sequence was: $NH_4^+ > Cs^+ > Rb^+ > Na^+ > Cl^-$, F^-, SO_4^{2-}. A detailed kinetic analysis of channel gating demonstrated the existence of two channel open states. For acetylcholine (ACh), the typical values of the time constants of the short-lived and long-lived open states were ~0.5 ms and ~ 4 ms. The frequency of occurrence of the long-lived state increased with ACh concentration. The simplest interpretation is that both singly and doubly liganded states of the AChR undergo transitions to the open conformation. Attempts to map functional domains in the AChR molecule to its primary structure involved the use of subunit-specific monoclonal antibodies. Antibodies specific to the β and γ subunits inhibited single channel activity pointing to a role of such subunits in the control of the ion channel. The reconstituted brain sodium channel had a γ = 25 pS in 0.5 M NaCl. The apparent selectivity sequence for the batrachotoxing (BTX*) activated channel was $Na^+ > K^+ > Rb^+ >> Cl^-$. Channel opening was voltage dependent and favored by depolarization. Probability density analysis of dwell times in the open and closed states indicates the occurrence of one open state and several distinct closed states. Tetrodotoxin (TTX*) reversibly blocked the channel with a Ki = 8.3 nM at -50 mV. Therefore, the process of synaptic transduction as well as that of electric excitability has been reduced to studies on the molecular physiology of purified channel proteins in lipid bilayers. The stage is set to investigate how chemical and genetic modifications in the structure of these channel proteins affect their function.

*This symbol designates terms defined in the glossary on page .99.....

AD _____

ANNUAL/FINAL REPORT

MAURICIO MONTAL, M.D., Ph.D.

Supported by

U.S. ARMY MEDICAL RESEARCH AND DEVELOPMENT COMMAND
Fort Detrick, Frederick, Maryland 21701-5012

Contract No. DAMD17-82-C-2221

The Regents of the University of California
The University of California, San Diego B-019
La Jolla, California 92093

Approved for public release; distribution unlimited

The findings in this report are not to be construed as an official Department of the Army position unless so designated by other authorized documents.

SUMMARY

The purpose of these investigations was to reconstitute functional nicotinic cholinergic receptors as well as voltage-sensitive sodium channels in model lipid membranes. This goal has been singularly important since the beginning of the biochemical studies of purified channel proteins more than a decade ago. Our approach consists of first purifying the channel protein from the native membrane and thereafter its reconstitution back into an experimental lipid membrane. The channel protein can be functionally reconstituted into lipid vesicles to which a variety of biochemical and immunological assays are conveniently and readily applied. The channel proteins are also reconstituted into planar lipid bilayers, a system that distinctly allows a detailed characterization of the function of the protein at the level of single channels. The reconstituted *Torpedo* acetylcholine receptor displays the functional integrity of the agonist-regulated cation channel in terms of activation and desensitization by cholinergic ligands, by exhibiting state transitions associated with cholinergic ligand occupancy as well as inhibition by specific cobra toxin. The reconstituted vesicles containing the *Torpedo* acetylcholine receptor are thereafter transformed into monolayers at the air/water interface and bilayers are thereafter formed by the apposition of two such monolayers. Planar lipid bilayers can be assembled either across teflon apertures which separate two aqueous compartments or at the tip of patch electrode pipets. The electrical characteristics of the reconstituted membrane are studied under voltage clamp conditions. The single-channel conductance (45 pS in 0.5 M NaCl) is ohmic and independent of the specific agonist. The apparent ion selectivity sequence, derived from single-channel current recordings is: $N_4+ > Cs^+ > Rb^+ > Na^+$ Cl^-, F^-, SO_4^{2-}. The reconstituted acetylcholine receptor channel has two distinct open states: at an applied voltage of 100 mV, the typical channel lifetimes of the short and long openings are 0.5 ms and about 4 ms, respectively. The time constants of these two states depend on the choice of agonists, following the sequence: suberyldicholine > acetylcholine > carbamylcholine. The frequency of occurrence of the long open state increases with agonist concentration, while the corresponding lifetimes of the short and long kinetic processes involved in channel closure are not altered systematically by agonist concentration. The simplest inference derived from these observations is that both singly and doubly liganded states of the acetylcholine receptor molecule undergo transitions to the open conformation. The autocorrelation analysis further supports this notion and, in addition indicates that these two open states can be entered or exited via at least two pathways, in other words, can be reached from at least two closed states. This new information obtained from single-channel analysis suggests a major revision to the accepted kinetic schemes for the gating of the acetylcholine receptor channel. Three monoclonal antibodies which are specific for extracellular or cytoplasmic domains of the β and γ subunits of the acetylcholine receptor inhibit the acetylcholine receptor channel in the reconstituted membrane, suggesting that the β and γ subunits are critical for channel gating.

The voltage-sensitive sodium channel was purified from rat brain and reconstituted into phospholipid vesicles. The reconstituted sodium channel exhibited in the vesicle sodium transport was activated by batrachotoxin (BXT) and inhibited by tetrodotoxin (TTX). The functional activity of the reconstituted sodium channel was further characterized by transferring the channel

protein from the reconstituted vesicles into preformed planar lipid bilayers, using the fusion technique. The purified sodium channels in the planar lipid bilayer were detected in the presence of BTX to eliminate inactivation. The cation selectivity and the single-channel conductance of the reconstituted channel are comparable to those of native sodium channels. The block of reconstituted sodium channels by TTX is reversible and dependent on orientation and voltage. Channel opening is favored by depolarization and is strongly voltage-dependent. Probability density analysis of dwell times in the closed and open states of the channel indicates the occurrence of one open state and several distinct closed states. Several kinetic schemes that are consistent with the experimental data are considered.

The molecular physiology of signal transduction and electrical excitability has been reduced to studies on the transmembrane events proceeding in the purified acetylcholine receptor or voltage-sensitive sodium channel molecules. The concepts and techniques required for the resolution and reconstitution of the system are now well established. The full cycle of solubilization, purification and reconstitution of these channel proteins can be achieved without impairment of channel function. Therefore, the stage is set to investigate how both chemical and genetic modifications in the structure of these channel proteins affect their function.

FOREWORD

Torpedo californica electric organ (Pacific Biomarie, Venice, CA)
[^{125}I]-αBGT
Na-cholate (Sigma, St. Louis, MO) and Interchem (Montlucon, France)
L-αphosphatidylcholine type IIS (Sigma, St. Louis, MO)
Naja naja siamensis toxin III
Con A-agarose (Sigma, St. Louis, MO)
Benzoquinoium chloride (Stirling-Winthrop Pharmaceuticals (New York, NY)
Cholesterol (Sigma, St. Louis MO)
Triton X-100 (Sigma, St. Louis, MO)
Dowex 50W-8X100 (Sigma, St. Louis, MO)
Trizma base (Sigma, St. Louis, MO)
CCh (Sigma, St. Louis,MO)
ACh (Sigma, St. Louis, MO)
Echothiophate iodide (Ayerst Laboratories, Inc., New York NY)
Black TFE is available from fluorocarbon, P.O. Box 3339, 1754 South Clementine Street, Anaheim, CA 92083.
Teflon film (Saunders Corp., Los Angeles, CA) (No. S-25, thickness 12.5 μm) (Yellow Springs, OH (Membrane Kit 5937 or 5776, thickness 12.5 μm).
Syringe needle (gauge 27) Hamilton or B-D Yale
BRANSONIC (Heat Systems Ultrasonic, (Plainview NY or Laboratory Supplies Co., Inc., Hicksville, NY (Model G112SPIT)
Multi-well disposo-tray (Linbro (Flow Laboratories, Inc., McLean, VA 22102; Catalog No. 76-336-05).
Standard hematocrit capillaries made of flint glass (BLU-TIP, plain; ID. 1.1-1.2 mm, Lancer, St. Louis, MO).
Current-to-voltage converter (Analogue Devices 528 or Burr Brown 3523J or National Semiconductor LF357AH).
Extracellular patchclamp system (List L/M EPC-5 and EPC-7, List Electronics, Darmstadt, Federal Republic of Germany, and Medical Systems Corp., New York, NY.
Ag/AgCl electrodes (pellet electrodes E-255 and E 206 (In Vivo Metric Systems Metric Systems, Healdsburg, CA).
DC source (Omnical 2001, WPI Instruments, New Haven, CT).
RACAL 4DS tape recorder (frequency response DC - 10 kHz, Hythe, Southampton, England).
PDP 11/34 computer (Digital Equipment Corp. Marlboro, MA)
Porous polystyrene bead (Bio-Beads SM-2) BioRad, Irvine, CA)
Latex beads (Dow Chemical Company, Midland, MI).
Whole rat brains (obtained from Pel Freez Biologicals, Rogers, Arkansas).
PE (Sigma, St. Louis, MO).
Brain PC (Sigma, St. Louis, MO).
Palmitoyl-2-oleoyl phosphatidylethanolamine (POPE) (Avanti Polar Lipids Birmingham, AL).
1-Palmitoyl-2-oleoyl phosphatidylcholine (POPC) (Avanti Polar Lipids, Birmingham, AL).
Diphytanoyl phosphatidylcholine (Avanti Polar Lipids, Birmingham, AL).

TABLE OF CONTENTS

PUBLICATIONS SUPPORTED BY THIS CONTRACT

Articles

1. Suarez-Isla B.A., Wan, K., Lindstrom, J. and Montal, M. (1983). Single channel recordings from purified acetylcholine receptors reconstituted in bilayers formed at the tip of patch pipets. Biochemistry 22:2319-2323.

2. Labarca, P., Lindstrom, J. and Montal, M. (1984). The acetylcholine receptor channel from *Torpedo californica* has two open states. J. Neurosci. 4:502-507.

3. Labarca, P., Lindstrom, J. and Montal, M. (1984). Acetylcholine receptor in planar lipid bilayers: Characterization of the channel properties of the purified nicotinic acetylcholine receptor from *Torpedo californica* reconstituted in planar lipid bilayers. J. Gen. Physiol. 83:473-496.

4. Montal, M., Labarca, P., Fredkin, D.R., Suarez-Isla, B.A. and Lindstrom, J. 1984). Channel properties of the purified acetylcholine receptor from *Torpedo californica* reconstituted in planar lipid bilayer membranes. Biophys. J. 45:165-174.

5. Montal, M., Lindstrom, J., Fredkin, D.R. and Labarca, P. (1984). Ion conduction and gating in the cholinergic receptor channel of *Torpedo californica* reconstituted in planar lipid bilayers. In: Charge and Field Effects in Biosystems. (M.J. Allen and P.N.R. Usherwood, eds.) Abacus Press, United Kingdom, pp. 111-122.

6. Anholt, R., Lindstrom, J. and Montal. (1985). The molecular basis of neurotransmission: Structure and function of the nicotinic acetylcholine receptor. In: The Enzymes of Biological Membranes (A. Martonosi, ed.) Plenum Press, New York, 3:335-401 (second edition).

7. Labarca, P., Rice, J.A., Fredkin, D.R., Montal, M. (1985). Kinetic analysis of channel gating: Application to the cholinergic receptor channel and the chloride channel from *Torpedo californica*. Biophys. J. 47:469-478.

8. Hartshorne, R.P., Keller, B.U., Talvenheimo, J.A., Catterall, W.A. and Montal, M. (1985). Functional reconstitution of the purified brain sodium channel in planar lipid bilayers. Proc. Natl. Acad. Sci. USA 82:240-244.

9. Hamamoto, T., Carrasco, N., Matsushita, K., Kaback, H.R. and Montal, M. (1985). Direct measurement of the electrogenic activity of o-type cytochrome oxidase from *Escherichia coli* reconstituted into planar lipid bilayers. Proc. Natl. Acad. Sci. USA 82:2570-2573.

10. Fredkin, D.R., Montal, M. and Rice, J.A. (1985). Identification of aggregated Markovian models: Application to the nicotinic acetylcholine receptor. Proc. of the Berkeley Conference in Honor of Jerzy Neyman and Jack Kiefer, Vol. I, (L.M. Le Cam and R.A. Olshen, eds.) Wadsworth Publishing Co., Belmont, CA. pp. 269-289.

11. Montal, M. (1986). Functional reconstitution of membrane proteins in planar lipid bilayer membranes. In: Techniques for Analysis of Membrane Proteins (C.I. Ragan and R. Cherry, eds.), Chapman and Hall, United Kingdom, 5:97-128.

12. Hamamoto, T. and Montal, M. (1985). Functional reconstitution of bacterial cytochrome oxidases in planar lipid bilayers. In: Methods in Enzymology Vol. 126 (S. Fleischer and B. Fleischer, eds.) Academic Press, New York, Chapter 12, 123-138.

13. Labarca, P., Montal M.S., Lindstrom, J. and Montal, M. (1985). The occurrence of long openings in the purified cholinergic receptor channel increases with acetylcholine concentration. J. Neurosci. 5:3409-3413.

14. Blatt, Y., Montal, M.S., Lindstron, J. and Montal, M. (1986). Monoclonal antibodies specific to the β and γ subunits of the *Torpedo* acetylcholine receptor inhibit single channel activity. J. Neurosci. 6:481-486.

15. Montal, M., Anholt, R. and Labarca, P. (1986). The reconstituted acetylcholine receptor. In: Ion Channel Reconstitution (C. Miller, ed.) Plenum Press, New York, Chapter 8, 157-204.

16. Hartshorne, R., Tamkun, M. and Montal, M. (1986). The reconstituted sodium channel from brain. In: Ion Channel Reconstitution (C. Miller, ed.) Plenum Press, New York, Chapter 13, 337-362.

17. Montal, M., Hartshore, R. and Keller, B (1987). Studies on sodium channels reconstituted in lipid bilayers: Inferences about molecular mechanisms derived from single channel recordings. In: Proteins of Excitable Membranes (B. Hille and D.M. Fambrough, eds.) John Wiley and Sons, New York and Society of General Physiologists Series 41:149-165.

18. Greenblatt, R.E., Blatt, Y. and Montal, M. (1985). The structure of the voltage-sensitive sodium channel: Inferences derived from computer aided analysis of the *Electrophorus electricus* channel primary structure. FEBS Lett. 193:125-134.

19. Keller, B.U., Hartshorne, R.P., Talvenheimo, J.A., Catterall, W.A. and Montal, M. (1986). Sodium channels in planar lipid bilayers: Channel gating kinetics of purified sodium channels modified by batrachotoxin. J. Gen. Physiol. 88:1-23.

20. Hartshorne, R.P., Keller, B.U., Talvenheimo, J.A., Catterall, W.A. and Montal, M. (1986). Functional reconstitution of purified sodium channels from brain in lipid bilayers. Ann. New York Acad. Sci. 479:293-305.

Abstracts

1. Labarca, P., Fredkin, D.R., Lindstrom, J. and Montal (1983). Desensitization of purified acetylcholine receptors reconstituted in planar lipid bilayers. Biophys. J. 41:134a.

2. Montal, M., Labarca, P., Fredkin, D.R., Suarez-Isla, B.A. and Lindstrom, J. (1983). Channel properties of the purified acetylcholine receptor reconstituted in planar lipid bilayers. International Symposium on New Perspectives on Membrane Dynamics (CNRS-INSERM-NATO). May 15-19, 1983 Strasbourg, Francej pp. 100-103.

3. Hamamoto, T. and Montal, M. (1984). Transduction of redox energy into transmembrane voltage by cytochrome C oxidase from the thermophilic bacterium PS-3 reconstituted into planar lipid bilayers. Biophys. J. 45: Abst. 38a.

4. Labarca, P., Rice, J., Lindstrom, J. and Montal, M. (1984). Covariance analysis of single channel currents from purified acetylcholine receptor and chloride channels in planar lipid bilayers. Biophys. J. 45: Abst. 387a.

5. Blatt, Y., Montal, M.S., Lindstrom, J. and Montal, M. (1984). Effect of antireceptor monoclonal antibodies on single channel currents of purified acetylcholine receptor reconstituted in lipid bilayers. Biophys. J. 45: Abst. 311a.

6. Hartshorne, R., Killer, B., Talvenheimo, J., Catterall, W. and Montal, M. (1984). Functional reconstitution of the purified brain sodium channel in planar lipid bilayers. Soc. Neurosci. Abst. Vol. 10, Part 2, p. 864.

7. Montal, M., Lindstrom, J., Montal, M.S., Blatt, Y. and Labarca, P. (1984). Studies on acetylcholine receptor reconstituted in lipid bilayers: Inferences about molecular mechanisms derived from single channel recordings and antireceptor antibodies. PAABS IV CONGRESO, Argentina.

8. Keller, B., Hartshorne, R., Talvenheimo, J., Catterall, W. and Montal, M. (1985). Channel gating kinetics of purified sodium channels modified by batrachotoxin in planar lipid bilayers. Biophys. J. 47:Abst. 439a.

9. Montal, M., HJartshorne, R. and Keller, B. (1985). Studies on sodium channels reconstituted in lipid bilayers: Inferences about molecular mechanisms derived from single channel recordings. J. Gen. Physiol. 86:4a.

STATEMENT OF THE PROBLEM

Two characteristics that are fundamental to the function of the nervous system are the excitability of its elements and the communication of excitability among its elements. These features are based on the activity of ion channels, i.e., membrane channel proteins. Our aim is to understand how a channel protein works. Our approach to this problem is based on the premise that understanding the mechanism of action of channel proteins depends upon the convergence of knowledge about the structure of the protein with a detailed characterization of its function at the molecular level. As a first step in this endeavor, the channel protein is purified from the native membrane and therefore it is reconstituted back into an experimental membrane that readily allows the characterization of its function at the level of single channels. Thus the study of the molecular physiology of electrical excitability and of signal transduction is reduced to investigations into the molecular properties of purified sodium channels or acetylcholine receptors reconstituted in planar lipid bilayers. The nicotinic acetylcholine receptor from *Torpedo californica* and the voltage-sensitive sodium channel from *Electrophorus electricus* and rat brain provide an opportunity to pursue this goal because more is known about these proteins than about any other membrane channel protein of the nervous system. Also, they represent the two main groups of membrane channel proteins that mediate information transfer in the brain. Our efforts were focused on: (1) To establish the technology to purify the channel protein from the native tissue and to reconstitute it into lipid bilayers. (2) To validate that the reconstituted channel exhibits reliable functional activity and retains the characteristic properties of the authentic channel. (3) To exploit the relative simplicity of the reconstituted channel to elucidate the detailed mechanisms of channel protein function.

The investigations of the acetylcholine receptor are described in section α and those of, the voltage-sensitive sodium chanel, in section β.

α-THE RECONSTITUTED ACETYLCHOLINE RECEPTOR

α-INTRODUCTION

The nicotinic acetylcholine receptor (AChR) is the postsynaptic membrane protein that transduces the binding of acetylcholine (ACh) into the transient opening of a cation selective channel. This signal transduction event is the fundamental process in the transfer of information across synaptic functions in excitable tissues (1,2,3,4,5).

Classical protein biochemistry together with the application of monoclonal antibody technology and recombinant DNA technology has contributed greatly to our present understanding of the molecular structure of the AChR. The salient structural features of the AChR are summarized schematically in Figure 1. Briefly, the AChR from *Torpedo* is a ~ 250,000 dalton pentamer composed of four homologous glycopeptides present as an $\alpha_2\beta\gamma\delta$ complex (6,7,8,9,10). Each AChR monomer contains two nonequivalent ACh binding sites distinguishable by their affinity for antagonists and their reactivity with affinity labels, such as the agonist analogue bromoacetylcholine (11) or the antagonist 4-(N-maleimido) benzyl trimethyl ammonium iodide (MBTA) (12), both of which attach to the α subunits (4,13,2,14). In the native membrane of *Torpedo*, the AChR occurs predominantly as a dimer, formed by a disulfide bridge between the δ subunits of adjacent monomers (15,16).

All four AChR subunits are transmembrane polypeptides (17,18,19,20,21) and the complete amino acid sequences of all four subunits have been deduced from the nucleotide sequences of cDNA clones (Fig. 1) (22,23,10,24,25). Analysis of hydrophobic sequences has led to the identification of several putative transmembrane segments for each of the subunits (10,24,25,26,27,28,29,30). Since the carboxyl and amino termini of the AChR subunits appear to be exposed on opposite sides of the membrane, each subunit must traverse the membrane an odd number of times (31,28,26,29). The exact transmembrane quaternary arrangement of the five subunits, as well as the precise conformation of the cation channel and its mechanism of agonist-induced gating, remains unclear. Figure 1 summarized many structural features of the *Torpedo* AChR. Notice that the bulk of the macromolecule protrudes from the synaptic side of the membrane. All subunits are glycopeptides and traverse the membrane at least once. Receptor monomers are linked as dimeric units via a disulfide bond between the δ subunits. The α subunits are shown to contain the ACh binding sites (12), main immunogenic region (MIR) and binding sites for mAbs 10 and 13 (147). The position of mAb 124 at a sterically masked location is tentative. The binding site of mAb 8 near the membrane interphase is based on Gullick et al. (209), and the intracellular position of the antigenic determinant to which mAb 166 binds is according to Anderson et al. (210) and Gullick et al. (211). A local anesthetic binding site has been indicated on the extracellular surface of the δ subunit according to Wennagle et al. (212). Subunit topography is indicated as proposed by Kistler et al. (208). Relative dimensions are based on Ross et al. (213) and Wise et al. (214). It should be noted that the shapes of the subunits are merely schematic and hypothetical. The positions of antigenic regions and ligand binding sites are, similarly, only schematic illustrations and are not intended to indicate precise topographic locations.

The amino acid sequences of the four subunits deduced by Noda et al. (10) from the corresponding nucleotide sequences of cloned cDNAs are presented in the lower portion of the figure. The alignment for maximum homology is according to Noda et al. (10). The boses indicate the occurrence of identical amino acids at homologous positions. Notice that each subunit possesses a signal peptide. In this alignment, the proposed active site disulfide would be formed between cysteines 132 and 146 of the α-subunit and the proposed δ-δ disulfide might be formed via the cysteine at position 526. Four transmembranes hydrophobic α helical domains proposed by (10,24) and (25) are indicated M1, M2, M3 and M4. In addition, (28) and (26) have proposed a fifth transmembranous domain in each subunit, indicated in the figure as M5. This domain consists of an amphipatic α helix which contains charged amino acids on one side and apolar amino acids on the other side, so that alignment of these corresponding amphipatic domains of the five subunits would form a transmembrane channel with a hydrophylic core (28,26); see also (160). In this scheme the N-termini would be located on the synaptic side of the AChR whereas the C-termini would be intracellular (3).

Functional reconstitution of the nicotinic AChR in model membranes enables investigation of its function *in vitro* under conditions in which both the protein and lipid composition of the reconstituted membrane can be varied in a controlled manner along with the concentration of agonist and ions in the medium. Furthermore, the isolated AChR can be manipulated and modified biochemically prior to or after reassembly and the effects of such treatments on AChR function can then be assessed in the reconstituted membrane. Thus a reconstituted system allows the investigation of structure/function relationships within the receptor molecule and may ultimately contribute towards a complete understanding of the molecular events which underlie ACh-regulated opening of the postsynaptic channel.

The following sections contain a review of the techniques and concepts which evolved during the study of the reconstituted AChR.

1. METHODS.

METHODS I: Solubilization, purification and reconstitutionof functional AChRs.

A.1-Preparation of AChR-rich electric organ membranes.

The procedure described here is based on the method of Elliot et al. (32), according to which AChR-rich membrane vesicles are purified on the basis of their relatively high density due to their high concentration of AChR. It is essential to use protease inhibitors during the initial homogenization step to prevent proteolytic degradation of the AChR. Frozen *Torpedo californica* electric organ (Pacific Biomarine, Venice, CA) typically 400 g, is broken into chunks, mixed with 1 volume of room temperature 10 mM Na-phosphate buffer, pH 7.5, 109 mM NaN_3, 5 mM EDTA, and agitated occasionally for about 15 min to allow the tissue to thaw partially. All subsequent steps should be performed at 4°C. Iodoacetamide and phenylmethanesulfonylfluoride are added to 5 mM and 1 mM, respectively. The mixture is homogenized in a 1 gallon Waring blender for 2 min, and aliquots of about 200 ml are rehomogenized for 2 min in a small quart 1 Waring blender at

high speed. The homogenate is then centrifuged at low speed for 10 min at 5,000 rpm in a Beckman JA-21 rotor. The supernatant is strained through cheesecloth to remove large fragments of tissue. To increase the yield of AChR, the pellet can be rehomogenized in an equal volume of buffer and centrifuged as before and the strained supernatant can be pooled with the first one. The low speed pellet is discarded and the supernatant is centrifuged in a Beckman type 19 rotor at 16,000 rpm for 90 min. This crude membrane pellet can serve as the starting material for solubilization of AChRs to be further purified on toxin-agarose (see below).

In order to prepare membranes more enriched in AChR, the high speed pellet is resuspended in 3 volumes of 10 mM Na-phosphate buffer, pH 7.5, 10 mM NaN_3, 5 mM EDTA, in a Virtis homogenizer 4 x 15 s at medium high speed. After a brief spin in a serological centrifuge to drain the foam, 60% sucrose is added to the suspension to a final concentration of 32% (w/w) as measured with a refractometer. This suspension is layered at 12 ml/tube over 14 ml of 36% (w/w) sucrose in 10 mM Na-phosphate buffer, pH 7.5, 10 mM NaN_3, 5 mM EDTA. After centrifugation for 60 min at 45,000 rpm in a Beckman Ti-50.2 rotor, the floating fat pad and pellet are discarded. The band of AChR-rich membranes is collected, diluted with an equal volume of distilled water, and then centrifuged for 30 min at 20,000 rpm in the Ti-50.2 rotor. The resulting membrane pellet is suspended in a small volume of 10 mM Na-phosphate buffer, pH 7.5, 100 mM NaCl, 10 mM NaN_3, using an 18-gauge needle and syringe. Specific activities of these membranes range between 1.0 and 2.0 µmoles [^{125}I]-alpha-bungarotoxin (αBGT) binding sites per gram protein, and major contaminants, as revealed by polyacrylamide gel electrophoresis in sodium dodecyl sulfate (SDS), are bands at 43,000 molecular weight and several high molecular weight bands at about M_r 100,000.

A.2-Alkaline extraction of AChR-rich electric organ membranes.

This method, used to further purify the above AChR-rich membranes, is based on the notion that extraction of AChR-rich electric organ membranes with low ionic strength pH 11 buffer removes peripheral membrane proteins, in this case, the 43,000 protein (33,34,35,36). Electric organ membranes enriched in AChR are diluted with cold distilled water and the pH of the suspension is raised to pH 11.2 by slowly adding 0.2 M NaOH while stirring. The alkali-treated membranes are pelleted by centrifugation for 30 min at 20,000 rpm in a Beckman Ti-50.2 rotor. The glassy pellets are suspended by 10 mM Na-phosphate buffer, pH 7.5 100 mM NaCl, 10 mM NaN_3. The pH is measured and adjusted to 7.5, using 10-fold concentrated Na-phosphate buffer. The specific activity of the alkali-washed membranes is routinely 3.2 ± 0.2 µmoles [^{125}I]-αBGT binding sites per gram protein. These membranes should be devoid of the 43,000 protein, but high molecular weight contaminants are usually still present. The membrane suspensions can be frozen in aliquots in a methanol-dry ice bath and stored at -20°C without loss of activity.

A.3-Solubilization of AChR-rich membranes.

AChR-rich membranes are dissolved in 2% Na-cholate (recrystallized (37) if obtained from Sigma, or used if obtained from Interchem, Montlucon, France) in the presence of the desired concentration of crude soybean lipids (L-αphosphatidylcholine type IIS, Sigma, MO; routinely 5 mg/ml) in 10 mM Na-

phosphate buffer, pH 7.5, 100 mM NaCl. Crude soybean lipids are prepared as a 150 mg/ml stock dispersion in distilled water by sonication under argon or nitrogen in a Bransonic bath sonicator. The solubilized membranes are gently shaken for 1 h at 4°C. Undissolved material can be removed either by centrifugation at 165,000 x g for 30 min or, for small volumes, by centrifugation for 15 min in an Eppendorf microfuge at 4°C. Both procedures give comparable AChR concentrations in the supernatants.

A.4-Purification of solubilized AChRs on toxin-agarose.

The extract of electric organ membranes is added to toxin-agarose (0.5 mg of *Naja naja siamensis* toxin III (38) per ml of Sepharose C14B) and is shaken gently for 1 h. Application of about 4 nmoles AChR/ml gel leads routinely to binding of approximately two-thirds of the AChRs in the extract to the resin. The resin is poured into a column and washed with 250 to 300 volumes of cholate/lipid buffer (2% Na-cholate, 5 mg/ml of soybean lipid, 100 mM NaCl, 10 mM Na-phosphate buffer, pH 7.5). Conventionally, AChRs eluted from the affinity column are collected on a DEAE gel, from which they can be eluted at high salt concentrations. However, the presence of lipid in the solution prevents the use of DEAE, since the lipid adsorbs to and coats the ion exchange column. Instead, AChRs can be collected on a column of Con A-agarose (one-tenth the volume of the toxin-agarose column) connected to the toxin-agarose column. AChR can be eluted from the toxin-agarose by 1 mM benzoquinonium chloride (Stirling-Winthrop Pharmaceuticals (New York, NY), a competitive antagonist, or 1 M carbamylcholine (CCh) in cholate/lipid buffer, recirculating through the two columns overnight by means of a peristaltic pump. Benzoquinonium is preferable as eluting agent, since it is effective at a 1,000-fold lower concentration than CCh and its presence can be visually monitored because of the pink color of the solution. The same benzoquinonium solution can be used repeatedly for several preparations. As the AChR is eluted from the toxin-agarose, it is bound to the Con A-agarose, which can then be washed free of the eluting ligand. Incubation at room temperature rather than in the cold is essential for optimal elution from the Con A-agarose. The AChR can be eluted using 1 column volume of 1 M α-methyl-D-mannoside, 5 mM NaN_3, 1 mM EDTA in cholate/lipid buffer for 2 h at room temperature. The elution yield from the Con A column amounts to ~ 25% of the AChR originally bound to the toxin-agarose. The specific activity of the eluate is routinely ~ 8 μmoles [^{125}I]-αBGT binding sites per gram protein. The total yield of toxin-agarose-purified AChR, compared to the AChR content in the initial homogenate, ranges between 5 and 10%. Polyacrylamide gel electrophoresis in SDS reveals usually only the four AChR polypeptides, free of contaminants, after either staining with Coomassie Brilliant Blue or using the more sensitive ammoniacal silver stain procedure (39).

A.5-Measurement of AChR concentration.

AChR concentration is measured by immune precipitation as the concentration of [^{125}I]-αBGT binding sites (40). α-Bungarotoxin can be purified from the crude venom of *Bungarus multicinctus*, obtained from Miami Serpentarium, according to Ravdin and Berg (41), and iodinated (42). Aliquots (0.5 ml) of vesicles diluted to about 10^{-8} M αBGT binding sites in 0.5% Triton X-100, 100 mM NaCl, 10 mM Na-phosphate buffer, pH 7.5, are incubated with 3 x 10^{-8} [^{125}I]-αBGT for 15 min

at room temperature. Then 5 µl of a 3-fold concentration of a 40% ammonium sulfate cut of rat anti-*Torpedo* AChR serum is added for at least 1 h. Thereafter, goat-anti-rat IgG is added for 30 min. The immune precipitate is pelleted by 2 min centrifugation in an Eppendorf microfuge. The washed pellets are counted in a γ counter. Counts of ^{125}I in pellets from reaction mixtures without AChR are subtracted from all samples. All assays should be performed in triplicate. To measure protein, the method of Lowry et al. (43) can be used with bovine serum albumin as standard and using cholate/lipid buffer as the blank.

A.6-Incorporation of AChRs into liposomes.

The total lipid concentration in the membrane extract or the column eluate is adjusted to 25 mg/ml, using a sonicated dispersion of soybean lipids in distilled water. Supplementary cholesterol can be included when desired by mixing a 100 mg/ml solution of soybean lipids in chloroform with a 100 mg/ml solution of cholesterol (Sigma, MO) in chloroform in the desired proportions. After evaporation of the chloroform under nitrogen or argon, the dry lipid film is suspended in a 2% Na-cholate solution in 100 mM NaCl, 10 mM Na-phosphate buffer, pH 7.5, by sonication. It is essential to remove all traces of chloroform so that no chloroform odor is perceptible prior to the addition of AChR. Recommended final concentration of the components in the reconstitution mixture are 25 mg/ml total lipid, 2% Na-cholate, 100 mM NaCl, 10 mM Na-phosphate buffer, pH 7.5, and 1-2 µM AChR. Liposomes containing AChR are formed through removal of the detergent by dialysis of 16-18 h against 500 volumes of 10 mM Na-phosphate buffer, pH 7.5, 100 mM NaCl, 10 mM NaN_3, followed by dialysis for the same period against 500 volumes of 145 mM sucrose, 10 mM NaN_3, 10 mM Na-phosphate buffer, pH 7.5. When desired, the resulting reconstituted preparation can be subjected to a freeze-thaw cycle by placing it in a freezer at 20°C or in liquid nitrogen, followed by ambient temperature. This results in sealing of leaky vesicles and leads to vesicle fusion (44).

A.7-Measurement of AChR orientation.

The fraction of AChRs in native or reconstituted vesicles accessible to [^{115}I]-αBGT, operationally defined as the "sidedness" of the membranes, is measured by comparing the total AChR concentration observed after solubilization in Triton X-100 (as described above) with the AChR concentration observed with intact vesicles. The assay is conducted in 100 mM NaCl, 10 mM Na-phosphate buffer, pH 7.5 (45).

A.8-Assay of AChR function.

AChR function in the reconstituted vesicles is assayed at room temperature as the amplitude of the cumulative uptake of $^{22}Na^+$ or $^{86}Rb^+$ (New England Nuclear) during a 10 s incubation period in the presence of agonist. Entrapped $^{22}Na^+$ or $^{86}Rb^+$ can be separated from the external radioisotope by passage through a Dowex cation exchange column (46).

Dowex 50W-8X100 (Sigma, St. Louis, MO) is washed with distilled water by decantation until the supernatant is clear. Trizma base (Sigma, St. Louis, MO) is then added to equal volumes of resin and water at the ratio of 440 g/kg of resin.

After stirring for 1 h, additional Trizma is added if necessary to bring the pH to 9.8. Then the Tris is decanted and the beads washed with many changes of water until the pH approaches that of the water. Disposable columns (about 0.5 x 8 cm) are poured in short Pasteur pipets loosely plugged with glass wool. A small plastic funnel is attached to the top of each column with tygon tubing. The capacity of these columns is sufficiently large to allow repeated use for up to three assays. Immediately before the first use, each column is washed in 3 ml of 170 mM sucrose, 3.3 mg of bovine serum albumin. When $^{22}Na^+$ is used, the assay should be conducted behind lead shielding. $^{22}Na^+$ or $^{86}Rb^+$ (5 µl of 0.2 mCi/ml) and 5 µl of water or a 10-fold concentrated solution of the agonist are mixed together in Eppendorf microfuge tubes. The assay is initiated by rapidly injecting 40 µl of vesicles in 10 mM Na-phosphate buffer, pH 7.5, 145 mM sucrose, 10 mM NaN_3, with a Pipetman pipeter. After mixing with the pipeter, the mixture is transferred onto a Dowex column in a total elapsed time of about 10 s. Sucrose solution (3 ml of 175 mM) is carefully added to elute the vesicles. Eluates are counted in a γ counter for $^{22}Na^+$ or in a scintillation counter for ($^{86}Rb^+$). For each sample, triplicate CCh (Sigma, MO) responses and triplicate water blanks should be measured. The agonist-activated cation uptake is defined as the difference between the cpm in the water samples and those containing agonist. Standard errors are generally with 10% of the mean. When ACh (Sigma, MO) is used as agonist, the assay should be preceded by a 30 min preincubation period of the vesicles with 1 µM echothiophate iodide (Ayerst Laboratories, Inc., New York, NY) or a similarly effective ACh esterase inhibitor.

The apparent internal volume of the vesicles can be measured by mixing 40 µl of vesicles, 5 µl of $^{22}Na^+$ or $^{86}Rb^+$, and 5 µl of H_2O as above, in triplicate, but incubating at 40°C for 48 h prior to passage through Dowex.

METHODS II:Reconstitution of functional AChRs in planar lipid bilayers.

A.2.1-Bilayers across apertures in Teflon septi.

A.2.1a-The chamber.

The chamber consists of two compartments fabricated in black Teflon, which is chosen for its flexibility. Reconstituted studies also in progress in our laboratory which utilize this system include light-activated proteins (e.g., rhodopsin, bacteriohodopsin and reaction centers from photosynthetic bacteria) (47,48). (Black Teflon TFE is available from fluorocarbon, P.O. Box 3339, 1754 South Clementine Street, Anaheim, CA 92083). Figure 2A illustrates the chamber routinely used. The aperture in the front provides access to the bilayer for light-activation experiments. There are two holes (1.5 mm) in each compartment, through which sections of polyethylene tubing are inserted to connect the chamber with the syringe used to raise or lower the water level (Fig. 2B). These holes can be used also for perfusion experiments to replace the aqueous phase in each compartment. The chamber capacity is 1.0 ml. The chamber interior should be smooth, avoiding steps that hinder the continuous flow of the interface, when the water levels are displaced. The cleaning of the chamber is of utmost importance. The routine procedure is to rinse thoroughly with water and then with chloroform,

ethanol, ether and acetone in this sequence. Thereafter, the chambers are immersed in boiling 1 M HCl (15 min), then in 1 M NaOH (15 min) and finally in water (30 min).

A.2.1b-Fabrication of the septum and the aperture.

The two compartments of the chamber are separated by a Teflon film pierced in the center with an aperture (~ 200 μm diameter). The Teflon film can be obtained from Saunders Corp., Los Angeles, CA (No. S 25, thickness 12.5 μm) or from Yellow Spring Instruments, Yellow Springs, OH (Membrane Kit 5937 or 5776, thickness 12.5 μm; this is the high sensitivity membrane used in oxygen electrodes). The septum is fabricated (49), as a "sandwich" of the thin film (12.5 μm) between two thick Teflon O-rings (50 μm). The aperture is cut with an electrically sharpened syringe needle (gauge 27, Hamilton or B-D Yale). Sharpening is conducted in 5 M HCl solution, applying 1.5 V (with the positive pole connected to the needle), and by repeated immersion and removal of the needle tip. The Teflon film is supported on a new plexiglass plate. The needle is mounted on a syringe and inserted in a device that guides the needle while gentle pressure is applied against the Teflon film. The hole is cut by a single turn around the axis. The quality of the hole is checked under a microscope but the ultimate test is the ease to form membranes, their resistance and stability. The hole should be coated with 2 μl of 0.5% (v/v) hexadecane in hexane or in chloroform:methanol (2:1).

A.2.1c-Routine procedure to reconstitute AChRs in planar lipid bilayers.

The chambers are filled with 0.5 ml of the indicated buffer prior to the addition of the vesicles. For routine studies, the medium is 0.5 M NaCl, 0.5 to 5 mM $CaCl_2$, 2.5 mM Tricine or HEPES buffer, pH 7.4, and 50 μM (4,4'-diisothiocyanatostilbene-2,2'-disulfonic acid DIIDS). At this DIIDS concentration, the *Torpedo electroplax* chloride channel is blocked (51). The composition of the electrolyte solution in the two chambers is the same. If symmetric bilayers are formed, the same protocol is applied to both monolayer chambers. Alternatively, when asymmetric bilayers are formed, the AChR-containing monolayer compartment (*cis*) is prepared as previously described, while the monolayer compartment which contains only lipid (*trans*) is derived from liposomes devoid of AChR. The liposomes, from partially purified soybean phospholipids (37), at a concentration of 20 mg/ml in 80 mM Tricine buffer, pH 8.0, are prepared by a 10 min sonication under argon in a BRANSONIC (Heat Systems Ultrasonic, Plainview, NY) or Laboratory Supplies Co., Inc., Hicksville, NY (Model G112APIT) water bath sonicator. These liposomes, 50 μl samples, are then subjected to the same incubation conditions as the reconstituted AChR vesicles described above. After a few minutes, each monolayer achieves a surface pressure of ~ 30 dyne/cm. Thereafter the level of the AChR-containing compartment is raised over the aperture in the Teflon septum by introducing additional buffer into the chamber from a reservoir. Next, the second monolayer is apposed to the septum and a bilayer formed across the aperture. Membrane formation is continuously followed by monitoring the membrane capacitance. The reconstituted bilayers exhibit a capacitance of ~ 0.8 $\mu F/cm^2$. After formation, the membranes are left uperturbed for 10 min. The electrical conductance is monitored by

applying voltages of up to ± 200 mV. Bilayers with changes in conductance during this period are discarded. Thereafter, the pharmacological agent under study is introduced into the AChR compartment and mixed with a magnetic stirrer.

A.2.2-Bilayers at the tip of patch pipets.

A.2.2a-The chamber.

The chamber is commercially available. A single well is cut out from a Multi-well disposo-tray available from Linbro (Flow Laboratories, Inc., McLean, VA 22102; Catalog No. 76-336-05). Each tray has 48 flat-bottom wells (0.8 x 0.6 cm); the well capacity is ~ 0.4 ml. Each well is used only once.

A.2.2b-Fabrication of the patch pipet.

A detailed description of pipet fabrication is provided in Hamill et al. (52). Standard hematocrit capillaries made of flint glass (BLU-TIP, plain; ID. 1.1-1.2 mm, Lancer, St. Louis, MO) are used. The capillaries are immersed in 1N nitric acid overnight, rinsed thoroughly with deionized water and stored in deionized water. Immediately before pulling, the capillaries are rinsed with methanol and dried by a nitrogen gas flush. The pulling procedure is performed in a vertical pipet puller (David Kopf 700C, Tujunga, CA) and consists of two steps: First, the capillary is extended (8 mm) to produce an intermediate thin section. This section is then recentered with respect to the heating element by an upward displacement of ~ 5 mm. The final pull produces two pipets with an opening (tip diameter) of approximately 0.8 μm with a steep taper. The tip size can be controlled by adjusting the heater current in the second pull. No further treatment, such as fire polishing or coating, is necessary. The tip size is adjusted to yield ~ 10 MΩ of open pipet resistance when filled and immersed in 0.5 M NaCl, 0.5 mM $CaCl_2$ and 2.5 mM HEPES, pH 7.4. Pipets should be used within 4 h after fabrication.

The two compartments separated by the membrane are connected to the amplifier by means of two Ag/AgCl electrodes. The active electrode, identified as the pipet electrode, is connected to a BNC connector pin of the shielded pipet holder, a componet of the patch clamp system (see A.2.3). The pipet, previously filled with buffer, is placed in the pipet holder. The holder is connected to the headstage of the patch clamp system, which is designed to be mounted directly on a micromanipulator. The reference electrode is immersed in the chamber used for bilayer formation and is connected to the high quality ground connection on the headstage of the patch clamp system. The pipet potential is determined with reference to this ground. Positive or negative pressures are applied to the pipet with a syringe.

A.2.2c-Routine procedure to reconstitute AChRs in planar lipid bilayers.

The process of bilayer formation from monolayers at the air-water interface at the tip of patch pipets is fundamentally analogous to that of lipid bilayer formation from two monolayers at the air-water interface across an aperture in a Teflon partition that separates two aqueous compartments (53,54,55,56,57). The method is a follows:

Step 1. Lipid protein monolayers are derived from the reconstituted AChR vesicles. A patch pipet is introduced into the solution under positive pressure in order to avoid its occlusion.

Step 2. The pipet is removed from the solution. The lipid head groups of the monolayers are attached to the polar glass pipet while the hydrocarbon tails contact air.

Step 3. The pipet is reimmersed in the solution. This leads to the apposition of the hydrocarbon tails of the attached monolayer to those of the original monolayer and the resulting formation of a bilayer at the tip of the patch pipet.

It should be noted that the interaction of the lipid monolayer with the bilayer support is different in the two modalities: While the lipid hydrocarbon tails interact with the hydrophobic Teflon septum, the lipid polar head groups interact with the polar glass pipet.

The reconstituted bilayers exhibit membrane resistances in the range of 5 GΩ<RGΩ< 25GΩ. All the planar bilayer experiments are performed at 22 ± 2°C.

A.2.3-Electrical recordings and data processing.

The current recordings from bilayers in Teflon septi are obtained with a current amplifier designed for high speed and high resolution. The critical strategy is the minimization of the effective feedback capacitance on the current-to-voltage converter (Analogue Devices 528 or Burr Brown 3523J or National Semiconductor LF357AH). This allows measurements of signals at a gain of 10^{10} A/V with one pA of noise (peak-to-peak amplifier time constant, (τ = 250 μs) and at a gain of 10^9 A/V with 2 pA of noise (amplifier τ = 120 μs) (53,58). For the current recordings from patch pipets, a commercially available extracellular patchclamp system is used (List L/M EPC-5 and EPC-7, List Electronics, Darmstadt, Federal Republic of Germany, and Medical Systems Corp., NY (55,59,60,61). Voltage is applied and current is measured with Ag/AgCl electrodes E 255 and E 206 from In Vivo Metric Systems, Healdsburg, CA). Constant voltage is supplied by a DC source (Omnical 2001, WPI Instruments, New Haven, CT), and the *trans*-side of the membrane is defined as zero voltage. Accordingly, a negative applied voltage corresponds to a depolarization in the electrophysiological convention. Membrane current is recorded directly on a storage oscilloscope or amplified and stored on a RACAL 4DS tape recorder (frequency response DC - 10 kHz, Hythe, Southampton, England) for subsequent analysis. After

filtering, the recordings are digitized at a sampling interval of 100 μs in a PDP 11/34 computer (Digital Equipment Corporation, Marlboro, MA) The digitized records are inspected on a computer-generated display and compared to a matching routine in which the computer generated a virtual reproduction of the actual recording: the computer-generated rectangular pulses are checked for fidelity in matching the channel openings and closings. The duration of the generated rectangular pulses corresponds to the open times, while the intervals between the pulses are the closed times. The parameters of the generated rectangular pulses, position and width, are stored in the computer. The single channel conductance is calculated from conductance histograms fitted by the sum of two Gaussian functions corresponding to the closed and open channel states. Histograms of dwell times in the open and closed states of the generated pluses are automatically produced. Histograms of dwell times, normalized to have a total area equal to 1 are fitted by a probability density function of the form:

$$f(t) = \sum_{i=1}^{N} A_{ie}^{-1}/\tau_i$$

The amplitudes, A_i, and the time constants, τ_i, of the exponential fit obtained by a chi-square minimization algorithm are derived (58,62,59).

A.2.4-Efficiency and reliability of the reconstituted system.

Efficiency is operationally used to describe the fraction of the total bilayers formed, under a given condition, that exhibit functional activity. Efficiency is stringently dependent on the quality of the AChR preparation: the higher the specific activity, the higher the reconstitution efficiency. With high quality preparations (2), the efficiency should be better than 90%. It should be stressed that the technique of forming a bilayer samples discrete areas of monolayer and therefore, nonrandom distributions of AChR in the monolayer will affect the reconstitution efficiency.

2. RECONSTITUTION OF ACETYLCHOLINE RECEPTORS IN LIPID VESICLES

2.1- Preservation of the functional integrity of the agonist-regulated cation channel of the AChR during solubilization of the electric organ membrane.

Although once a challenging problem, solubilization of the AChR and its reincorporation in lipid vesicles with full retention of its functional properties is now a routine procedure (for reviews, see 63,64,65).

The main principle for the successful reconstitution of functional AChR is the notion that the integrity of its agonist-regulated ion channel is critically dependent upon the continuous presence of stabilizing lipid (66,67,68,69,-45,70,71,72). This lipid dependence is illustrated in Figure 3. Only about 10% of the initial cation channel activity survives when extracts of native membranes (1.67 mg/ml protein) are incubated in 2% cholate. This residual activity results from protection by endogenous lipids in the extract. However, the presence of relatively low amounts of supplementary soybean lipids preserves channel function. Similarly, Heidmann et al. (73) showed that the characteristic allosteric properties of the membrane-bound AChR are preserved by the presence of protective lipids in the micellar solution, while the capacity of the AChR to bind [^{125}I]-αBGT is not affected.

As shown in Figure 4A, extraction of native membranes is maximal at 2% cholate and amounts to be recovery of about 68% of the initial AChRs in the extract at cholate:lipid ratios of 10:1 (w/w). A class of M_r 43,000 proteins anchors AChRs to the cytoskeleton (74,75,76,77,78,79). Alkaline extraction methods, which remove these proteins, do not increase the extraction yield (33,34,36).

When detergent concentrations above 3% cholate are used, a strong irreversible inactivating effect of the detergent on the channel becomes evident, even though the same 10:1 (w/w) cholate:lipid ratio is maintained (Fig. 4B). This channel inactivation observed at elevated detergent concentrations can be accounted for by the high concentration of lipid-free cholate micelles which displace the lipid protecting the AChR channel. Taking into account the 20-fold molar excess of cholate over lipid in the micellar solution, under optimal conditions (2% cholate, 2 mg/ml of soybean lipid), it is evident that the affinity of the lipids for the AChR must be significantly higher than the affinity of cholate for the AChR. This suggests that the AChR channel must be shielded from the detergent molecules and the aqueous medium by a protective annulus of lipids (Fig. 4). Cholate forms expandable micelles in which the planar cyclopentenophenanthrene rings are apposed, while the hydroxyl groups attached to the rings interact with the aqueous environment. This peculiar micellar structure of cholate may enable it to carry AChRs as lipoprotein complexes so that the ion channel is protected by a lipid annulus (Fig. 4) (70).

Although the use of other detergents, such as the nonionic dialyzable detergent octylglucoside, has been reported (80), cholate dialysis is the most widely used technique for the incorporation of functionally intact AChRs in lipid vesicles, since there is consensus that AChR function is recovered after exposure to mixed micelles of cholate and lipid.

2.2- Formation of reconstituted vesicles.

Although low concentrations of lipids are sufficient to protect the cation channel during solubilization in cholate, approximately 10-fold higher lipid concentrations are required to preserve the integrity of the channel during the reassembly of lipid and AChR into vesicles. When AChRs are reconstituted under optimal conditions (lipid:protein > 16:1), they reassemble into lipid vesicles at a constant protein:lipid ratio so that the AChR packing density is 5-fold lower than that in the native electric organ membrane (Fig. 5). Reconstitution under suboptimnal lipid:protein ratios leads to a denser packing of AChRs in the reconstituted membranes and a corresponding irreversible inactivation of a fraction of the AChR channels (70). Freeze-fracture replicas of reconstituted preparations reveal the presence of two populations of vesicles: large vesicles containing intramembranous particles which correspond in size to AChRs, and smaller liposomes free of particles (Fig. 6). About 70% of the AChRs are oriented with their agonist binding sites on the external surface of the vesicles. Immune precipitation of reconstituted vesicles with monoclonal antibodies provides evidence that receptors in a single vesicle are oriented either all right side out or all inside out (70).

Considering that AChRs make up about 7% by weight of the reconstituted membranes (70) and taking into account the partial specific volume of the AChR (6), the average area occupied by a phospholipid molecule (81) and the isopycnic density of liposomes without AChRs (70), it is estimated that a 2,000 A vesicle contains approximately 100 AChR monomers (44).

In order to reduce limitations of the intravesicular volume on the agonist-activated radiosotope uptake measured at equilibrium (discussed indetail below), attempts have been made to prepare vesicles with a large internal volume per AChR Popot et al. (71) reported the preparation of large vesicles (mean diameter 950 ± 550A) by partial cholate dialysis and subsequent gel filtration. We reported that subjecting reconstituted vesicles to a freeze-thaw cycle enhances the sealing of the vesicles and causes vesicle fusion. Inclusion of cholesterol (20% w/w) during the reconstitution procedure greatly enhances vesicle fusion during a subsequent freeze-thaw cycle. This, however, results in a more random orientation of AChRs in the reconstituted vesicles (44).

Size analysis of the reconstituted vesicles, performed by electron microscopy after negative staining, established three general patterns of vesicle organization, as summarized in Figure 7: 1) Liposomes formed in the presence of AChR have larger mean diameters than the corresponding preparations formed in the absence of AChR. 2) Freezing and thawing of the preparations shifts the mean value of the diameter to larger values and causes the appearance of a large number of vesicles greater thatn 1,000 A in diameter. 3) Cholesterol-supplemented liposomes containing AChRs undergo extensive fusion during freezing

and thawing, and the resulting vesicles have a mean diameter of 760 Å; 25% of the vesicles are now larger than 1,000 Å in diameter and 50% of the total included volume is contained in 3.5% of the vesicles with diameters larger than 1,400 Å (44). Fusion with liposomes can be expected to lower the packing density of AChRs in the reconstituted membranes, leading to a further increase in the available internal volume per AChR for cation accumulation during the agonist-induced permeability response (discussed in more detail below).

It is evident from the above discussion that the number of AChR-containing vesicles, the density of AChRs per vesicle, the internal volume per AChR in the reconstituted vesicles, the orientation of the reconstituted receptors and the dynamics of vesicle fusion during the free-thaw cycle all are variable parameters which can be influenced by, among other factors, the lipid composition of the membranes. It should therefore be emphasized that experiments in this model system have to be interpreted with caution, since alterations in radioisotope flux measurements may result from alterations in the structure of the reconstituted membranes instead reflect a change in AChR function.

2.3- Assessment of the pharmacological integrity of the reconstituted AChR.

2.3.1-State transitions.

It is essential with any reconstituted system to verify the pharmacological integrity of the component of interest in order to justify the use of the system as a model for the function of its elements *in vivo*. Reconstituted vesicles containing pharmacologically intact AChRs should exhibit an agonist-activated, dose-dependent translocation of cations which can be blocked by known inhibitors, such as snake neurotoxins, d-tubocurarine and local anesthetics. Furthermore, preincubation with the neurotransmitter should prevent channel opening indicating the occurrence of desensitization.

There is widespread agreement that AChRs can exist in at least three different conformational states-- a "resting state," in which the cation channel is closed; an activated state, in which the cation channel is open; and a "desensitized state," in which the cation channel remains closed in the presence of agonist (cf. 1,2,5,3). These state transitions are illustrated in Figure 8. Ligand binding to the AChR in its resting state results in opening of the channel, which remains open for several milliseconds, allowing the passage of cations. Prolonged exposure to the agonist will stabilize the AChR in its desensitized state, which is characterized by a higher affinity (by two orders of magnitude) for the ligand than the resting state (82,83,84,85,86,87,88,89). Evidence suggests that the desensitization process occurs in two stages, a fast step ($\tau_{1/2} \approx 300$ ms), which initiates the desensitization process, followed by a slow step ($\tau_{1/2} \approx 6$-7 s), which stabilizes the desensitized conformation (90,91,92,93,94). Recovery of the desensitized AChR to its resting state after removal of the agonist is a slow process occurring over minutes (86,90).

In the absence of agonist, most of the AChRs are in the resting low affinity state, but a significant fraction of the unliganded AChRs pre-exist in the high affinity desensitized conformation. This equilibrium is described by the allosteric constant M (Fig. 8). Reported values for M for *Torpedo californica*

range between 4.5 (84) and 10 (95,96,86). Since AChR activation and desensitization processes can go to completion within the incubation period of the assay (~ 10 s), as described in the preceding section, it is clear that measurements of integrated $^{22}Na^{+}$ or $^{86}Rb^{+}$ uptake are not sensitive to the intermediate kinetics which lead to the accumulation of the measured amount of radioisotope inside the vesicles prior to the stabilization of a relatively long-lived desensitized state. However, important qualitative information about the functional characteristics of reconstituted AChRs can still be obtained, for example, through manipulation of the AChR concentratioin. The dose reponse characteristics of AChR activation by agonists depend on the concentration of AChR. When the AChR concentration is high with respect to the dissociation constant for the agonist, bound agonist will constitute a significant fraction of the total agonist concentration. The midpoint of the dose response curve will, as a result, be displaced as function of AChR concentration and will asymptotically approach a constant value at infinite dilution of AChR (Fig. 9) (44). This displacement effect is twice as large for ACh as for CCh, reflecting their respective higher binding affinity for ACh of both the resting and desensitized states of the AChR. The effect of AChR concentration on the midpoint of the dose dependence of AChR desensitization is even more dramatic (Fig. 9), since the desensitized AChR has higher affinity (by two orders of magnitude) than the resting AChR for both agonists. Thus it appears from functional measurements that reconstituted AChRs distinguish between ligands and, at least qualitatively, undergo state transitions in a way similar to AChRs in the native membrane.

2.3.2-Inhibition by cobratoxin: a tool for the assessment of intravesicular volume limitations onthe radioisotope uptake assay.

Inhibition of AChR function by cobratoxin gives information about the extent of intravesicular volume limitations on the measured radioisotope uptake after activation by agonist. Since the probability of channel opening is greatest when two agonist molecules are bound per AChR, the concentration dependence of inhibition of AChR function by cobratoxin is expected to be parabolic (97). In native membranes, the dense packing of AChRs (Fig. 10A) and the concomitant limitation of the internal volume/AChR (~2 x 10^{-20} liters/AChR) lead to equilibration of the intravesicular volume with the external concentration of the radioisotope before termination of the assay. Hence a large fraction of AChRs have to be occupied by cobratoxin before a reduction in the agonist-induced uptake of cations is observed (Fig. 10A) (34,45,44).

A mathematical model of the cobratoxin titration experiment that considers different extents of volume limitation on the cation uptake response was developed (44). This generates a family of curves which approach the predicted parabolic inhibition curve as restraints on the available internal volume per AChR are relieved (Fig. 10B) (44). At relatively low extents of volume limitations per AChR (indicated by the parameter γ as defined in the legend to Fig. 10B), shallow sigmoids may, within experimental error, appear linear. This apparent linearity is enhanced if one assumes heterogeneity in vesicle sizes. Figures 10C-E show the range of observed toxin titration behaviors of regular reconstituted vesicles after freezing and thawing. The inhibition curves vary

slightly, depending on the extent to which fusion has occurred as a result of the freeze-thaw cycle. $^{22}Na^+$ uptake induced by a lower agonist concentration generates toxin titration curves shifted in the direction of the predicted parabola (Figs. 10C and 10E). Cholesterol-supplemented vesicles, after freezing and thawing, have relatively large internal volumes/AChR (ν 25 x 10^{-20} liters/AChR) and show only slight deviations from this parabolic curve. Deviations are small at saturating concentrations of CCh, and the predicted titration curve is followed closely at mM CCh, a concentration which elicits between one-third and one-half of the maximal response (Fig. 10F).

The relative contributions of desensitization and volume limitations in determining the amplitute of the $^{22}Na^+$ uptake response vary with the agonist concentration. At low agonist concentrations, when few AChRs are activated, desensitization is expected to be the primary limitation on the $^{22}Na^+$ or $^{86}Rb^+$ uptake. At higher agonist concentrations, volume limitations will become important in an increasing fraction of the vesicles. In these vesicles, equilibration of the intravesicular volume with the external radioisotope concentration will occur at submaximal agonist concentrations. Accordingly, the midpoint of the dose/response curve for AChR activation shirts to lower agonist concentrations. Limitations on internal volume per AChR may complicate investigation of AChR function but are much less serve in reconstituted vesicles (~8 x 10^{-20} liters/AChR) than in the native membrane (~ 2 x 10^{-20} liters/AChR). They can be entirely prevented at low agonist concentrations through the use of cholesterol-supplemented liposomes and a freeze-thaw cycle to promote the formation of large scaled vesicles (~ 25 x 10^{-20} liters/AChR).

2.4- Identification of membrane components essential for postsynaptic signal transduction.

2.41-The AChR monomer as the functional entity.

A unique advantage of a reconstituted system is that it allows the fractionation of the native membrane into its individual components and the subsequent determination of their respective importance in the recovery of specific functions after reassembly.

The fact that the presence of supplementary lipids prevents inactivation of the ion channel in cholate solution during the purification of AChRs by affinity chromatography allowed the isolation and reconstitution of functionally intact AChRs (67,69,45,71). These studies establish that the $\alpha_2\beta\gamma\delta$ structure is sufficient to express the transduction of ligand binding into the opening of a cation-specific channel. Moreover, with few exceptions (98), it is generally agreed that AChR monomers and dimers are functionally equivalent (71,99,100,101). This notion is based on the observation that purified monomers and dimers, reconstituted separately inlipid vesicles, are indistinguishable with respect to agonist-induced activtion and desensitization (99), and that functional activity of reconstituted AChRs is unaffected after mild treatment with reducing agents, which converts dimers into monomers (99,71). Furthermore, the observation that AChRs remain functional after extensive trypsinization (102) or after depletion

of non-receptor peripheral proteins (103), treatments which also convert dimers into monomers, constitutes additional evidence in support of the notion that the $\alpha_2\beta\gamma\delta$ monomeric form of the AChR represents its functional unit.

2.4.2-Subfractionation of the AChR monomer.

Reconstitution studies aimed at the complete dissociation of the five component subunits and their *in vitro* reassembly into a functional complex so far have not been successful. This is not surprising in light of the fact that the sequential assembly of AChR subunits during *in vivo* synthesis is a complex process, in which maturation of the toxin binding site requires a 15-30 min posttranslational period (104,105). Moreover, after assembly, the subunits of the mature AChR can be dissociated only under denaturing conditions. Partial renaturation of the α subunits isolated by preparative gel electrophoresis in SDS was reported; it was expressed either as recovery of low affinity αBGT binding displaceable by cholinergic ligands after removal of the detergent (106,107) or as high affinity binding of the toxin, which was not displaceable by agonists (108).

The most elegant study on the formation of AChR assemblies consisting of different complements of the five subunits was conducted by Mishina et al. (109). They coupled-cloned cDNAs of all four AChR subunits to a simian virus 40 vector, amplified the messages in COS monkey cells, and injected the resulting mRNAs into *Xenopus oocytes*. Translation of the mixture of injected mRNAs encoding all four subunits of the AChR resulted in the synthesis of functional AChRs in the ooxytes. From studies in which mRNAs coding for some of the subunits were selectively deleted during injection, they deduced that all four subunits are required for the assembly of a functional AChR, although only the α subunit appeared indispensable for αBGT binding.

2.4.3-Effect of membrane lipid composition on AChR function.

Several laboratories have studied the effect of the lipid environment on AChR function (cf. (64)). Early studies with pure lipids established a mixture of phosphatidylethanolamine and phosphatidylserine (3:1 w/w) supplemented with cholesterol or other neutral lipids, such as α-tocopherol or certain quinones, as optimal lipid environment (110,111,112,113,114). However, as discussed above, changes in the lipid composition of the reconstitution mixture can alter the size and hence the volume of the resulting vesicles, as well as the orientation of AChRs in the liposomes (44,113,114,115). Therefore, the evaluation of AChR function must be approached with caution.

The best-documented report on the effect of the lipid environment on AChR function is the systematic study by Criado et al. (115), in which the alteration in vesicle structure was analyzed in parallel with alteration in AChR function. It was found that unsaturated phosphatidylethanolamine in combination with 18-35 moles % cholesterol hemisuccinate permit a maximal ion translocation reponse of the reconstituted AChR. The cumulative results of several studies using pure lipid mixtures indicate that AChR function is optimally retained in a fluid,

unsaturated, cholesterol-supplemented membrane environment. This is consistent with the fact that the native membrane of *Torpedo* electric organ is a fairly unsaturated membrane with a high content of cholesterol (116).

2.5-Limitations of equilibrium measurements of AChR function in reconstituted vesicles.

Equilibrium measurements in reconstituted vesicles, by virtue of their technical simplicity, are useful as a convenient and rapid screening system for macroscopic effects on AChR function (e.g., effects of monoclonal antibodies). They are, however, complicated by 1) restrictions onthe available volume per AChR for the accumulation of radiosotope during the assay time and 2) measurement of initial flux rates. Through the use of cholesterol-supplemented vesicles, volume restrictions can be minimized or, at low agonist concentrations, eliminated (Fig. 10F). The large amplitute obtained after freezing and thawing of reconstituted vesicles further allows measurement of AChR function at relatively low AChR concentrations, which have minimal effects on the midpoints of the dose/response curves for AChR activation and desensitization (Fig. 9, closed symbols). Thus the major limitation of the system remains the measurement of a cumulative cation uptake response which is insensitive to the intermediate kinetic steps involved in AChR function (e.g., during the assay time activation as well as desensitization processes take place which lead to displacements of the midpoint of the dose/response curve for AChR activation toward a lower agonist concentration). Methods to study the kinetics of neurotransmitter-regulated cations fluxes through AChR receptor channels in reconstituted systems consist of rapid stop-flow measurements in reconstituted vesicles (117) and of electrical measurements in planar lipid bilayers. The transformation of reconstituted vesicles containing AChR into planar lipid bilayer membranes is discussed in the following section.

3. RECONSTITUTION OF AChR IN PLANAR LIPID BILAYERS.

3.1- Rationale.

The ultimate criterion for the success of the AChR channel reconstitution resides in the detailed comparison of the channel properties of the purified AChR with those of the native system. Single-channel recordings from the purified AChR reconstituted in planar lipid bilayers provide an assay that resolves, in real time, molecular transitions proceeding in a single AChR molecule. Knowledge of the kinetic, pharmacological and ion conduction characteristics of the purified AChR is the prerequisite for the investigation of how manipulations in structure modify functioinal properties on a molecular level (see 4).

Planar lipid bilayers are assembled via apposition of two monolayers initially at the air-water interface (53,50,47). The bilayers can be formed either across apertures in Teflon septi (53,50,47) or at the tip of patch pipets (54,56,55,57). In both modalities, the monolayers are derived from the reconstituted AChR vesicles (118,119,120,98,121,58,62,59,60,122) described in detail in the previous section.

3.2- Transformation of reconstituted vesicles into monolayers at the air-water interface.

A necessary condition for the assembly of planar lipid bilayers from vesicle-derived monolayers is that the surface pressure, π, of the monolayer > 25 dynes (118,119). Surface pressure is extremely sensitive to the composition of the aqueous medium (subphase). Schindler and collaborators studied AChRs from *T. marmorato* and *californica* in planar lipid bilayers (120,123,98). The channel properties were found to depend on the surface properties of the monolayers and on the lipid composition of the reconstituted vesicles. Two requirements for the functional integrity of the reconstituted AChR channel were identified: 1) cholesterol, which appears to stabilize the channel and 2) a monolayer cohesive pressure of ~30 dynes/cm, which appears to reduce the aggregation of AChRs in the membrane.

The procedure we routinely use to derive monolayers from purified AChR reconstituted vesicles (see 2) with surface pressures sufficient to support the assembly of bilayers is as follows: a 50 µl sample of reconstituted vesicles (the AChR concentration ranges between 0.2 and 1.0 µM; soybean lipid is 32 mg/ml supplemented with 8 mg/ml cholesterol) is diluted with 25 mM HEPES (N-2-hydroxypiperazine-N'-2-ethane sulfonic acid)-Tris, pH 7.4, to a final volume of 250 µl and centrifuged at top speed in a Beckman Airfuge (122,000 x g) for 20 min. The pellet is resuspended in 0.5 M NaCl, buffered with 2.5 mM Tricine (N-tris-[hydroxymethyl]-methylglycine), or HEPES, pH 7.4, and $CaCl_2$ between 0.5 and 5 mM) in a final volume of 0.3 ml; sonicated for 15s; and incubated for 20 min at 20°C. Such a suspension is introduced into the bilayer chamber by gently delivering 20 µl drops (see section 3.3). The surface pressure of monolayers at the air-water interface can be monitored by the method of Wilhelmy in a monolayer trough with two movable barriers and several compartments (124). Figure 1 illustrates the time course of change in surface pressure caused by the formation of a monolayer at the air-water interface from a suspension of AChR reconstituted vesicles (5).

The actual transfer of purified AChRs from the reconstituted vesicles to monolayers can be determined using ^{125}I-αBGT-labeled AChRs (120,58). An aliquot of αBGT-labeled reconstituted vesicles is deposited into one chamber of the multicompartment surface trough. Monolayers at surface pressures of 14-18 dynes/cm are transferred to a vesicle-free comnpartment, compressed to a π of 30 dynes/cm and collected for analysis. The radiolabeled αBGT measured in the monolayer provides an estimate of the density of AChR (AChR molecules/cm^2) in the monolayer. Under the conditions described for bilayer reconstitution studies, the estimated AChR density is ~ 10^7/cm^2 (58).

3.3- Assessment of the pharmacological integrity of the reconstituted AChR channel.

The reconstituted AChR in planar lipid bilayers displays the macroscopic phenomena associated with the AChR in the native membrane, namely, activation and desensitization in the presence of cholinergic agonists. The agonist-activated membrane conductance increases with agonist concentration and is inhibited by cholinergic antagonists (d-tubocurarine and hexamethonium) and by αBGT

(121,58,122). At high current resolution, the opening and closing of single AChR channels are clearly discerned (121,98,125,58,62,122). Single-channel currents are activated by ACh, CCh and SubCh. Channel are not observed when the reconstituted vesicles are preincubated with an excess of αBGTx, which specifically inhibits the agonist-activated flux response in vesicles (see section 2.4.2).

3.3.1-Comparison of single-channel recordings obtained from planar lipid bilayers across Telfon apertures or at the tip of patch pipets.

So far, similar channel properties have been recorded from reconstituted AChRs with both modalities of bilayer support, namely, bilayers formed across apertures in Teflon septi or at the tip of patch pipets (122,55,58,62). Therefore, in the description of AChR channel properties that follows, no distinction is made with respect to the specific modality used. However, the technique of forming a lipid bilayer from two monolayers at the tip of a patch pipet allows recordings of single-channel currents to be obtained at a higher time resolution and with better single-to-noise ratio than those obtained from bilayers formed across Teflon aperture (55). Figure 12 shows single AChR channel currents recorded from planar lipid bilayers formed either across an aperture in Teflon (left-hand panel) or at the tip of a patch pipet (right-hand panel). Four stretches from a continuous record are illustrated. In both panels, two distinct channel states are clearly discerned, corresponding to the closed and open states of the channel. The single-channel conductance is estimated from the conductance histogram illustrated in Figure 13. Two Gaussian curves are identified, corresponding to closed and open channel states. The data noisy curve, are well fitted by the sum of two Gaussians (smooth curve). The first curve, with a mean peak value at zero current, corresponds to the channel closed state. The second is associated with the channel open state. At 100 mV, its peak value is centered around 4.2 pA and 4.7 pA, respectively, The single-channel conductance, γ, is the current difference between the two peaks divided by the applied voltage; In these recordings γ = 42 pS (0.44 M NAcl, left-hand panel) and δ = 47 pS (0.5 M NaCl, right-hand panel). The two Gaussian are well separated but their widths are larger for the records from bilayers in Teflon apertures, indicting a lower signal-to-noise ratio. Note that the width of the Gaussians is larger for the open state than for the closed state, a feature especially conspicuous in the record from patch pipets. This is a measure of th current noise and indicates that the open channel noise is > 10% larger than the noise of the closed channel. This result agrees with data obtained by Sigworth (126) in native membranes and appears to reflect the increased current introduced by the fluctuations of the protein domains forming the channel as the ions travese through it.

The properties measured in both systems are therefore practically identical but the records obtained from patch pipets are clearly superior.

3.3.2-Ion conduction through the reconstituted AChR channel saturation, selectivity and block.

The single AChR channel current-voltage relationship is linear in the range of -100 mV < V < 100 mV. The single-channel conductance is ohmic and independent of the type or concentration of the agonist for ACh, CCh or SubCh

(58,122). Single-channel currents increase with Na^+ activity to a maximum conductance of 95 pS and show a half-saturation point of 395 mM. The apparent ion selectivity sequence derived from single-channel current recordings is: NH_4^+ > Cs^+ > Rb^+ > Na^+ >> Cl^-, F^-, SO_4^{2-} (58). The selectivity and saturation characteristics of the open AChR channel in planar lipid bilayers are in agreement with those determined in muscle cells (127,128,129,130,131,132). In addition, a quaternary ammonium derivative of the local anesthetic lidocaine (QX-222) is known to block ion conduction through open AChR channels in muscle (133). A similar action is exerted on the purified *Torpedo* AChR reconstituted in lipid bilayers, as evidenced from the appearance of fast "flickering" between open and closed states and a drastic reduction in open channel lifetimes (58). This blocking action is voltage-dependent, being prominent when the *cis*-side of the bilayer is positive. In contrast, no detectable block is measured when QX-222 is present on the *trans*-side of the membrane, suggesting that the drug is effective only on the normally extracellular-facing side of the channel, in agreement with data on native AChR (134,135,136). Thus it is evident from single-channel studies that all tested aspects of ion conduction through the reconstituted AChR channel are functionally retained in the planar lipid bilayer.

3.3.3-Channel gating kinetics.

3.3.3a-The AChR channel has two open states.

Precise information about the number of open and closed states in which the AChR channel can exist, the pathways to enter into or exit from such states and the rates of transition between the various states is essential for a rigorous understanding of the AChR channel at the molecular level.

Single-channel recordings are especially appropriate to detailed statistical analysis. The major analytical tool is the computation of distribution of dwell times (lifetimes) in the open and closed states of the channel. Single-channel recordings obtained from cells by the patch clamp technique (137,138) and from the purified AChR reconstituted in planar bilayers (62,59,60,121) have led to a major revision of the kinetic schemes used to describe the function of the AChR channel. The conventional model of the AChR, in which channels are open or closed (Fig. 8) and the distribution of open times is well described by a single exponential with the predicted time constant, cannot account for the single-channel results.

A major conclusion derived from the analysis of single-channel current records from the reconstituted AChR channel is that the distribution of channel open times is well fit by a sum of two exponentials, reflecting on the existence of at least two open states (62,59,60). This is illustrated in Figure 14. Records in which only one channel is open at any given time are analyzed. The fitted curve (smooth curve) is superimposed on the histogram of the actual data (noisey curve). The area under the probability density function (A) and time constants (τ) for the short (S) and the long (L) components have been calculated. For ACh, at an applied voltage of 100 mV, the typical values of the time constants of the short and long openings are 0.5 ms and ~4 ms (60). The time constants of these two states depend on the choice of agonist, following the

sequence: SubCh > ACh > CHh in agreement with single-channel data from native AChR in cells (139,140). These two kinetically distinct, open states, however, have the same single-channel conductance (58,62,122,55,141).

3.3.b-The occurrence of the long-lived state increases with ACh concentration.

The high signal-to-noise ratio of the records obtained from patch pipets (Figs. 12,13) enables a clear identification of states and therefore a more accurate and reliable estimation of the kinetic parameters involved in channel gating. Exploiting the high resolution of these measurements, a detailed correlation between the frequency of occurrence of short and long opening and the concentration of ACh was obtained (60).

The probability density of open dwell times is well described by a sum of two exponentials of agonist concentrations in the range of 0.01 μM < ACh < 0.1 mM. This study indicates that the area ratio of the two components (A_L:A_S ratio) increases with the concentration of ACh, while the corresponding time constants, τ_S and τ_L, of the short and long kinetic processes involved in channel closure are not altered systematically by agonist concentration. Similar results are obtained with CCh (58). Thus the frequency of occurrence of the long openings increases with the concentration of agonist (60). Similar results have been obtained from single AChR channel recordings in adult muscle cells (D. Colquhoun and B. Sakmann, personal communication).

3.3.c-Inferences about molecular mechanisms of channel gating.

The results of the kinetic analysis described above allow one to reject a set of kinetic schemes which predict either that the A_L:A_S ratio is a constant or that the time constants vary with agonist concentration (142). Below is a minimum kinetic scheme that is consistent with the experimental data.

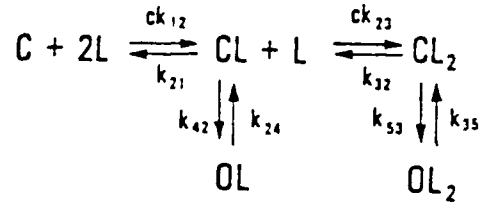

(1)

where C represents closed channel states and O, open states and L denotes the ligand. This scheme is consistent with the independence on agonist concentration of both τ_s and τ_L, implying that liganding is to closed states. Such amodel predicts a linear dependence with unitary slope of the A_L:A_S ratio on agonist concentration when plotted as the log A_L:A_S versus log [ACh]. The function, determined experimentally, indeed shows a unitary slope within the range of ACh concentration between 0.01 μM and 0.1 μM. At higher ACh concentrations, the A_L:A_S ratio approaches a constant value. Such behavior does not appear to arise

from channel blocking by the agonist (13), since the τ's calculated from the distribution of open times are independent of ACh concentration. Formally, this deviation could be accounted for by introducing an additional short-lived, doubly liganded open state to the right of Cl_2 in scheme (1). Models equivalent to (1), consisting of multiple open states with higher extents of ligand occupancy or with a more complex closed states structure, could also account for the experimental results. The simplest inference derived from our observations is that both singly and doubly liganded states of the AChR molecule undergo transitions to the open conformation.

Note that the dependence on ACh concentration of the permeability response, assayed in the same reconstituted vesicles from which the planar bilayers are derived, shows that the fraction of desensitized AChRs increases from ~ 50% at 0.01 μM ACh to 100% at 0.1 μM ACh (Fig. 9). This is the range of ACh concentrations at which the A_L:A_S ratio is most sensitive to the concentration of ACh.

3.3.3d-Autocorrelation analysis of AChR channel gating kinetics.

A different approach to the analysis of single channels that, in addition to the conventional computation of dwell times distributions, takes advantage of autocorrelation and autocovariance functions was developed. This method allows the extraction of information about the pathways connecting the open and closed states which is contained in such autocorrelation functions. It is applicable only to stationary processess in membranes containing a single channel. Extended accounts of both the theoretical formalism (143) and the experimental application to the AChR channel (59) have appeared.

The autocorrelation analysis for the open state of the AChR channel activated byh ACh is shown in Figure 15. The theory described by Fredkin et al. (143) states that the correlation function decays geometrically. Considering that a correlation is significant only if it is larger in absolute value than twice the approximate standard error of the estimate in the case of while noise (horizontal dashed lines), it is evident that substantial correlation is present near zero. This result indicates that there are at least two entry/exit states through which the open and closed aggregates communicate (59).

The conditional probability analysis of single-channel currents of the purified AChR (62) provides evidence of two kinetically distinct open states. The autocorrelation analysis further supports that notion and indicates that these two open states can be entered or exited via at least two pathways, in other words, can be reached from at least two closed states. This new information, extracted from the autocorrelation analysis, is an independent demonstration for the existence of at least two open states and supports the kinetic scheme outlined above (60). Jackson et al (142) applied a different correlation test, based on the analysis of pairs of openings to AChR channel in cultured cells, and reached a similar conclusion.

3.3.3e-Desensitization

Single-channel currents occur in paroxysms of channel activity followed by quiescent periods during which little or no activity is observed (Figure 16A) (90,122,58). This pattern is more pronounced as the agonist concentration increases, and is reflected in histograms of channel opening frequencies (122). Long single-channel records are divided into 100 ms sections (trials) and the histograms show how many 100 ms trials have 0, 1,2, etc., openings. Figure 16B shows a typical histogram for 1 mM CCh. The peak at zero openings corresponds to the quiescent periods. The peak at ~ 6 openings/100 ms trial corresponds to the number of openings in a typical paroxysm. Monte Carlo simulations with the simplest three-state model, consisting of two closed (unliganded, C, and liganded, CL) and one open state (OL), do not resemble the recorded pattern of channel activity, especially at high agonist concentration. Inclusion of a desensitized liganded state (DL) reproduces the qualitative features of channel records (122). The occurrence of paroxysms of channel activity thus seems to result from the transit of AChR through its active conformation, from which it can open several times before desensitizing (Fig. 16B-16D) (144,90).

3.3.3f-Monoclonal antibodies specific to the β and γ subunits affect channel gating.

A library of monoclonal antibodies (mAbs) against the AChR have been used to identify regions of the AChR involved in channel function. mAbs directed against determinants on specific subunits have been evaluated with regard to their ability to alter the single-channel properties of the reconstituted AChR (145,40,146,147,148,149,150).

mAbs that bind to the main immunogenic region on the extracellular domain of the α-subunit and away from the ACh binding site (Fig. 1) and to a cytoplasmic determinant on the δ-subunit altered neither the single-channel conductance nor the channel open times. In contrast, three mAbs directed against determinants on the β- and γ-subunits inhibited channel activity (145,149,150)(Fig. 17). mAb 10, which binds to an extracellular domain of the β-subunit and also cross-reacts with the α-subunit (Fig. 1), caused inhibition of the AChR channel when added to the same compartment as ACh (Figure 17A). Ab 148, which recognizes a cytoplasmic domain of the β-subunit, and mAb 168, directed against a cytoplasmic domain of te γ-subunit, inhibited single AChR channel activity only when added to the compartment opposite that containing ACh, in agreement with their specificity for determinants on the cytoplasmic surface of the AChR (cf. (151,152)) (Figs. 17B and 17C). The inhibition of channel activity can be accounted for by a reduction in the number of active channels and not be an alteration in single-channel characteristics. In agreement, mAb 10 was previously shown to inhibit the CCh-activated influx of $^{22}Na^{+}$ into reconstituted vesicles when added after their formation (145). In contrast, mAbs 148 and 168 inhibited the flux response only if present during the vesicle reassembly process, implying that inhibition was conditional to binding to a cytoplasmic AChR domain (152). It is interesting, that the monovalent Fab fragments of these mAbs do not affect channel activity.

4. CONCLUSIONS AND FUTURE PROSPECTS.

The molecular physiology of postsynaptic signal transduction has been reduced to studies on the transmembrane events proceeding in the purified AChR molecule. The concepts and techniques required for the resol'tion and reconstitution of the system are now well established. The full cycle of solubilization, purification and reconstitution of the AChR can be achieved without impairment of channel function. Therefore, the stage is set to investigate how both chemicl and genetic modifications in the structure of the AChR affect its channel gating.

One interesting protein modification is phosphorylation, which is widely recognized as a regulatory mechanism in signal transduction (cf. (153)). The *Torpedo* AChR is a substrate for three distinct protein (154) kinases, namely, a C-AMP-dependent protein kinase, protein kinase C and an endogenous tyrosine-specific protein kinase (155). The latter phosphorylates a single intracellular site of the β-γ- and δ-subunits. The effect of AChR phosphorylation on channel function can be evaluated using reconstituted AChR in planar lipid bilayers. The foreseable trends are likely to encompass the use of mAbs to probe AchR function (149,150,145,156,157,158) in comjunction with site-directed antibodies (31,159). The successful application of site-specific oligonucleotide mutagenesis to the AChR (160) will give impetus to expanding the use of molecular genetics to channel proteins. Individually, the results of these approaches are open to several interpretations. However, it is anticipated that the integration of the information obtained using site-directed mutagenesis, peptide-specific antibodies and chemical modification to known sites on the AChR subunits and the single-channel recordings in reconstituted receptors will eventually head to the clarification of the structure function relationships in the AChR.

β-THE RECONSTITUTED SODIUM CHANNEL FROM BRAIN

β-INTRODUCTION

The voltage-sensitive sodium channel mediates the inward sodium current during the depolarizing phase of an action potential. Because of its central role in impulse conduction, it has been the subject of extensive investigations by electrophysiological and biochemical techniques to understand its structure and function. Sodium channels have been solubilized in detergents and purified from eel electroplax (161,162), rat muscle (163,164), chicken heart (165) and rat brain (166,167,168). The only functional property of sodium channels that is measurable in detergent solution is the binding of certain sodium-channel specific neurotoxins. Therefore, it is necessary to reconstitute the purified channel protein to establish that it is functionally intact. This section describes the reconstitution into lipid vesicles (169,170) and planar lipid bilayers (171) of sodium channels purified from rat brain and the measurement of sodium channel function in these two systems.

1.1-Sodium channel specific neurotoxins.

Several types of sodium-channel-specific neurotoxins (172) have been extremely useful in these studies. The first class consists of the sodium channel blockers saxitoxin (STX) and tetrodotoxin (TTX). These are small, positively charge, water-soluble, heterocyclic guanidines that bind with nanomolar K_Ds to a site on the extracellular-facing side of the sodium channel. [^{3}H)-STX binds with similar affinity to both detergent-solubilized and membrane-bound sodium channels, making it an excellent marker for the sodium channel protein during its purification (173). Binding of these toxins to the channel protein results in an inhibition of ion flux. Since these compounds cannot permeate lipid bilayers, they have no effect on the channel when they have access only to the normally intracellular-facing side (174). Thus STX and TTX are also valuable for determining the orientation of reconstituted sodium channels.

The second group of toxins is represented by the sodium channel activators batrachotoxin (BTX) and veratridine (Ver.). These are small (molecular weight = 536 and 674, respectively) lipid-soluble molecules that can interact with sodium channels from either side of the bilayer. These toxins shift the voltage dependence of activation by ~ 50 mV in the hyperpolarized direction so that the voltage at which 50% of the channels are activated (V_{50})is near -90 mV (175). In addition, they eliminate both fast and slow (BTX only) inactivation, resulting in persistently activated channels over a wide voltage range (176). The ionic selectivity and single-channel conductance of sodium channels is also decreased by these toxins (177,178).

The third type is a scorpion toxin (LqTX) purified from the venom of the North African scorpion *Leiurus quinquestriatus*. This toxin is a 6,700 molecular weight positively charged polypeptide that binds to a site on the extracellular-facing side of the sodium channel in a highly voltage-dependent manner (179). The K_D at -55 mV is 2 nM, while at 0 mV, it is 1,000 nM. LqTX acts to slow the rate of inactivation of the sodium channel (180).

1.2- Sodium channel purification and subunit composition.

The sodium channel was purified from a Triton X-100 solution of rat brain membranes, as outlined in Table I, by selecting the fractions that contained high concentration of [^{3}H]=STX binding sites (181). The purity at each step can be assessed by comparing its specific activity to the specific activity of 3,200 pmoles/mg calculated for pure sodium channel from its molecular weight. On this basis, the channel proteins 90% pure after the sucrose gradient step.

The sodium channel protein purified from rat brain consists of three subunits, $\alpha(M_r \sim 260,000)$, $\beta 1$ ($M_r \sim 39,000$) and $\beta 2$ ($M_r \sim 37,000$) (182,181). as shown in silver-stained SDS gels (Fig. 18) (183). Several lines of evidence support this conclusion. First, in sucrose density gradients, all three polypeptides cosediments as a stoichiometric complex whose distribution exactly coincides with the distribution of [^{3}H]-STX binding sites in the gradient (181). Second, with native sodium channels in synaptosomes and inprimary neuronal cultures from rat brain, the α-subunit and the $\beta 1$-subunit are specifically

covalently labeled by photoactivated derivaties of LqTX (184,185,186). Third, the α-subunit and the β2-subunit are covalently attached by at least one disulfate bond (182). And fourth the β-subunits are not proteolytically derived from α or a larger precursor during the purification because the amino terminus of all three subunits is blocked (168,183).

1.3- Why reconstitute?

Since the only functional property measurable with purified sodium channels in detergent solution is the binding of STX and TTX, a number of obvious questions about the structural and functional integrity of the purified protein remain to be answered, for example, has the entire structure of the sodium channel been purified or only a portion of it that contains the STX/TTX binding site? To answer these questions, purified sodium channels are reconstituted into lipid vesicles and into planar bilayers. These systems nicely complement each other. Purified sodium channels reconstituted in lipid vesicles provide a convenient system for studying the average properties of a large population of channels over a time scale that is slow compared to the opening and closing rates of the channel. This system is well suited for quantitative measurement of : 1) ligand binding 2) the fraction of functional ion channels reconstituted and their orientation and 3) neurotoxin-activated ion flux, provided that care is taken to ensure initial rate conditions throughout the time course of the assay. The planar lipid bilayer system excells in those areas in which the vesicle system is weakest: measurement of the current through one or a small number of channels with excellent time resolution under conditions in which the trans-bilayer voltage is well controlled. This system allows detailed measurements of the conductance, voltage dependence, kinetic constants and ion selectivity of single sodium channels. While neurotoxin binding measurement is impractical, neurotoxin effects can be readily demonstrated and their concentration dependence determined if the off and on rates are slow enough to be resolved and fast enough to permit a representative sampling of the data in a reasonable time. Note that the reconstituted vesicles are the source of sodium channels for the planar lipid bilayer experiments. Therefore, successful reconstitution in planar lipid bilayers is strictly dependent on the functional integrity of the sodium channels in the reconstituted vesicles. A description follows of the methods used to reconstitute purified sodium channels, first, into lipid vesicles and then in planar lipid bilayers and to review the properties of the reconstituted sodium channel.

2. RECONSTITUTION OF PURIFIED SODIUM CHANNELS INTO PHOSPHOLIPID VESICLES.

2.1-Methods.

2.1.1-Vesicle preparation.

Reconstitution of solubilized integral membrane proteins requires the slow removal of detergent in the presence of phospholipid. Detergents commonly used for reconstitution have relatively high critical micelle concentrations and are removable by dialysis. However, the sodium channel was solubilized and purified

using Triton X-100A, which cannot be dialyzed because of its low critical micelle concentration. This detergent can be removed by porous polystyrene beads (Bio-Beads SM-2) (187) and this is the basis of our reconstitution procedure.

Purified rat brain sodium channels were reconstituted into egg phosphatidylcholine (PC) (Sigma) vesicles according to the following protocol (169): Triton X-100 (10% w/v) in Na_2SO_4 reconstitution medium (67.5 mM Na_2SO_4, 25 mM HEPES, pH adjusted to 7.4 with Tris base, 0.5 mM $MgSO_4$, and 150 mM sucrose) containing 5% w/v PC was added to sucrose gradient samples containing 30-40 pmoles of purified sodium channels to yield a final concentration of 1.75% Triton X-100 and 0.85% PC. Small amounts of [^{14}C] were added to serve as a tracer vesicle phospholipid. Detergent was removed with Bio-Beads (0.2 ml/ml sample) during an overnight incubation at 4°C. The Bio-Beads were then replaced with an identical volume of fresh Bio-Beads. The sample was incubated for an additional two h at 4°C and the Bio-Beads were removed by filtration. Under these conditions, Bio-Beads removed more than 98% of the Triton X-100 (determined using [^{3}H]-Triton X-100). The Bio-Beads also removed 10-20% of the protein and lipid, which is one drawback of this procedure.

Sodium channels were also reconstituted into vesicles composed of 40% egg PC and 60% purified rat brain lipid (w/w). A solution of 10% Triton X-100, 1% brain lipid, 0.25% PC in Na_2SO_4 reconstitution medium was added to purified sodium channels to give a final lipid concentration of 0.06%. Vesicles were formed during an overnight incubation with 0.3 ml Bio-Beads per ml of solution, as described above.

2.1.2-Characterization of the reconstituted vesicles.

Internal volume was measured by including radioactive markers such as [^{14}C]-glucose or $^{22}Na^+$ prior to reconstitution by detergent removal. The nonspecific release of these markers is low. The efflux of $^{22}Na^+$ from these vesicles occurred with a $t_{1/2}$ of 4 h at 4°C. The reconstituted vesicles were passed over a glass fiber filter (Whatman GF/F) or through a Dowex ion exchange column to separate internal and external [^{14}C] glucose of $^{22}Na^+$, respectively (46). Total internal volume was calculated from the initial isotope concentration. Little or no [^{14}C]-glucose or $^{22}Na^+$ was bound to vesicle phospholipid, which was determined by treating the vesicles with low concentrations of Triton X-100 prior to measuring internal isotope levels.

Vesicle size was measured by both gel filtration and freeze-fracture electron microscopy (170). We used a BioGel A150 column(1.0 x 25 cm) calibrated with uniform-size latex beads obtained from Dow Chemical Company. Vesicle diameters up to 2000 Å were accurately determined with such a column. Comigration of [^{3}H] STX binding activity and vesicle phospholipid through the column demonstrated quantitative reconstitution. Vesicle aggregation can artificially create large particles and vesicles with diameters larger than 2,000 Å cannot be resolved. These problems can be avoided in freeze-fracture electron microscopy, which was the method of choice to assess vesicle size (188).

2.1.3-Assay of neurotoxin binding to the reconstituted sodium channel.

STX binding was measured by incubating the reconstituted vesicles with 2-10 nM [^{3}H]-STX in choline chloride binding medium as previously described in detail (189). Separation of bound and free [^{3}H]-STX was by filtration through a Whatman GF/F filter. Since the vesicles contained a trace amount of [^{14}C]-PC, the filters were analyzed for both ^{3}H and ^{14}C radioactivity to quantitate [^{3}H]-STX binding and vesicle retention, respectively. Approximately 20% of the vesicles were not retained by the filter. Nonspecific binding was determined in the presence of 1 μM TXX.

To determine the orientation of the reconstituted channel across the vesicle membrane, the binding of 10 nM [^{3}H]-STX to vesicles in the presence of increasing concentrations of Triton X-100 was measured (170). Following a 30 min incubation at 4°C, free and bound [^{3}H]-STX were separated by centrifugation through 1.5 ml columns of Sephadex G-50 as described for binding to the solubilized STX receptor (173). Triton X-100, 0.2%, allowed [^{3}H]-STX access to internally oriented, inside-out STX binding sites without solubilizing protein. At higher detergent concentrations, the binding activity declined because of solubilization and denaturation of the reconstituted STX receptor. The maximum percent increase in the [^{3}H]-STX binding observed with increasing detergent was taken as an indication of the fraction of inside-out STX receptor sites.

LqTX was purified from the venom of *Leiurus quinquestriatus* and labeled with ^{125}I (190,179). The binding of this radiolabeled polypeptide to the reconstituted channel was measured by incubating vesicles in reconstitution medium with 0.1 mM [^{125}I]-LqTX at 36°C for 15 min. The mixture was then diluted with ice-cold wash medium and filtered through a Whatman GF/F filter to separate bound and free toxin. Prior to use, the filters were incubated in wash medium containing 1 mg/ml bovine serum albumin for 30-45 min. This preincubation was necessary to reduce [^{125}]I-LqTX binding to the filter. Incubation times longer than 1 h or with more than 1 mg/ml bovine serum albumin further reduced [^{125}I-LqTX binding but also decreased vesicle retention by the filter. LqTX binding in the presence of a membrane potential was measured as described elsewhere (170).

Analysis of nonspecific [^{125}I]-LqTX binding was more complicated than measuring binding in the presence of an excess of unlabeled LqTX. Both glass fiber filters and protein-free phospholipid vesicles demonstrated low affinity, but saturable, [^{125}I]-LqTX binding. To correct for this, vesicles were formed with heat-denatured sodium channels (15 min at 36°C) under conditions identical to those used to form vesicles with active channels. The [^{125}I-LqTX binding to these vesicles, which contained no [^{3}H]-STX binding activity, was taken as nonspecific binding. Routinely, at concentrations of [^{125}I]-LqTX below 0.2 nM, nonspecific binding constituted 25% to 35% of total binding (Fig. 20). Of this fraction, ~ 40% represented binding to GF/F filters and the remainder, nonspecific binding to reconstituted vesicles. Binding to phospholipid vesicles was characterized by high capacity and low affinity (K_D = 5 μM). In contrast, the binding to reconstituted sodium channels had a 100-fold K_D, 60 nM (170).

2.1.4-Assay of Na^+ transport by the reconstituted sodium channel.

The small diameter of reconstituted vesicles complicates the quantitative measurement of initial rates of ion transport. Equilibrium is likely to be reached in less than a second when measuring rates of net ion influx. The small internal volume of the vesicles also results in a low signal-to-noise ratio, especially if the measured ions also bind to vesicle phospholipid. Tanaka et al. (191) used a stop-flow approach to measure initial rates of ion transport by reconstituted sodium channels purified from skeletal muscle. We used an alternative procedure (169) based on an assay system developed by Epstein and Racker (192) to measure $^{22}Na^+$ uptake by reconstituted vesicles. Vesicles were first incubated with neurotoxins to activate the channel. To initiate uptake, a 20 µl aliquot of vesicles formed in the presence of Na_2SO_4 reconstitution medium was diluted 10-fold with 180 µl of Tris-SO_4 medium (105 mM Tris-SO_4, pH 7.4, 0.5 mM $MgSO_4$, 25 mM HEPES adjusted to pH 7.4 with Tris base and the sucrose concentration required to maintain osmolarity with the vesicle medium) containing 10 µCi/ml $^{22}NaCl$ and the appropriate neurotoxins. The diluted sample was incubated at 36°C for 20 s, unless indicated otherwise, then applied to a Dowex AG50W-X8 (Tris form) column (10 x 0.5 cm) in a Pasteur pipette and immediately eluted with 1 ml of 0.38M sucrose containing 1 mg/ml of bovine serum albumin. Recovery of the vesicles in the column eluate, as determined by [^{14}C]-PC, approached 100%. $^{22}Na^+$ uptake terminated within 3 s as the cations were adsorbed to the resin.

Dilution into Na^+-free medium generates a 10-fold outward-oriented Na^+ electrochemical gradient. Vesicles containing neurotoxin-activated sodium channels are selectively permeable to Na^+ ions and therefore should generate an inside negative membrane potential of ~ 62 mV, as predicted by the Nernst equation (170). The observed $^{22}Na^+$ uptake represents isotopic equilibration rather than net influx and therefore occurs over a slower time course than would otherwise by expected, since the ratio $[Na^+]in/[Na^+]out=10$, $^{22}Na^+$ is concentrated within those vesicles containing active channels. This effect greatly enhances the signal-to-noise ratio of the assay system. Sodium must be the only ion capable of crossing the vesicle bilayer if the gradient and membrane potential are to be maintained. The lack of permeant counter ions, coupled with the inside negative membrane potential, also prevents isotope loss during passage over the Dowex resin.

2.2-Assessment of the functional activity of the reconstituted sodium channel.

2.2.1-Description of reconstituted vesicles.

Figure 19 is a freeze-fracture electron micrograph of reconstituted sodium channels in egg PC vesicles. The arrow points to a vesicle with an intramembranous particle (~ 100 Å), presumably a sodium channel. The size of the vesicles is distributed in two populations, one with a mean diameter of 850 Å ± 35 Å ($S_oE.$) and the other significantly larger, with a mean diameter of 2,300 Å ± 50 Å (S.E.). Intramembranous particles are present in both populations, so there is no evidence that sodium channels are preferentially incorporated into

vesicles of one size group. The average number of STX receptors per vesicle (0.75 to 2.1 from 6 different batches of vesicles) is kept low to facilitate ion flux measurements (170).

2.2.2-[^{3}H]STX binding and receptor orientation.

Scatchard analysis of [^{3}H]STX binding to purified reconstituted sodium channels shows a single class of binding sites with a K_D of 2 nM (170). This value agrees well with the 2.3 nM K_D of [^{3}H]STX binding to sodium channels in synaptosomes (173). The orientation of the STX receptors was determined as described in section 2.1.4 on six different batches of reconstituted sodium channels. The percentage of externally oriented STX receptors ranged from 40% to 60% with a mean of 50% ± 4% (S.E.M.).

2.2.3-Scorpion toxin binding by the reconstituted sodium channel.

LqTX binding activity is an extremely sensitive biochemical indicator of the functional state of the sodium channel. Binding of this polypeptide toxin to native channels is influenced by both membrane potential and occupancy of the alkaloid toxin receptor site (172). LqTX binding is also affected by the hydrophobic environment of the sodium channel. Concentrations of Triton X-100 that are 10-fold lower than those that solubilize the membrane completely inhibit toxin binding (173).

Sodium channels reconstituted into egg PC vesicles do not bind ^{125}I-LqTX. Solubilization per se does not irreversibly denature the LqTX receptor, since Triton X-100-solubilized channels can be reconstituted prior to purification with recovery of LqTX binding activity (189). There are three possible reasons for the lack of ^{125}I-LqTX binding following reconsitution into PC vesicles: 1) The LqTX receptor may be irreversibly denatured during the purification; 2) a protein component essential for LqTX binding may separate from the sodium channel during purification; and 3) a membrane constituent necessary for LqTX binding other than sodium channel protein itself may be removed during purification. Endogenous lipid is a possible candidate within this third category.

To examine the role of endogenous membrane lipid, whole rat brains (obtained from Pel Freez Biologicals,Rogers, Arkansas) were subjected to a modified Folch extraction and the resulting lipid purified by silicic acid chromatography (170). This lipid fraction was a mixture of PC, phosphatidylethanolamine (PE), phosphatidylserine and cholesterol and was protein-free.

Binding of ^{125}I-LqTX to reconstituted sodium channels in rat brain lipid/PC vesicles is illustrated in Figure 20. In the absence of unlabeled LqTX, reconstituted vesicles containing untreated sodium channels bound 1.95 fmole of ^{125}I=LqTX, while vesicles containing heat-denatured sodium channels bound 0.45 fmole (23%) of total binding). The difference between these two values represents specific binding (0). Specifically bound ^{125}I-LqTX was competitively displaced by unlabeled LqTX with a K_D of 100 nM. In contrast, 100 nM unlabeled LqTX had little effect on nonspecific binding to vesicles with denatured sodium

channels. Concentrations of unlabeled LqTX > 100 nM displace nonspecivially bound ^{125}I-LqTX. This nonspecific binding component, with a high binding capacity and a K_D of 5-10 μM, was not characterized further.

To verify that the observed binding to vesicles was to the reconstituted sodium channel protein and not the vesicle lipid, a thermal inactivation protocal was performed. Purified sodium channels were incubated at 36°C for the times indicated in Figure 21. The heated sodium channel preparation was then reconstituted using rat brain lipid and PC and both [^{3}H]STX and ^{125}I-LqTX binding were measured. The STX binding activity of the solubilized sodium channel is very sensitive to thermal inactivation, whereas the reconstituted material shows thermal stability (169). As shown in Figure 21, both [^{3}H]STX (O) and ^{125}I-LqTX (Δ) binding decay in parallel. Thus the specific LqTX binding to purified sodium channels reconstituted with brain lipids represents binding to the sodium channel protein.

The LqTX binding recovered after reconstitution with endogenous lipid was not affected by either membrane potential or occupany of the alkaloid toxin receptor site. Either the channel has yet to be reconstituted in the proper lipid environment or the residual Triton X-100 is a problem. Recent results of (193) indicate that bovine brain PC and PE can effectively substitute for the purified rat brain lipid, allowing reconstitution of LqTX binding. This approach is likely to lead to the recovery of voltage-dependent, alkaloid toxin-sensitive LqTX binding.

2.2.4-Sodium transport by the reconstituted sodium channel.

To demonstrate that the three polypeptides copurifying with STX binding activity also contain components necessary for ion transport, neurotoxin-activated Na^+ uptake by the reconstituted vesicles was examined. The time course of Na^+ uptake by the reconstituted vesicles is illustrated in Figure 22. In the absence of neurotoxins, the uptake is slow (O). With veratridine Ver (100 μM), the extent of Na^+ uptake was stimulated 8-fold (O), with half-maximal stimulation at 28 μM. This value is similar to that measured for Ver-activated Na^+ transport in synaptosomes (194). If 1 μM TTX was included both inside and outside the vesicles, the extent of the Ver-stimulated Na^+ uptake ( ) was reduced to the control level at the early time points. At longer times there was a small measurable uptake even in the presence of TTX. This uptake can be accounted for by reversible dissociation of TTX from a fraction of the activated channels, allowing Na^+ uptake at long incubation times.

2.2.5-Concentration dependence of TTX inhibition of Na^+ transport by the reconstituted sodium channel.

The extent of Ver-stimulated Na^+ uptake detected in the presence of increasing TTX concentrations is shown in Figure 23. In these vesicles ~ 40% of the reconstituted TTX binding sites faced the vesicle exterior (determined as described in section 2.2.4). TTX, which was present only on the extravesicular compartment, maximally inhibited 40% of the Ver-activated Na^+ uptake, as expected. The maximal percentage of inhibition of Na^+ uptake observed with externally added TTX was consistently equal to the fraction of right-side-

out-oriented TTX receptors. In this experiment, the K_I as 18 nM. The average value of the K_I of TTX was 14 nM ± 6 nM (S.D., n=3), similar to the 10 nM K_D for TTX binding to native channels in rat brain membranes (173).

2.2.6-Ionic selectivity of the reconstituted sodium channel.

A qualitative assessment of the ionic selectivity of the reconstituted channel can be obtained from the flux assay described (170). The Ver-activated sodium channels also transport RB^+ and Cs^+ with an apparent selectivity ratio with respect to Na^+ of 1.0:0.25:0.10.

2.2.7-The majority of the reconstituted sodium channels are functional.

To verify that only the three STX receptor subunits are sufficient for Na^+ transport in the reconstituted system, it is valuable to estimate the fraction of reconstituted STX receptors that bind LqTX and transport Na^+. If only 1% of the STX receptors transported Na^+, for example, it is conceivable that an "impurity" in the preparation representing 1% of total protein could be a sodium channel component required for ion transport.

The fraction of reconstituted STX receptor sites that bind LqTX toxin is readily calculated. Scatchard analysis of the binding indicates that 76% ± 6% (S.E.M) of the reconstituted channels which bind STX also bind LqTX of the fractionof STX binding sites that transport Na^+ can be estimated in two ways. First, the initial rates of $^{22}Na^+$ influx through Ver-activated sodium channels in synaptosomes and in reconstituted vesicles are compared under similar conditions. Sodium channels in rat brain synaptosomes transport Na^+ at a rate of 1.4×10^6 ions/min/STX binding site (194) as compared to 1.0×10^6 ions/min/STX binding site for the reconstituted channel. Accordingly, 70% of the reconstituted channels are active and transport sodium at comparable rates to sodium channels *in situ*. The fraction of STX binding sites associated with functional ion channels can also be calculated from the fraction of vesicular internal volume accessible to Ver-induced Na^+ efflux and the distributions of STX binding sites in the vesicles as desscribed in detail by (170). By this method, the fraction of STX binding sites representing functional sodium channels would range between 30% and 73% of the total STX receptor sites. Thus the two independent estimates of sodium channel ion transport activity indicate that a large fraction, up to 70%, of the reconstituted STX receptors contribute to the measured ion flux. This value is in agreement with the fraction of reconstituted STX binding sites that bind LqTX (76%). Since the sodium channel used for these reconstitution studies was ~ 90% pure by SDS gel electrophoresis, the complex of the α-, β1-and β2-subunits is sufficient for reconstitution of both neurotoxin-stimulated ion transport and LqTX binding.

3. RECONSTITUTION OF PURIFIED SODIUM CHANNELS IN PLANAR LIPID BILAYERS

3.1-Methods.

The basic procedurefor forming planar lipid bilayers from n-decane solutions of phospholipids across an aperture in a partition separting two aqueous compartments is described by Mueller et al. (195,196). The procedure for fusing

vesicles with planar bilayers was first described by Drachev et al. (197), applied to vesicles containing ion channels by Miller and Racker (198), elaborated on by Cohen et al (199,200) and used to incorporate sodium channels into bilayers by Krueger et al. (201).

3.1.1-Aperture fabrication.

The aperture across which the bilayer is formed is a critical component of the system. Its area controls the major source of noise - the capacitance of the bilayer. Smooth, circular apertures 30 - 300 µm in diameter are readily produced in a 25µm thick Teflon film (Yellow Springs Instruments #5775, Yellow Springs, OH) when an electrical spark generated by an automobile ignition coil is passed through the Teflon. The ignition coil, with its associated capacitor connected across its low voltage terminals, is connected to a 12 or 22 V battery through a potentiometer and a toggle switch. An automotive spark plug with its ground electrode removed makes a convenient high voltage electrode. It is necessary first to create a small defect in the Teflon film by poking it with a needle or the tip of a pulled glass rod; then support the Teflon so that it is approximately centered in a 2-5 mm gap between the high voltage and ground electrodes and discharge a spark through it by closing and opening the circuit between the battery and the coil. The size of the aperture is determined by the battery voltage and the number of sparks passed through the hole. A 12V battery produces a ~90 µm aperture with a single spark and both higher and lower voltages yield smaller holes. The spark vaporizes and melts the Teflon to create a smooth aperture that is an excellent support for stable, long-lasting bilayers.

3.1.2-Vesicle formation

Purified sodium channels are reconstituted into lipid vesicles composed of 35% bovine brain PE (Sigma) and 65% bovine brain PC (Sigma) by the procedure described in section 2.1.1, using 0.25-0.4 ml of BioBeads per ml of reconstitution mixture. The resulting vesicles are composed of 2 mg/ml PC, 1.05 mg/ml PE and 5-15 pmoles/ml STX receptor in 50 mM NaCl, 10 mM HEPES/Tris, pH 7.4, 0.5 mM $MgSO_4$ and 400 mM sucrose.

3.1.3-Experimental set-up.

The Tefon sheet containing the aperture is attached with silicone grease to a partition containing a 2 mm hole that separates two 450 µl chambers that have been milled from a block of Teflon. The small aperture reduces both the capacitance of the system and its microphonic noise pick-up. The Teflon block rests upon a battery-powered magnetic stirrer enclosed in a Faraday cage mounted on a vibration-free table. The *cis*-chamber contains 0.5 M NaCl and 1-5 µl of vesicles containing reconstituted purified sodium channels (5-75 fmoles) in medium A (10 mM HEPES/Na^+, pH 7.4, 0.15 mM $CaCl_2$, 0.1 mM $MgCl_2$ and 0.05 mM EGTA). The *trans*-chamber initially contains 0.2-0.4 M NaCl in medium A plus 1 µM BTX. The chambers are connected by Ag/AgCl pellet electrodes (In Vivo Metric Systems, Healdsburg, CA) to a List Medical Electronics EPC-7 patch clamp amplifier in voltage clamp mode. The EPC-5 amplifier does not work because of the high capacitance of the bilayer. The *trans*-electode is set to the command voltage

relative to the *cis* electrode, which is held at virtual ground. The EPC-7 output is filtered at 3 kHZ, monitored on an oscilloscope and recorded on a RACAL 4DS FM tape recorder. All experiments are performed at 21°C ± 2°C.

3.1.4-Bilayer formation

To form stable bilayers, the area of Teflon around the aperture is first thoroughly cleaned in hexane, then precoated on both sides with a thin film of 5% lipid in n-decane (Sigma) and dried for 3-5 min under a gentle stream of nitrogen. The precoating step is important: Not enough yields bilayers that spontaneously break in a few minutes; excess coating yields bilayers whose areas diminish over the course of several minutes, turning into thick (> 1,000 A) films. The chambers are filled with their aqueous solutions, a small amount of the 5% lipid solution is spread across the *cis* side of the aperture with a clean sable point brush (#2) from which most of the bristles have been removed. Voltage steps 0.1 - 1 mV in amplitude and 5 ms in duration are applied to the electrodes to monitor bilayer formation by capacitance change (196). A clean brush is then used to repeatedly wipe away the excess lipid solution until a bilayer is formed, as indicated by a large increase in capacitance. A few more brush strokes may be needed to increase the specific capacitance of the bilayer and torus to 0.25-0.35 $\mu F/cm^2$. An alternative method to form bilayers that works well for small apertures starts by spreading on a small amount of lipid solution on the *cis* side of the aperture with a brush and then using a clean brush to break the high resistance seal across the aperture. Carefully lowering the aqueous solution in the *cis*-chamber with a pipet until the parture is exposed to air and then slowly raising the solution to its original level forms a bilayer across the aperture. This may require several tries.

The lipid compositon of the bilayer is also important. We have used a mixture of 40 mg/ml 1-palmitoyl-2-oleoyl phosphatidylethanolamine (POPE) and 10 mg/ml 1-palmitoyl-2-oleoy- phosphatidylcholine (POPC) (Avanti Polar Lipids, Birmingham, AL) in n-decane, as suggested by Weiss (202), to form stable long-lasting bilayers. We have also used a nonoxidizable lipid, diphytanoyl phosphatidylcholine (Avanti Polar Lipids) as a 50 mg/ml solution in n-decane. This lipid works better for small apertures (< 100 μm diameter) because it thins to form the bilayer configuration more readily and vesicles are more likely to fuse with it. Bilayers of both types typically have high resistances (> 300 GΩ), are electrically stable between -150 mV and + 150 mV and will last several hours.

3.1.5-Channel incorporation into lipid bilayers.

The fusion approach is used to incorporate lipid vesicles containing purified sodium channels into planar lipid bilayers. After formation of a planar bilayer, vesicles containing reconstituted sodium channels are added to the *cis* chamber and the solutions in the *cis* and *trans* chambers are gently stirred for 3 min while maintaining an applied voltage (V) of 70 mV across the bilayer. The current through the bilayer is then examined at V=70 mV and -70 mV to determine whether any channels have been incorporated. If not, the bilayer capacitance is rechecked and the stirring step repeated until one or more channels are seen (171). Sodium channels are usually observed within 30 min when using 2 μl of vesicles, a 0.5 M $_{cis}$ -0.2 M_{trans} NaCl gradient and a POPE/POPC bilayer in a 220

μm aperture. Channel incorporation is stopped by eliminating the osmotic gradient across the bilayer with the addition of 4 M NaCl to the *trans* chamber to yield a final concentration of 0.5 M. In approximately 30% of the bilayers, under the conditions above, channel incorporation could be stopped with only one sodium channel in the bilayer. Decreasing the size of the bilayer, the *trans*-bilayer osmotic gradient, or the vesicle concentration will increase the percentage of single channel bilayers but will also prolong the time required before channel incorporation occurs.

3.1.6-Voltage convention

Since sodium channels are oriented randomly in the vesicles (section 2.2.2), their orientation in the bilayer is necessarily random. This could cause confusion when comparing a voltage-dependent property of channels oriented in opposite directions. To avoid this ambiguity, the voltage sensed by the channel is defined according to the electrophysiological convention (V= V"intracellular"side - V "extracellular" side). The "extracellular" side of a sodium channel can be readily determined by the sidedness of TTX block at the end of an experiment. Alternatively, the polarity of the applied voltage sensed as a hyperpolarization that closes a channel will also indicate its orientation. When both methods have been employed to determine the orientation of a channel, the results have always agreed (n=25).

3.2-Properties of purified sodium channels in planar lipid bilayers.

3.2.1-TTX sensitivity.

The most specific test of whether an ion channel in a planar lipid bilayer is a sodium channel is its susceptibility to block by TTX or STX. Figure 24 demonstrates that the ionic current through purified sodium channels is reversibly blocked by TTX in an orientation-dependent manner (171). The bilayer in Figure 24 contains four active channels. Prior examination of the polarity of the voltage that closes the channels by hyperpolarization indicated that there are three *cis*-facing channels and one *trans*-facing channel. Following addition of TTX to the *trans* chamber in Figure 24A, the one *trans*-facing sodium channel is blocked for the rest of the experiment, while the three *cis*-facing channels are unaffected. Addition of TTX to the *cis* side of the bilayer in Figure 24B reduced the current in three discrete steps to the value it had prior to channel incorporation as the three *cis*-facing channels are blocked. The intial segment of Figure 24C, on a 10-fold slower time scale, shows that the channels remain blocked as long as TTX is present. Following perfusion of the *cis* chamber to remove TTX, the three *cis*-facing channels reappear, demonstrating that TTX block is reversible. The TTX sensitivity of these single-channel events is unequivocal evidence that they are mediated by the sodium channel protein.

The concentration and voltage dependence of TTX block of purified BTX-activated sodium channels are presented in Table II. The concentration dependence of block is well described by a simple one-to-one binding curve. At -50 mV the K_I for TTX block is 8.3 nM, while at 70 mV the K_I is 135 nM (171). The voltage dependence of this shift in K_I corresponds to an e-fold increase in K_I

for each 43 mV depolarization. Similar values for the K_I of TTX block and its voltage dependence were found with synaptosomal sodium channels incorporated into planar bilayers by Krueger and French (personal communication) (Table III).

3.2.2-Channel oplening is voltage-dependent.

The next property of purified sodium channels evaluated in the planar bilayer system is the voltage dependence of gating in the presence of BTX. BTX should shift the voltage dependence of sodium channel activation in the hyperpolarized direction and eliminate inactivation. Figure 25 shows the single channel current through a BTX-modified purified sodium channel at the holding potentials indicated. The excellent time resolution and low noise (0.3 pA RMS noise at 3kHz) of these records approach those of patch recording and are examples of what can be achieved using small membrane areas. In the first current record, at -135 mV, the channel is closed nearly all of the time except for a few brief openings indicated by downward deflections. At more positive voltages, the channel spends an increasing fraction of time open. The voltage at which the channel is open 50% of the time (V_{50}) is -95 mV. At -55 mV and more positive voltages, the channel is open most of the time, with occasional closures. As expected for a BTX-modified channel, it does not inactivate.

For purified sodium channels the average value of V_{50} is -91 mV 1 17 mV (S.E.M. n=22) (171). This S.E.M. is in good agreement with the V_{50} of: -93 mV for BTX-modified synaptosomal sodium channels in planar bilayers (203), -94 mV for BTX-modified rat sarcolemmal sodium channels in planar bilayers (204), -90 mV for BTX-modified sodium channels in frog node of Ranvier (175), and -85 for BTX-modified sodium channels in NG-108-15 neuroblastoma cells (176). The V_{50} of purified sodium channels varies from channel to channel. For most of the channels, V_{50} is between -80 mV and -105 mV, with the extreme values being -130 mV and -64 mV. Figure 25A shows the voltage dependence of channel opening for three different channels selected because of their widely differing V_{50} values. Channel opening is steeply voltage-dependent over a limited voltage range for each channel. The curves are parallel to each other and shifted along the voltage axis. Figure 26B shows a linear transformation (203) of these curves whose slope is proportional to the apparent gating charge (q) of the sodium channel. Despite the differences in V_{50}, the apparent gating charge for each of these three channels is essentially the same. The apparent gating charge for purified BTX-modified sodium channels is 3.8 ± 0.3 (S.E.M. n=5) electronic charges (171). Similar values of q were found for BTX-modified sodium channels from frog node of Ranvier, 3.5 (175), rat brain, 4-6 (203), and NG-108-15 neuroblastoma cells, 4-5 (177). The agreement for the values of q and the average V_{50} between purified reconstituted sodium channels and native sodium channels is evidence that the voltage sensing and gating mechanisms are present and functionally intact in the purified protein. However, the variation of V_{50} needs to be addressed.

What is the origin of the variation in V_{50} from channel to channel? The trivial explanation of an uncompensated electrode offset potential can be ruled by experiments showing that the reversal potential for the Na^+ current is always within 1 or 2 mV of the calculated Nernst potential for Na^+. The fact that the voltage dependence curves are parallel (Fig. 26) rules out the possibility that

the channels are incorporated into the bilayer so that they sense only a fraction of the applied electric field. Lipid surface charge effects are unlikely, since these experiments are conducted with symmetric bilayers of uncharged lipids in solutions with symmetric ionic compositions. Is the variability due to alteration of the channel protein during its purification? Probably not, because similar results were obtained with BTX-modified sodium channels incorporated into planar bilayers from native membranes (202,204) and with patch-clamped BTX-modified sodium channels in neuroblastoma cells (177). At present, we favor the possibility that the variation in V_{50} reflects a naturally occurring heterogeneity in the sodium channel population, perhaps arising from variations in fixed charge on or near the voltage-sensing mechanism. The planar bilayer system is ideally suited for investigations of possible biochemical mechanisms modifying the voltage dependence of sodium channels in a well-defined environment.

3.2.3-Progress towards voltage-dependent activation.

A major objective of this research is the examination of voltage-dependent activation and inactivation of purified sodium channels in the absence of BTX. The high capacitance associated with bilayers in 220 μm apertures in which the initial results were obtained precluded the observation of channel opening after a depolarizing voltage step. A large, slowly decaying capacitive current saturates the amplifier for 5 ms after the change of voltage. Reducing this capacitive transient has been the impetus behind examining bilayers in small apertures. With diphytanoyl PC/decane bilayers in 70 μm apertures, 30 mV steps result in the loss of only the first 0.3 ms of data when the capacitance cancellation circuity in the EPC-7 is used. Digital subtraction techniques can further reduce this loss. Since the electrical noise of these bilayers is low (Fig. 25), the current can be filtered at 3 kHz, which would allow channel openings as short as 300 μs to be clearly resolved from the noise.

Channel activity in the absence of BTX has not yet been observed. Either nonfunctional channels are being incorporated into the bilayer, or, in the absence of BTX, sodium channels are not incorporated into the bilayer under the conditions used. The following experiment favors the second possibility. Under conditions chosen to promote fusion (5 μl) of vesicles, a 0.5 M_{cis} - 0.2 M *trans* NaCl gradient and a diphytanoyl PC bilayer in 220 μm aperture), we attempted to incorporate sodium channels into the bilayer, using the procedure described in section 3.1.5, in the absence of BTX for 1 h (0.5 μl of ethanol was added in place of the solution of BTX in ethanol). To stop any additional fusion, concentrated NaCl was then added to the *trans*-chamber, yielding a final concentration of 0.5 M. To determine whether any sodium channels had been incorporated during the 1 h incubation, BTX (1 μM final *trans*) was added and the current through the bilayer was monitored ror 30 min. No sodium channels were seen. The contents of the *trans*-chamber were then diluted with distilled water to a final concentration of 0.3 M NaCl. In each of four separate experiments, sodium channels (1 to 3) were then seen within 10 min. These results clearly indicate that BTX is required for vesicle fusion under these conditions. Whether BTX promotes fusion by increasing the osmotic gradient across the vesicle bilayer by increasing its sodium permeability or by causing a hydrophobic surface on the

sodium channel to become exposed is not known. We are currently examining other methods of promoting channel incorporation into the bilayer to allow us to study the purified sodium channel in the absence of BTX.

3.2.4-Single-channel conductance and ionic selectivity.

Purified sodium channels are selectively permeable to Na^+. This is evident from the single-channel current-voltage curves for Na^+, K^+ and Rb^+ in Figure 27 (171). The average single-channel conductance (γ) in 0.5 M solutions of these ions is γ_{Na^+} = 25.2 pS ± 0.5 pS (S.E.M. n=10), γ_{K^+} = 3.5 pS ± 0.2 pS (S.E.M. n=3), and γ_{Rb^+} = 1.2 pS ± 0.1 PS. (S.E.M. n=3). The single-channel conductance for Na^+ of 25.2 pS is a little lower than the 30 pS found (201), and a bit higher than the 24 pS found (204) for native rat brain sodium channels incorporated into planar bilayers and activated by BTX. The permeability ratios of K^+ and Rb^+ relative to Na^+ are 0.14 ± 0.02 and 0.05 ± 0.01, respectively. These permeability ratios agree well with the permeability ratios directly measured from ion flux determinations with BTX-activated sodium channels in N18 neuroblastoma cells (P_{K+} = 0.17 and P_{Rb^+} = 0.08 (205), and sodium channels purified from rat muscle (P_{K+} = 0.14 and P_{Rb^+} = 0.02 (191). This agreement is not as good with the relative permeability of K^+ (0.07) (201), determined from reversal potential measurements on BTX-activated rat brain sodium channels in planar bilayers. The relative permeability of sodium channels calculated from reversal potential measurements varies with the ionic composition of the medium (206), which may account for this difference.

4. CONCLUSIONS

The functional properties of purified sodium channels from rat brain reconstituted into lipid vesicles and planar lipid bilayers are compared with those of native rat brain sodium channels in Table II. The functional characteristics of the purified sodium channel are comparable to those of the native sodium channel in nearly evfery aspect tested. Of particular importance is the finding that a large fraction of the STX binding sites are associated with functional ion channels (170). This rules out the possibility that trace amounts of other polypeptides are involved in sodium channel function. In addition, it indicates that the sodium channels sampled in the planar bilayer studies are likely to be prepresentative of the whole population. The conclusion from the reconstitution studies in both lipid vesicles and planar bilayers is clear. The complex of α-, β1- and β2-subunits that make up the purified STX binding protein contains functional binding sites for TTX, LqTX, BTX and Ver and forms a functional ion-conducting pore that exhibits both the ionic selectivity and the voltage-dependent gating of the native sodium channel in the presence of BTX. Thus the α- β1- and β2-subunits are sufficient to account for the entire structure of the sodium channel from rat brain.

The initial goal of reconstitution, to establish whether all the functional elements of the sodium channel are in the purified protein, has now been achieved. The immediate objectives are to determine which subunits and domains of subunits are involved in opening and closing the channel, forming its structure, and governing its voltage regulation. Moreover, reconstitution techniques provide an especially sensitive assay to investigate the influences of

the lipid environment on sodium channel function. It is anticipated that the combination of recombinant DNA technology to modify the gene(s) encoding the sodium channel (207), biochemical alterations of purified sodium channels and rconstitution studies as described here will prove valuable in pursuing an understanding of how voltage controls the gating of this channel protein.

LITERATURE CITED

1. Changeux, J.-P. (1981) The acetylcholine receptor: An allosteric membrane protein. *Harvey Lect.* 75:85-254.

2. Changeux, J.-P., Devillers-Thiery, A. and Chemouilli, P. (1984) Acylcholine receptor: an allosteric protein. *Science* (Washington, D.C.) 225: 1335-1345.

3. Anholt, R., Lindstrom, J. and Montal, M. (1984) The molecular basis of neurotransmission: Structure and function of the nicotinic acetylcholine receptor, in: *The Enzymes of Biological Membranes* (A. Martonosi, ed.) Plenum Press, New York, Second Ed. 3: 335-401.

4. Karlin, A. (1980) Molecular properties of nicotinic acetylcholine receptors, in: *The Cell Surface and Neuronal Function*, (G. Poste, G. Nicholson and C. Cotman, eds.) Elsevier/North Holland Biomedical Press, New York, pp. 191-260.

5. Conti-Tronconi, B.M. and Raftery, M.A. (1982) The nicotinic cholinergic receptor: Correlation of molecular structure with functional properties. *Ann. Rev. Biochem.* 51: 491-530.

6. Reynolds, J.A., and Karlin, A. (1978) Molecular weight in detergent solution of acetylcholine receptor from *Torpedo californica* . *Biochemistry* 17:2035-2038.

7. Lindstrom, J., Merlie, J. and Yogeeswaran, G. (1979) Biochemical properties of acetylcholine receptor subunits from *Torpedo californica*. *Biochemistry* 18: 4465-4470.

8. Raftery, M.A., Hunkapiller, M.W., Strader, C.D. and Hood, L.E. (1980) Acetylcholine receptor: Complex of homologous subunits. *Science* 208:1454-1457.

9. Raftery, M.A., Dunn, S.M.J., Conti-Tronconi, B.M., Middlemas, D.S. and Crawford, R.D. (1983) The nicotinic acetylcholine receptor: Subunit structure, functional binding sites and ion transport properties. *Cold Spring Harbor Symp. Quant. Biol.* 48: 21-33.

10. Noda, M., Takahashi, H., Tanabe, T., Toyosato, M., Kikotani, S., Furutani, Y., Hirose, T., Takashima, H., Inayama, S., Miyata, T., and Numa, S. (1983) Structural homology of *Torpedo californica* acetylcholine receptor subunits. *Nature* 302: 528-532.

11. Damle, V., McLaughlin, M. and Karlin, A. (1978) Bromoacetylcholne as an affinity label of the acetylcholine receptor from *Torpedo californica*. *Biochem. Biophys. Res. Commun.* 84: 845-851.

12. Weill, C.L., McNamee, M.G. and Karlin, A. (1974) Affinity labeling of purified acetylcholine receptor from *Torpedo californica*. *Biochem. Biophys. Res. Commun.* 61:997-1003.

13. Karlin, A., Cox, R., Kaldany, R.-R., Lobel, P. and Holtzman, E. (1983) The arrangement and funtions of the chains of the acetylcholine receptor of *Torpedo* electric tissue. *Cold Spring Harbor Symp. Quant. Biol.* 48: 1-8.

14. Kao, P.W., Dwork, A.J., Kaldany, R.R.-J., Silver, M.L., Wideman, J., Stein, S. and Karlin, A. (1984) Identification of the α subunit half-cystine specifically labeled by an affinity reagent for the acetylcholine receptor binding site. *J. Biol. Chem.* 259: 11662-11665.

15. Chang, H.W. and Bock, E. (1977) Molecular forms of the acetylcholine receptor: Effects of calcium ions and a sulfhydryl reagent on the occurrence of oligomers. *Biochemistry* 16: 4513-4520.

16. Hamilton, S.L., McLaughlin, M. and Karlin, A. (1979) Formation of disulfide-linked oligomers of acetylcholine receptor in membrane from *Torpedo* electric tissue. *Biochemistry* 18: 155-163.

17. Tarrab-Hazdai, R., Geiger, B., Fuchs, S. and Amsterdam, A. (1978) Localization of acetylcholine receptor in excitable membrane from the electric organ of *Torpedo*: Evidence for the exposure of receptor antigenic sites on both sides of the membrane. *Proc. Natl. Acad. Sci. USA* 75: 2497-2501.

18. Strader, C.B.D., Revel, J.-P. and Raftery, M.A. (1979) Demonstration of the transmembrane nature of the acetylcholine receptor by labeling with anti-receptor antibodies. *J. Cell. Biol.* 83: 499-510.

19. Wennogle, L.P. and Changeux, J.-P. (1980) Transmembrane orientation of proteins present in acetylcholine receptor-rich membranes from *Torpedo marmorata* studied by selective proteolysis. *Eur. J. Biochem.* 106: 381-393.

20. Strader, C.D. and Raftery, M.A. (1980) Topographic studies of *Torpedo* acetylcholine receptor subunits as a transmembrane complex. *Proc. Natl. Acad. Sci. USA* 77: 5807-5811.

21. Froehner, S.C. (1981) Identification of exposed and buried determinants of the membrane-bound acetylcholine receptor from *Torpedo californica* *Biochemistry* 20: 4905-4915.

22. Noda, M., Takahashi, H., Tanabe, T., Toyosato, M., Fusutani, Y., Hirose, T., Asai, M., Inayama, S., Miyata, T. and Numa, S. (1982) Primary structure of α-subunit precursor of *Torpedo californica* acetylcholine receptor deduced from cDNA sequence. *Nature* 299:793-797.

23. Noda, M., Takahashi, H., Tanabe, T., Toyosato, M., Kikyotani, S., Hirose, T., Asai, M., Takashima, H., Inayama, S., Miyata, T. and Numa, S. (1983) Primary structures of α-subunit precursors of *Torpedo californica* acetylcholine receptor deduced from cDNA sequences. *Nature* 301:251-255.

24. Claudio, T., Ballivet, M., Patrick, J. and Heinemann, S. (1983) Nucleotide and deduced amino acid sequences of *Torpedo californica* acetylcholine receptor α subunit. *Proc. Natl. Acad. Sci. USA* 80: 1111-1115.

25. Devilliers-Thiery, A., Giraudat, J., Bentaboulet, M. and Changeux, J.P. (1983) Complete mRNA coding sequence of the acetylcholine binding α-subunit of *Torpedo marmorata* acetylcholine receptor: A model for the transmembrane organization of the polypeptide chain. *Proc. Natl. Acad. Sci. USA* 80:2067-2071.

26. Guy, H.R. (1984) A structural model of the acetylcholine receptor channel based on partition energy and helix packing calculations. *Biophys. J.* 45: 249-261.

27. Fairclough, R.H., Finer-Moore, J., Love, R.A., Kristofferson, D., Desmeules, P.J. and Stroud, R.M. (1983) Subunit organization and structure of an acetylcholine receptor. *old Spring Harbor Symp. Quant. Biol.* 48: 9-20.

28. Finer-Moore, J. and Stroud, R.M. (1984) Amphipathic analysis and possible fomation of the ion-channel in an acetylcholine receptor. *Proc. Natl. Acad. Sci. USA* 81: 155-159.

29. Young, E.F., Ralston, E., Blake, J., Ramachandran, J., Hall, Z.W. and Stroud, R.M. (1985) Topological mapping of acetylcholine receptor: Evidence for a model with five transmembrane segments and a cytoplasmic COOH-terminal peptide. *Proc. Natl. Acad. Sci. USA* 82: 626-630.

30. Criado, M., Hochschwender, S., Sarin, V., Fox, L.J. and Lindstrom, J. (1985) Evidence for unpredicted transmembrane domains in acetylcholine receptor subunits. *Proc. Natl. Acad. Sci. USA* 82:2004:2008.

31. Lindstrom, J., Criado, M., Hochschwender, S., Fox, J.L. and Sarvin, V. (1984) Immunochemical tests of acetylcholine receptor subunit models. *Nature* 311: 573-575.

32. Elliott, J., Blanchard, S.G., Wu, W., Miller, J., Strader, C.D., Hartig, P., Moore, H.-P., Racs, J. and Raftery, M.A. (1980) Purification of *Torpedo californica* postsynaptic membranes and fractionation of their constituent proteins. *Biochem. J.* 185: 667-677.

33. Neubig, R.R., Krodel, E.K., Boyd, N.D. and Cohen, J.B. (1979) Acetylcholine and local anesthetic binding to *Torpedo* nicotinic postsynaptic membranes after removal of nonreceptor peptides. *Proc. Natl. Acad. Sci. USA* 76: 690-694.

34. Moore, H.-P., Hartig, P.R. and Raftery, M.A. (1979) Correlation of polypeptide commposition with functional events in acetylcholine receptor-enriched membranes from *Torpedo californica*. *Proc. Natl. Acad. Sci. USA* 76: 6265-6269.

35. Elliott, J., Dunn, S.M.J., Blanchard, S.G. and Raftery, M.A. (1979) Specific binding of perhydrohistrionicotoxin to *Torpedo* acetylcholine receptor. *Proc. Natl. Acad. Sci. USA* 76: 2576-2579.

36. Barrantes, F.J., Neugebauer, D.-Ch. and Zingsheim, H.P. (1980) Peptide extraction by alkaline treatment is accompanied by reangement of the membrane bound acetylcholine receptor from *Torpedo marmorata*. *FEBS Lett.* 112: 73-78.

37. Kagawa, Y. and Racker, E. (1971) Partial resolution of the enzymes catalyzing oxidative phosphorylation: XXV Reconstitution of vesicles catalyzing ^{32}Pi-ATP exchange. *J. Biol. Chem.* 246:5477-5487.

38. Karlsson, E., Arnberg, H. and Eaker, D. (1971) Isolation of the principal neurotoxins of two *INaja naja* subspecies. *Eur. J. Biochem.* 21: 1-16.

39. Oakley, B.R., Kirsch, D.R. and Morris, N.R. (1980) A simplified ultrasensitive silver stain for detecting proteins in polyacrylamide gels. *Anal. Biochem.* 105: 361-363.

40. Lindstrom, J., Einarson, B. and Tzartos, S. (1981) Production and assay of antibodies to acetylcholine receptors, in: *Methods in Enzymology: Immunochemical Techniques,* 74: 432-460.

41. Ravdin, P.M. and Berg, D.K. (1979) Inhibition of neuronal acetylcholine sensitivity by α-toxins from *Bungarus multicinctus* venom. *Proc. Natl. Acad. Sci.*76: 2072-2076.

42. Lindstrom, J., Lennon, V., Seybold, M. and Whittingham, S. (1976) Experimental autoimmune myasthenia gravis and myasthenia gravis: Biochemical and immunochemical aspects. *Ann. N.Y. Acad. Sci.*274: 254-274.

43. Lowry, O.H., Rosebrough, N.Y., Farr, A.L. and Randall, R.Y. (1951) Protein measurement with the Folin phenol reagent. *J. Biol. Chem.*193: 265-275.

44. Anholt, R., Fredkin, D.R., Deerinck, T., Ellisman, M., Montal, M. and Lindstrom, J. (1982) Incorporation of acetylcholine receptors into liposomes: Vesicle structure and acetylcholine receptor function. *J. Biol. Chem.* 257:7122-7134.

45. Lindstrom, J., Anholt, R., Einarson, B., Engel, A., Osame, M. and Montal, M. (1980) Purification of acetylcholine receptors, reconstitution into lipid vesicles, and study of agonist-induced cation channel regulation. *J. Biol. Chem.* 255:8340-8350.

46. Gasko, O.D., Knowles, A.F., Shertzer, H.G., Snolinna, E.M. and Racker, E. (1976) The use of ion-exchange resins for studying ion transport in biological systems. *Anal. Biochem.* 72: 57-65.

47. Montal, M., Darszon, A., and Schindler, H. (1981) Functional reassembly of membrane proteins in planar lipid bilayers. *Quart. Rev. Biophys.* 14:1-79.

48. Montal, M. (1986) Functional reconstitution of membrane proteins in planar lipid bilayer membranes. In: *echniques for Analysis of Membrane Proteins* (C.I. Ragan and R. Cherry, eds.) United Kingdon, Chapman and Hall Chapter 5, 97-128.

49. Schindler, H. and Feher, G. (1976) Branched bimolecular lipid membranes. *Biophys. J.* 16: 1109-1113.

50. Montal, M. (1974) Formation of bimolecular membranes from lipid monolayers. *Meth. Enzymol.*32:545-556.

51. Miller, C. and White, M.M. (1984) Dimeric structure of single chloride channels from *Torpedo electroplax. Proc. Natl. Acad. Sci. USA* 81: 2772-2775.

52. Hamill, O.P., Marty, A., Neher, E., Sakmann, B. and Sigworth, F. (1981) Improved patch-clamp techniques for high resolution current recording from cells and cell-free patches. *Pfluegers Arch. Eur. J. Physiol.* 391: 85-100.

53. Montal, M. and Mueller, P. (1972) Formation of bimolecular membranes from lipid monolayers and a study of the electrical properties. *Proc. Natl. Acad. Sci. USA* 69:3561-3566.

54. Wilmsen, V., Methfessel, C., Hanke, N. and Boheim, G. (1983) Channel current fluctuation studies with solvent-free lipid bilayers using Neher-Sakmann pipettes, in: *Physical Chemistry of Transmembrane Ion Motions* (G. Spach, ed.) pp. 479-485. Elsevier Science Publishers, B.V. Amsterdam.

55. Suarez-Isla, B.A., Wan, K., Lindstrom, J. and Montal, M. (1983) Single channel recordings from purified acetylcholine receptors reconstituted in bilayers formed at the tip of patch pipets. *Biochemistry* 22:2319-2323.

56. Schuerholz, Th. and Schindler, H. (1983) Formation of lipid-protein bilayers by micropipette-guided contact of two monolayers. *FEBS Lett.* 152: 187-190.

57. Coronado, R. and Latorre, R. (1983) Phospholipid bilayers made from monolayers on patch-clamp pipettes. *Biophys. J.* 43:231-236.

58. Labarca, P., Lindstrom, J. and Montal, M. (1984) Acetylcholine receptor in planar lipid bilayers: Characterization of the channel properties of the purified nicotinic acetylcholine receptor from *Torpedo califonrnica* reconstituted in planar lipid bilayers. . *Gen. Physiol.* 83: 473-496.

59. Labarca, P., Rice, J., Fredkin, D. and Montal, M. (1985) Kinetic analysis of channel gating: Application to the cholinergic receptor channel and to the chloride channel from *Torpedo californica. Biophys. J.* 47: (April issue).

60. Labarca, P., Montal, M.S., Lindstrom, J. and Montal, M. (1985) The occurrence of long openings in the purified cholinergic receptor channel increases with acetylcholine concentration. *J. Neurosci.* 5:3409-3413.

61. Hamamoto, T. and Montal, M. (1985) Functional reconstitution of bacterial cytochrome oxidases in planar lipid bilayers. *Methods in Enzymology,* Vol. 96, part II (S. Fleischer and B. Fleischer, eds.) Academic Press, N.Y. Chapter 12, 123-138.

62. Labarca, P., Lindstrom, J. and Montal, M. (1984) The acetylcholine receptor channel from *Torpedo californica* has two open states. *J. Neurosci.* 4: 502-507.

63. Anholt, R. (1981) Reconstitution of acetylcholine receptors in model membranes. *rends Biochem. Sci.*6: 288-291.

64. McNamee, M.G. and Ochoa, E.L.M. (1982) Reconstitution of acetylcholine receptor function in model membranes. *Neuroscience* 7: 2305-2319.

65. Anholt, R., Montal., M. and Lindstrom, J. (1983) Incorporation of acetylcholine receptors in model membranes: An approach aimed at studies of the molecular basis of neurotransmission. *Peptide and Protein Reviews,* (Hearn, M. ed.) 1: 95-137.

66. Epstein, M. and Racker, E. (1978) Reconstitution of carbamylcholine-dependent sodium ion flux and desensitization of the acetylcholine receptor from *orpedo californica. J. Biol. Chem.* 253:6660-6662.

67. Huganir, R.L., Schell, M.A., Racker, E. (1979) Reconstitution of the purified acetylcholine receptor from *Torpedo californica. FEBS (Fed. Eur. Biochem. Soc.) Lett.* 108: 155-160.

68. Huganir, R.L. and Racker, E. (1982) Properties of proteoliposomes reconstituted with acetylcholine receptor from *Torpedo californica. J. Biol. Chem.* 257: 9372-9378.

69. Changeux, J.-P., Heidmann, T., Popot, J. and Sobel, A. (1979) Reconstitution of a functional acetylcholine regulator under defined conditions. *FEBS Lett.* 105: 181-187.

70. Anholt, R., Lindstrom, J. and Montal, M. (1981) Stabilization of acetylcholine receptor channels by lipids in cholate solution and during reconstitution in vesicles. *J. Biol. Chem.* 256:4377-4387.

71. Popot, J.-L., Cartaud, J. and Changeux, J.-P. (1981) Reconstitution of a functional acetylcholine receptor: Incorporation into artificial lipid vesicles and pharmacology of the agonist-controlled permeability changes. *Eur. J. Biochem.* 118: 203-214.

72. Wu, W.C.S. and Raftery, M.A. (1979) Carbamylcholine-induced rapid cation efflux from reconstituted membrane vesicles containing purified acetylcholine receptor. *Biochem. Biophys. Res. Commun.* 89: 26-35.

73. Heidmann, T., Sobel, A., Popot, J.-L. and Changeux, J.-P. (1980) Reconstitution of a functional acetylcholine receptor: Conservation of the conformational and allosteric transitions and recovery of the permeability response role of lipids. *Eur. J. Biochem.* 110: 35-55.

74. Sobel, A., Weber, M. and Changeux, J.-P. (1977) Large-scale purification of the acetylcholine receptor protein in its membrane-bound and detergent-extracted forms from *Torpedo marmorata* electric organ. *Eur. J. Biochem.* 80: 215-224.

75. Cartaud, J., Sobel, A. Rousselet, A., Devaux, P. and Changeux, J.-P. (1981) Consequences of alkaline treatment for the ultra-structure of the acetylcholine receptor-rich membranes from *Torpedo marmorata* electric organ. *J. Cell. Biol.* 90: 418-426.

76. Sealock, R. (1982) Visualization at the mouse neuromuscular junction of a submembrane structure in common with *Torpedo* postsynaptic membranes. *J. Neurosci.* 2: 918-923.

77. Froehner, S.C., Gulbrandsen, V., Hyman, C. Jeng, A.Y., Neubig, R.R. and Cohen, J.B. (1981). Immunofluorescence localization at the mammalian neuromuscular junction of the M_r 43,000 protein of *Torpedo* postsynaptic membranes. *Proc. Natl. Acad. Sci. USA* 78: 5230-5234.

78. Gysin, R., Wirth, M. and Flanagan, S.D. (1981) Structural heterogeneity and subcellular distribution of nicotinic synapse-associated proteins. *J. Biol. Chem.* 256: 11373-11376.

79. St. John, P.A., Froehner, S.C., Goodenough, D.A. and Cohen, J.B. (1982) Nicotinic postsynaptic membranes from *Torpedo*: Sidedness, permeability to macromolecules, and topography of major polypeptides. *J. Cell Biol.* 92: 333-342.

80. Gonzalez-Ros, J.M., Paraschos, A. and Martinez-Carrion, M. (1980) Reconstitution of functional membrane-bound acetylcholine receptor from isolated *Torpedo californica* receptor protein and electroplax lipids. *Proc. Natl. Acad. Sci. USA* 77: 1796-1800.

81. Shah, D.O. and Schulman, J.M. (1967) Enzymic hydrolysis of various lecithin monolayers employing surface pressure and potential technique. *J. Colloid Interface Sci.* 25: 107-119.

82. Weber, M., David-Pfeuty, T. and Changeux, J.-P. (1975) Regultion of binding properties of the nicotinic receptor protein by cholinergic ligands in membrane fragments from *Torpedo marmorata*. *Proc. Natl. Acad. Sci. USA* 72: 3443-3447.

83. Lee, T., Witzemann, V., Schimerlik, M. and Raftery, M.A. (1977) Cholinergic ligand induced affinity changes in *Torpedo californica* acetylcholine receptor. *Arch. Biochem. Biophys.* 183: 57-63.

84. Weiland, G. and Taylor, P. (1979) Ligand specificity of state transitions in the cholinergic receptor: Behavior of agonists and antagonists. *Mol. Pharmacol.* 15: 197-212.

85. Sine, S. and Taylor, P. (1979) Functional consequences of agonist-mediated state transitions in the cholinergic receptor. *J. Biol. Chem.* 254: 3315-3325.

86. Boyd, N.D. and Cohen, J.B. (1980) Kinetics of binding of [^{3}H]-acetylcholine and ^{3}[H]-carbamylcholine to *Torpedo* postsynaptic membranes: Slow conformational transitions of the cholinergic receptor. *Biochemistry* 19: 5344-5353.

87. Boyd, N.D. and Cohen, J.B. (1980) Kinetics of binding of [^{3}H]-acetylcholine to *Torpedo* postsynaptic membranes: Association and dissocation rate constants by rapid mixing and ultrafiltration. *Biochemistry* 19: 5353-5358.

88. Cash, D.J., Aoshima, H. and Hess, G.P. (1981) Acetylcholine-induced cation translocation across cell membranes and inactivation of the acetylchol'ne receptor: Chemical kinetic measurements in the millisecond time region. *Proc. Natl. Acad. Sci. USA* 78: 3318-3322.

89. Moore, H.-P.H. and Raftery, M.A. (1980) Direct spectroscopic studies of cation translocation by *Torpedo* acetylcholine receptor on a time scale of physiological relevance. *Proc. Natl. Acad. Sci. USA* 77: 4509-4513.

90. Sakmann, B., Patlak, J., and Neher, E. (1980) Single acetylcholine-activated channels show burst-kinetics in presence of desensitizing concentrations of agonist. *Nature* 286:71-73.

91. Neubig, R.R. and Cohen, J.B. (1980) Permeability control by cholinergic receptors in *Torpedo* postsynaptic membranes: Agonist dose-response relations measured at second and millisecond times. *Biochemistry* 19: 2770-2779.

92. Walker, J.W., McNamee, M.G., Pasquale, E., Cash, D.J. and Hess, G.P. (1981) Acetylcholine receptor inactivation in *Torpedo californica* electroplax membrane vesicles: Detection of two processes in the millisecond and second time regions. *Biochem. Biophys. Res. Commun.* 100: 86-90.

93. Walker, J.W., Takeyasu, K. and McNamee, M.G. (1982) Activation and inactivation kinetics of *Torpedo californica* acetylcholine receptor in reconstituted membranes. *Biochemistry* 21: 5384-5389.

94. Magleby, K.L. and Pallotta, B.S. (1981) A study of desensitization of acetylcholine receptors using nerve-released transmitter in the frog. *J. Physiol. (London)* 316: 225-250.

95. Barrantes, F.J. (1978) Agonist-mediated changes of the acetylholine receptor in its membrane environment. *J. Mol. Biol.* 124: 1-26.

96. Heidmann, T. and Changeux, J.-P. (1979) Fast kinetic studies on the interaction of a fluorescent agonist with the membrane-bound acetylcholine receptor from *Torpedo marmorata*. *Eur. J. Biochem.* 94: 255-279.

97. Sine, S.M. and Taylor, P. (1980) The relationship between agonist occupation and the permeability response of the cholinergic receptor revealed by bound cobra α-toxin. *J. Biol. Chem.* 255: 10144-10156.

98. Schindler, H., Spillecke, F. and Neumann, E. (1984) Different channel properties of *Torpedo* acetylcholine receptor monomers and dimers reconstituted in planar membranes. *Proc. Natl. Acad. Sci. USA* 81: 6222-6226.

99. Anholt, R., Lindstrom, J. and Montal, M. (1980) Functional equivalence of monomeric and dimeric forms of purified acetylcholine receptor from *orpedo californica* in reconstituted lipid vesicles. *Eur. J. Biochem.* 109:481-487.

100. Wu, W.C.S. and Raftery, M.A. (1981) Functional properties of acetylcholine receptor monomeric and dimeric forms in reconstituted membranes. *Biochem. Biophys. Res. Commun.* 99: 436-444.

101. Wu, W.C.S., Moore, H.-P. and Raftery, M.A. (1981) Quantitation of cation transport by reconstituted membrane vesicles containing purified acetylcholne receptor. *Proc. Natl. Acad. Sci. USA* 78: 775-779.

102. Huganir, R.L. and Racker, E. (1980) Endogenous and exogenous proteolysis of the acetylcholine receptor from *Torpedo californica*. *J. Supramol. Struct.* 14: 215-221.

103. Criado, M. and Barrantes, F.J. (1984) Conversion of acetylcholine receptor dimers to monomers upon depletion of non-receptor peripheral proteins. *Biochim. Biophys. Acta* 798: 374-381.

104. Merlie, J.P. and Sebbane, R. (1981) Acetylcholine receptor subunits transit a precursor pool before aquiring α-bungarotoxin binding activity. *J. Biol. Chem.* 256: 3605-3608.

105. Merlie, J.P., Sebbane, R., Tzartos, S. and Lindstrom, J. (1982) Inhibition of glycosylation with tunicamycin blocks assembly of newly synthesized acetylcholine receptor subunits in muscle cells. . *Biol. Chem.* 257: 2694-2701.

106. Haggerty, J.G. and Froehner, S.C. (1981) Restoration of ^{125}I-α-Bungarotoxin binding activity to theα subunit of *Torpedo* acetylcholine receptor isolated by gel electrophoresis in sodium dodecyl sulfate. *J. Biol. Chem.* 256: 8294-8297.

107. Gershoni, J.M., Palade, G.E., Hawrot, E., Klimowicz, D.W. and Lentz, T.L. (1982) Analysis of α-bungarotoxin binding to *Torpedo* acetylcholine receptor by electrophoretic transfer techniques. *J. Cell Biol.* 95: 422a.

108. Tzartos, S.J. and Changeux, J.-P. (1983) High affinity binding of α-bungarotoxin to the purified α-subunit and to its 27,000-dalton proteolytic peptide from *Torpedo marmorata* acetylcholine receptor: Requirement for sodium dodecyl sulfate. *EMBO J.* 2: 381-387.

109. Mishina, M., Kurosaki, T., Tobimatsu, T., Morimoto, Y., Noda, M., Yamamoto, T., Terao, M., Lindstrom, J., Takahashi, T., Kuno, M. and Numa, S. (1984). Expression of functional acetylcholine receptor from cloned cDNAs. *Nature* 307: 604-608.

110. Kilian, P.L., Dunlap, C.R., Mueller, P., Schell, M.A., Huganir, R.L. and Racker, E. (1980) Reconstitution of acetylcholine receptor from *Torpedo californica* with highly purified phospholipids: Effects of α-tocopherol, phylloquinone and other terpenoid quinones. *Biochem. Biophys. Res. Commun.* 93: 409-414.

111. Dalziel, A.W., Rollins, E.A. and McNamee, M.G. (1980) The effect of cholesterol on agonist-induced flux in reconstituted acetylcholine receptor vesicles. *FEBS Lett.* 122: 193-196.

112. McNamee, M.G., Ellena, J.F. and Dalziel, A.W. (1982) Lipid-protein interactions in membranes containing the acetylcholine receptor. *Biophys. J.* 37: 103-104.

113. Ochoa, E.L.M., Dalziel, A.W. and McNamee, M.G. (1983) Reconstitution of acetylcholine receptor function in lipid vesicles of defined composition. *Biochim. Biophys. Acta.* 727: 151-162.

114. Criado, M., Eibl, H. and Barrantes, F.J. (1982) Effects of lipids on acetylcholine receptor: Essential need of cholesterol for maintenance of agonist-induced state transitions in lipid vesicles. *Biochemistry* 21: 3622-3629.

115. Criado, M., Eibl, H. and Barrantes, F.J. (1984) Functional properties of the acetylcholine receptor incorporated in model lipid membranes. Differential effects of chain length and head group of phospholipids on receptor affinity states and receptor-mediated ion-translocation. *J. Biol. Chem.* 259: 9188-9198.

116. Gonzalez-Ros, J.M., Llanillo, M., Paraschos, A. and Martinez-Carrion, M. (1982) Lipid environment of acetylcholine receptor from *Torpedo californica*. *Biochemistry* 21: 3467-3474.

117. Hess, G.P., Cash, D.J. and Aoshima, H. (1983) Acetylcholine receptor-controlled ion transolcation: Chemical kinetic investigations of the mechanism. *Ann. Rev. Biophys. Bioeng.* 12: 443-473.

118. Schindler, H. (1979) Exchange and interactions between lipid layers at the surface of a liposome solution. *Biochim. Biophys. Acta* 555:316-336.

119. Schindler, H. (1980) Formation of planar bilayers from artificial or native membrane vesicles. *FEBS Lett.* 122:77-79.

120. Schindler, H., and Quast, U. (1980) Functional acetylcholine receptor from *Torpedo marmorata* in planar membranes. *Proc. Natl. Acad. Sci. USA* 77:3052-3056.

121. Nelson, N., Anholt, R., Lindstrom, J. and Montal, M. (1980) Reconstitution of purified acetylcholine receptors with functional ion channels in planar lipid bilayers. *Proc. Natl. Acad. Sci. USA* 77:3057-3061.

122. Montal, M., Labarca, P., Fredkin, D.R., Suarez-Isla, B.A. and Lindstrom, J. (1984) Channel properties of the purified acetylcholine receptor from *Torpedo californica* reconstituted in planar lipid bilayer membranes. *Biophys. J.* 45: 165-174.

123. Schindler, H. (1982) Concepts and techniques for membrane transport reconstitution. In: *ransport in Biomembranes: Model Systems and Reconstitution* (R. Antolini, A. Gliozzi and A. Gorio, eds.) Raven Press, New York, pp. 75-85.

124. Fromherz, P. (1975) Instrumentation for handling monomolecular films at an air-water interface. *Rev. Sci. Instrum.* 46:1380-1385.

125. Boheim, G., Hanke, W., Barrantes, F.J., Eibl, H., Sakmann, B., Fels, G. and Maelicke, A. (1981) Agonist-activated ionic channels in acetylcholine receptor reconstituted into planar lipid bilayers. *Proc. Natl. Acad. Sci. USA* 78:3586-3590.

126. Sigworth, F.J. (1982) Fluctuations in the current through open ACh-receptor channels. *Biophys. J.* 37:309 (Abstr.).

127. Adams, D.J., Dwyer, T.M., and Hille, B. (1980) The permeability of endplate channels to monovalent and divalent metal cations. *J. Gen. Physiol.* 75:493-510.

128. Adams, D.J., Nonner, W., Dwyer, T.W. and Hille, B. (1981) Block of end-plate channels by permeant cations in frog skeletal muscle. *J. Gen. Physiol.* 78:593-615.

129. Dwyer, T.M., Adams, D. and Hille, B. (1980) The permeability of the endplate-channel to organic cations in frog muscle. *J. Gen. Physiol.* 75:469-492.

130. Hamill, O.P. and Sakmann, B. (1981) Multiple conductance states of single acetylcholine receptor channels in embryonic muscle cells. *Nature* 294:462-464.

131. Horn, R. and Patlak, J. (1980) Single channel currents from excised patches of muscle membrane. *Proc. Natl. Acad. Sci. USA* 77: 6930-6934.

132. Dani, J.A. and Eisenman, G. (1984) Acetylcholine-activated channel current-voltage relations in symmetrical Na^+ solutions. *Biophys. J.* 45: 10-12.

133. Neher, E. and Steinbach, J.H. (1978) Local anesthetics transiently block currents through single acetylcholine receptor channels. *J. Physiol. (London)* 277:153-176.

134. Horn, R., Brodwick, M.S. and Dickey, W.D. (1980) Asymmetry of the acetylcholine channel revealed by quaternary anesthetics. *Science* (Wash. D.C.) 210: 205-207.

135. Ruff, R.L. (1982) The kinetics of local anesthetic blockade of end-plate channels. *Biophys. J.* 37:625-631.

136. Ogden, D.C., Siegelbaum, S.A., and Colquhoun, D. (1981) Block of acetylcholine-activated ion channels by an uncharged local anesthetic. *Nature* 289:596-598.

137. Neher, E. and Sakmann, B. (1976) Single channel currents recorded from membrane of denervated frog muscle fibers. *Nature* 260:799-802.

138. Colquhoun, D. and Sakmann, B. (1981) Fluctuations in the microsecond time range of the current through single acetylcholine receptor ion channels. *Nature* 294:464-466.

139. Jackson, M.B., Lecar, H., Askanas, V., Engel, W.K. (1982) Single cholinergic receptor channel currents in cultured human muscle. *J. Neurosci.* 2: 1465-1473.

140. Trautmann, A., and Feltz, A. (1980) Open time of channels activated by binding of two distinct agonists. *Nature* 286:291-293.

141. Tank, D.W., Huganir, R.L., Greengard, P. and Webb, W.W. (1983) Patch-recorded single-channel currents of the purified and reconstituted *Torpedo* acetylcholine receptor. *Proc. Natl. Acad. Sci. USA* 80:5129-5133.

142. Jackson, M.B., Wong, B.S., Morris, C.E., Lear, H., and Christian, C.N. (1983) Successive openings of the same acetylcholine receptor-channel are correlated in their open times. *Biophys. J.* 42: 109-114.

143. Fredkin, D.R., Montal, M. and Rice, J.A. (1985) Identification of aggregated Markovian models: Application to the nicotinic acetylcholine receptor. *Proc. of the Neyman-Kiefer Memorial Symposium,* Berkeley, CA (L.M. LeCam and R.A. Olshen, eds.) Wadsworth Publ. Co., Blemont, CA. Vol. 1:269-289.

144. Katz, B. and Thesleff, S. (1957) A study of the "desensitization" produced by acetylcholine at the motor end-plate. *J. Physiol.* 138:63-80.

145. Lindstrom, J., Tzartos, S., Gullick, W., Hochschwender, S., Swanson, L., Sargent, P., Jacob, M. and Montal, M. (1983) Use of monoclonal antibodies to study acetylcholine receptors from electric organs, muscle, and brain and the autoimmune response to receptor in myasthenia gravis. *Cold Spring Harbor Symp. Quant. Biol.* 48, 89-99.

146. Lindstrom, J.M., Tzartos, S.J. and Gullick, W.J. (1981) Structure and function of acetylcholine receptors studies using monoclonal antibodies. *Ann. N.Y. Acad. Sci.* 377: 1-19.

147. Tzartos, S.J. and Lindstrom J.M. (1980) Monoclonal antibodies used to probe acetylcholine receptor structure: Localization of the main immunogenic region and detection of similarities between subunits. *Proc. Natl. Acad. Sci. USA* 77: 755-759.

148. Tzartos, S. and Lindstrom, J. (1981) Production and characterization of monoclonal antibodies for use as probes of acetylcholine receptors. In: *Monoclonal Antibodies in Endocrine Research,* (Fellows, R. and Eisenbarth, G., eds.) Raven Press, New York, pp. 69-86.

149. Blatt, Y., Montal, M.S., Lindstrom, J. and Montal, M. (1984). Effect of antireceptor monoclonal antibodies on single channel currents of purified acetylcholine receptor reconstituted in lipid bilayers. *Biophys. J.* 45: Abstr. 311a.

150. Blatt, Y., Montal, M.S., Lindstrom, J. and Montal, M. (1986). Monoclonal antibodies specific to the β and γ subunits of the *Torpedo* acetylcholine receptor inhibit single channel activity. *J. Neurosci.* 6:481-486.

151. Sargent, P.B., Hedges, B.E., Tsavaler, L., Clemons, L., Tzartos, S. and Lindstrom, J.M. (1984) The structure and transmembrane nature of the acetylcholine receptor in amphibian skeletal muscle as revealed by cross-reacting monoclonal antibodies. *J. Cell Biol.*98: 609-618.

152. Wan, K.K. and Lindstrom, J.M. (1985) Effects of monoclonal antibodies on the function of acetylcholine receptors purified from *Torpedo californica* and reconstituted into vesicles. *Biochemistry* 24:1212-1221.

153. Nestler, E.J., Walaas, S.I. and Greengarad, P. (1984) Neuronal phosphoproteins: Physiological and chemical implications. *Science* 225: 1357-1367.

154. Huganir, R.L. and Greengard, P. (1983) C-AMP-dependent protein kinase phosphorylates the nicotinic acetylcholine receptor. *Proc. Natl. Acad. Sci. USA* 80: 1130-1134.

155. Huganir, R.L., Miles, K. and Greengard, P. (1984) Phosphorylation of the nicotinic acetylcholine receptor by an endogenous tyrosine-specific protein kinase. *Proc. Natl. Acad. Sci. USA* 81: 6968-6972.

156. Gonzalez-Ros, J.M., Ferragut, J.A. and Martinez-Carrion, M. (1984) Binding of anti-acetylcholine receptor antibodies inhibits the acetylcholine receptor-mediated cation flux. *Biochem. Biophys. Res. Commun.* 120: 368-375.

157. Goldberg, G., Mochly-Rosen, D., Fuchs, S. and Lass, Y. (1983) Monoclonal antibodies modify acetylcholine-induced ionic channel properties in cultured chick myoballs. *J. Membrane Biol.*76: 123-128.

158. Donnelly, D., Mihovilovic, M., Gonzalez-Ros, J.M., Ferragut, J.A., Richman, D. and Martinez-Carrion, M. (1984) A non-cholinergic site-directed monoclonal antibody can impair agonist-induced ion flux in *Torpedo californica* acetylcholine receptor. *Proc. Natl. Acad. Sci. USA* 81: 7999-8003.

159. Neumann, D., Fridkin, M. and Fuchs, S. (1984) Anti-acetylcholine receptor response achieved by immunization with a synthetic peptide from the receptor sequence. *Biochem. Biophys. Res. Commun.* 121, 673-679.

160. Mishina, M., Tobimatsu, T., Imoto, K., Tanaka, K., Fujita, Y., Fukuda, K., Kurasaki, M., Takahashi, H., Morimoto, Y., Hirose, T., Inayama, S., Takahashi, T., Kuno, M. and Numa, S. (1985) Location of functional regions of acetylcholine receptor α-subunit by site-directed mutagenesis. *Nature* 313: 364-369.

161. Agnew, W.S., Levinson, S.R., Brabson, J.S., and Raftery, M A. (1978) Purification of the tetrodotoxin-binding component associated with the voltage-sensitive sodium channel from *Electrophorus electricus* electroplax membranes. *Proc. Natl. Acad. Sci. USA* 75: 2606-2610.

162. Miller, J.A., Agnew, W.S. and Levinson, S.R. (1983) Principal glycopeptide of the tetrodotoxin/saxitoxin binding protein from *Electrophorus electricus* :Isolation and partial chemical and physical characterization. *Biochemistry* 22: 462-470.

163. Barchi, R.L., Cohen, S.A. and Murphy, L.E. (1980) Purification from rat sarcolemma of the saxitoxin-binding component of the excitable membrane sodium channel. *Proc. Natl. Acad. Sci. USA* 77: 1306-1310.

164. Barchi, R.L. (1983) Protein components of the purified sodium channel from rat skeletal muscle sarcolemma. *J. Neurochem.* 40: 1377-1385.

165. Lombet, A. and Lazdunski, M. (1984) Characterization, solubilization, affinity labeling and purification of the cardiac Na^+ channel using Tityus toxin). *Eur. J. Biochem.* 141: 651-666.

166. Hartshorne, R. P. and Catterall, W. A. (1981) Purification of the saxitoxin receptor of the sodium channel from rat brain. *Proc. Natl. Acad. Sci. USA* 78: 4620-4624.

167. Barhanin, J., Pauron, D., Lombet, A., Norman, R., Vijerberg, H., Giglio, J.R., and Lazdunski, M. (1983) Electrophysiological charaterization, solubilization, and purification of the Tityus) toxin receptor receptor associated with the gating component of the Na^+ channel from rat brain. *EMBO J.* 2: 915-920.

168. Grishin, E.V., Kovalenko, V.A., Pashkov, V.N., and Shamotienko, O.G. (1984) Isolation and characterization of sodium channel components. *Membrane Biochemistry* (U.S.S.R.) 1: 858-867.

169. Talvenheimo, J.A., Tamkun, M.M., and Catterall, W.A. (1982) Reconstitution of neurotoxin-stimulated sodium transport by the voltage-sensitive sodium channel purified from rat brain. *J. Biol. Chem.* 257: 11868-11871.

170. Tamkun, M.M., Talvenheimo, J.A., and Catterall, W.A. (1984) The sodium channel from rat brain: Reconstitution of neurotoxin-activated ion flux and scorpion toxin binding from purified components. *J. Biol. Chem.* 259: 1676-1688.

171. Hartshorne, R.P., Keller, B.U., Talvenheimo, J.A., Catterall, W.A., and Montal, M. (1985) Functional reconstitution of the purified brain sodium channel in planar lipid bilayers. *Proc. Natl. Acad. Sci. USA* 82:240-244.

172. Catterall, W.A. (1980) Neurotoxins that act on voltage sensitive sodium channels in excitable membranes. *Ann. Rev. Pharmacol. Toxicol.* 20: 15-43.

173. Catterall, W.A., Morrow, C. S., and Hartshorne, R.P. (1979) Neurotoxin binding to receptor sites associated with voltage-sensitive sodium channels in intact, lysed, and detergent solubilized brain membranes. *J. Biol. Chem.* 254: 11379-11387.

174. Narahashi, T., Anderson, N.C., and Moore, J.W. (1966) Tetrodotoxin does not block excitation from inside the nerve membrane. *Science* 153:765-767.

175. Khodorov, B.I. and Revenko, S.V. (1979) Further analysis of the mechanisms of action of batrachotoxin on the membrane of myelinated nerve. *Neuroscience* 4: 1315-1330.

176. Huang , L. M., Moran, N., and Ehrenstein, G. (1982) Batrachotoxin modifies the gating kinetics of sodium channels in internally perfused neuroblastoma cells. *Proc. Natl. Acad. Sci. USA* 79: 2082-2085.

177. Huang , L. M., Moran, N., and Ehrenstein, G. (1984) Gating kinetics of batrachotoxin modified sodium channels in neuroblastoma cells determined from single channel measurements. *Biophys. J.* 45: 313-322.

178. Quandt, F. and Narahashi, T. (1982) Modification of single Na^+ currents by batrachotoxin. *Proc. Natl. Acad. Sci. USA* 79: 6732-6736.

179 Catterall, W.A. (1977) Membrane potential dependent binding of scorpion toxin to the action potential Na^+ ionophore. *J. Biol. Chem.* 252: 8660-8668.

180. Koppenhöfer, E. and Schmidt, H. (1968) Die wirkung von scorpiongift auf die ionenströme des Ranvierschen schnürrings II. Unvollst ndige natrium inaktivierung. *Pflügers Arch.* 303: 150-161.

181. Hartshorne, R. P. and Catterall, W. A. (1984) The sodium channel from rat brain: Purification and subunit composition. *J. Biol. Chem.* 259: 1667-1675.

182. Hartshorne, R. P., Messner, D.J., Coppersmith, J.C., and Catterall, W. A. (1982) The saxitoxin receptor of the sodium channel from rat brain: Evidence for two nonidentical α subunits. *J. Biol. Chem.* 257: 13888-13891.

183. Messner, D.J. and Catterall, W.A. (1985) Separation and characterization of the subunits of the sodium channel. *Biochemistry* 260:10597-10604.

184. Beneski, D.A. and Catterall, W.A. (1980) Covalent labeling of protein components of the sodium channel with a photoactivable derivative of scorpion toxin. *Proc. Natl. Acad. Sci. USA* 77: 639-643.

185. Darbon, H., Jover, E., Couraud, F., and Rochat, H. (1983) Photoaffinity labeling of the α and β-scorpion toxin receptors associated with rat brain sodium channel. *Biochem. Biophys. Res. Comm.* 115: 415-422.

186. Sharkey, R.G., Beneski, D.A., and Catterall, W.A. (1984) Differential labeling of the α and β1 subunits of the sodium channel by photoreactive derivatives of scorpion toxin. *Biochemistry* 23: 6078-6086.

187. Holloway, P.W. (1973) A simple procedure for removal of Triton X-100 from protein samples. *Anal. Biochem.* 53: 304-308.

188. Szoka, F.Jr. and Papahadjopoulos, D. (1980) Comparative properties and methods of preparation of lipid vesicles (liposomes). *Ann. Rev. Biophys. Bioeng.* 9: 467-508.

189. Tamkun, M.M. and Catterall, W.A. (1981) Reconstitution of the voltage-sensitive sodium channel of rat brain from solubilized components. *J. Biol. Chem.* 256: 11457-11463.

190. Catterall, W.A. (1976) Purification of a toxic protein from scorpion venom which activates the action potential Na^+ ionophore. *J. Biol. Chem.* 251: 5528-5536.

191. Tanaka, J.C., Eccelston, J.F., and Barchi, R.L. (1983) Cation selectivity charateristics of the reconstituted voltage-dependent sodium channel purified from rat skeletal muscle sarcolemma. *J. Biol. Chem.* 258: 7519-7526.

192. Epstein, M. and Racker, E. (1978) Reconstitution of carbamylcholine-dependent sodium ion flux and desensization of the acetylcholine receptor from *Torpedo californica*, *J. Biol. Chem.* 253: 6660-6662.

193. Feller, D.J., Talvenheimo, J.A., and Catterall, W.A. (1984) Restoration of voltage dependent state change in the purified Na^+ channel from rat brain. *Soc. Neurosci. Abstr.*10: 863.

194. Tamkun, M.M. and Catterall, W.A. (1981) Ion flux studies of voltage-sensitive sodium channels in synaptic nerve ending particles. *Mol. Pharmacol.* 19: 78-86.

195. Mueller, P., Rudin, D.O., Tien, H.T., and Wescott, W.C. (1963) Methods for the formation of single bimolecular lipid membranes in aqueous solution. *J. Phys. Chem.* 67: 534-535.

196. Mueller, P. and Rudin, D.O. (1969) Bimolecular lipid membranes: Techniques of formation, study of electrical properties and induction of gating phenomenon, in: *Laboratory Techniques of Membrane Biophysics* (M. Passow and R. Stampfli, eds.), Springer-Verlag, Berlin, pp. 141-156.

197. Drachev, L.A., Jasaitis, A.A., Koulen, A.D., Kondrashin, H.A., Liberman, E.A., Hayrecek, I.B., Ostroumov, S.A., Semenov, A.Y., and Skulachev, V.P. (1974) Direct measurement of electric current generation by cytochrome oxidase, H^+-ATPase, and bacteriorhodopsin. *Nature* (Lond.) 249: 321-323.

198. Miller, C., and Racker, E. (1976) Ca^{2+} induced fusion of fragmented sarcoplasmic reticulum with artificial bilayers. *J. Memb. Biol.*30: 283-300.

199. Cohen, F.S., Akabas, M.H., and Finkelstein, A. (1982) Osmotic swelling of phospholipid vesicles causes then to fuse with a planar phospholipid bilayer membrane. *Science* (Wash. D.C.) 217: 458-460.

200. Cohen, F.S., Akabas, M.H., Zimmerberg, J., and Finkelstein, A. (1984) Parameters affecting the fusion of unilamellar phospholipid vesicles with planar bilayer membranes. *J. Cell Biol.* 98: 1054-1062.

201. Krueger, B.K., Worley, J.F., and French, R.J. (1983) Single sodium channels from rat brain incorporated into planar lipid bilayer membranes. *Nature (Lond.)* 303: 172-175.

202. Weiss, L.B., Green, W.N.,and Andersen, O.S. (1984) Single channel studies on the gating of batrachotoxin modified sodium channels in lipid bilayers. *Biophys. J.* 45: 67 (abstr.).

203. French, R.J., Worley, J.F.,and Krueger, B.K. (1984) Voltage-dependent block by saxitoxin of sodium channels incorporated into planar lipid bilayers,. *Biophys. J.*45: 301-310.

204. Moczydlowski, E., Garber, S.S., and Miller, C. (1984) Batrachotoxin-activated Na^+ channels in planar lipid bilayers: Competition of tetrodotoxin block by Na^+. *J. Gen. Physiol.*84: 687-704.

205. Huang , L. M., Catterall, W.A., and Ehrenstein, G. (1979) Comparison of ionic selectivity of batrachotoxin-activated channels with different tetrodotoxin dissociation constants. *J. Gen. Physiol.*73: 839-854.

206. Cahalan, M, and Begenisich, T. (1976) Sodium channel selectivity: Dependence on internal permeant ion concentration. *J. Gen. Physiol.*68: 111-125.

207. Noda, M., Shimizu, S., Tanabe, T., Takai, T., Kayano, T., Ikeda, T., Takahashi, H., Nakayama, H., Kanaoka, Y., Minamino, N., Kangawa, K., Matsuo, H., Raftery, M., Hirose, T., Inayama, S., Hayashida, H., Miyata, T., and Numa, S. (1984) Primary structure of Electrophorus electricus sodium channel deduced from cDNA sequence. *Nature* 312: 121-127.

208. Kistler, J. Stroud, R.M., Klymkowsky, M.W., Lalancette, R.A. and Fairclough, R.H. (1982) Structure and function of an acetylcholine receptor. *Biophys. J.* 37: 371-383.

209. Gullick, W.J., Tzartos, S. and Lindstrom, J. (1981) Monoclonal antibodies as probes of acetylcholine receptor structure. I. Peptide mapping. *Biochemistry* 20: 2173-2180.

210. Anderson, D.J., Blobel, G., Tzartos, S., Gullick, W. and Lindstrom, J. (1983) Transmembrane orientation of an early biosynthetic form of acetylcholine receptor a-subunit determined by proteolytic dissection in conjunction with monoclonal antibodies. *J. Neurosci.* 3: 1773-1784.

211. Gullick, W.J. and Lindstrom, J.M. (1983) Mapping the binding of monoclonal antibodies to the acetylcholine receptor from *Torpedo californica*. *Biochemistry* 22: 3312-3320.

212. Wennogle, L.P., Oswald, R., Saitoh, T. and Changeux, J.-P. (1981) Dissection of the 66,000 dalton subunit of the acetylcholine receptor. *Biochemistry* 20: 2492-2497.

213. Ross, M.J., Klymkowsky, M.W., Agard, D.A. and Stroud, R.M. (1977) Structural studies of a membrane-bound acetylcholine receptor from *Torpedo californica*. *J. Mol. Biol.*116: 635-659.

214. Wise, D.S., Karlin, A. and Schoenborn, B.P. (1979) An analysis by low-angle neutron scattering of the structure of the acetylcholine receptor from *Torpedo californica* in detergent solution. *Biophys. J.* 28: 473-496.

215. Brunner, Y., Skrabal, P. and Hauser, H. (1976) Single bilayer vesicles prepared without sonication: Physico-chemical properties. *Biochim. Biophys. Acta* 455: 322-331.

216. Heidmann, T. and Changeux, J.-P. (1980) Interaction of a fluorescent agonist with the membrane-bound acetylcholine receptor from *Torpedo marmorata* in the millisecond time range: Resolution of an intermediate conformational transition and evidence for positive cooperative effects. *Biochem. Biophys. Res. Commun.* 97: 889-896.

FIGURE LEGENDS

FIGURE 1. **A structural model of the AChR.** The figure presented is a modification of a model by Kistler et al. (208).

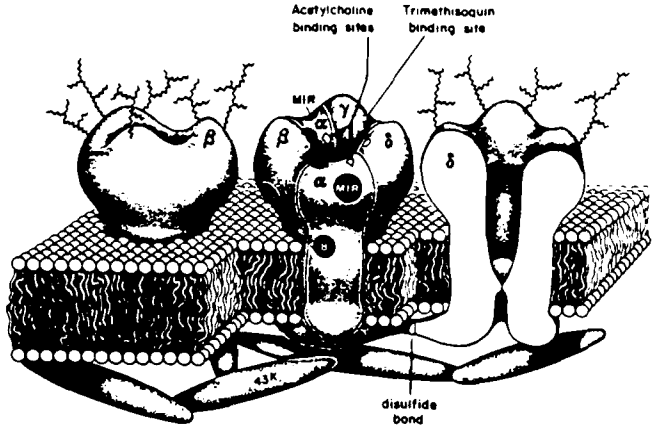

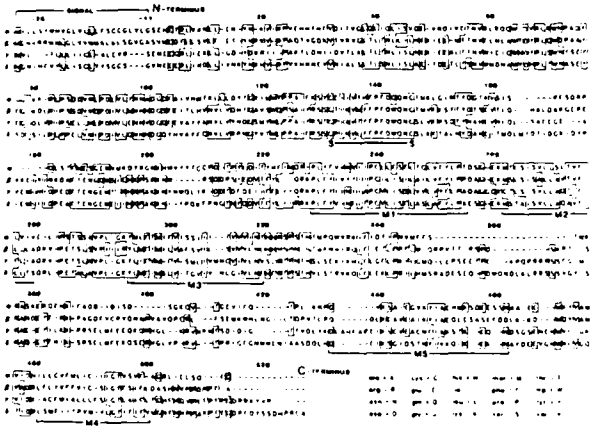

FIGURE 2. Experimental system for the formation of planar lipid bilayers across apertures in Teflon septi and for recording single AChR channel currents.

A- The chamber: Top: Photograph of the chamber. Middle and bottom: Diagram of the chamber with construction specifications, illustrating top (middle) and side (bottom) views. Dimensions in millimeters.

B- A complete set-up: The chamber is located inside an aluminum box (a Faraday cage). The chamber holder is fitted with water inlets and outlets to allow studies under constant temperature and at different temperatures. The syringes (disposable) used to displace the water levels are located to the right and also are enclosed in a metallic compartment. The syringes are connected to the chamber via polyethylene tubing. Two Ag/AgCl electrodes are immersed in Teflon reservoirs containing 1 M KCl and connected on one end, to the chamber compartments via salt bridges (1 M KCl in 2% w/v agar), and on the other, to the amplifier (retangular box at the left) via high quality chasis-BNC connector. The experimental set-up is mounted on a vibration-isolation platform.

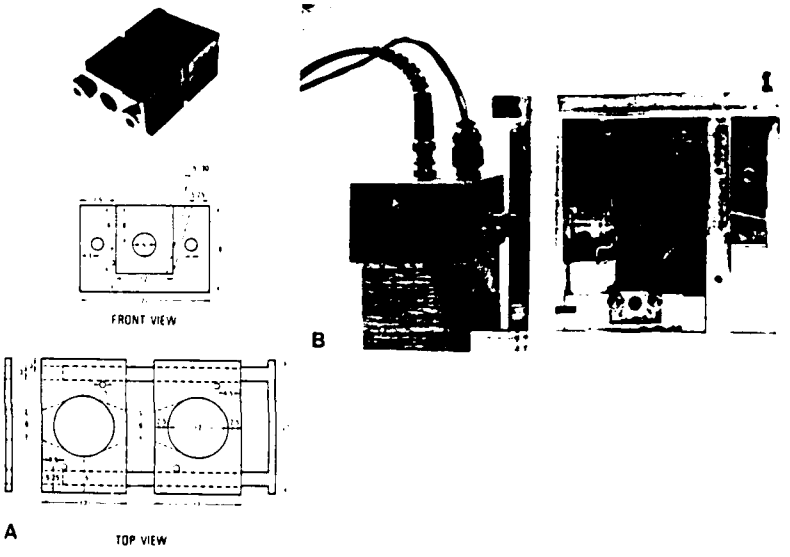

FIGURE 3. **Protection of ion channel function during solubilization of AChRs in the presence of supplementary soybean lipids.** Pelleted AChR-rich electric organ membranes (1.67 mg of protein) were solubilized in 0.5 ml of 2% cholate, 100 mM NaCl, 10 mM Na-phosphate buffer, pH 7.5, in the presence of the indicated amounts of soybean lipid added as a sonicated dispersion in distilled water. After gentle agitation for 16 h at 4°C, the lipid in all samples was adjusted to 25 mg in a final volume of 1 ml. The samples were agitated for 10 min and centrifuged for 30 min at 100,000 x g. Reconstituted vesicles were formed via removal of the cholate by dialysis (215). The cumulative $^{22}Na^{+}$ uptake in response to 10^{-4} M CCh was assayed (45).

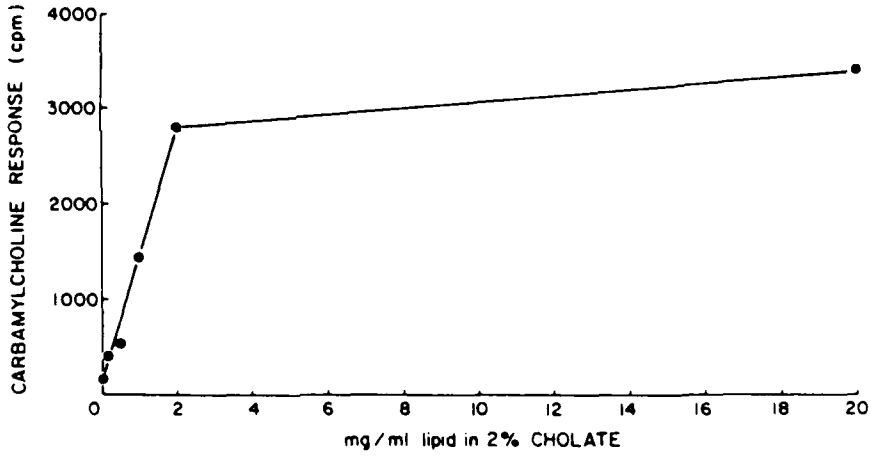

FIGURE 4. **Solubilization of AChRs from AChR-rich electric organ membranes (A) and preservation of AChR channel function in mixed micelles of sodium cholate and soybean lipids (B).** Aliquots of AChR-enriched membranes were centrifuged for 15 min in an Eppendorf microfuge. The pellets were suspended at a concentration of 4 mg/ml of protein in 100 mM NaCl, 10 mM Na-phosphate buffer, pH 7.5, supplemented with different concentrations of sodium cholate and soybean lipids, at a constant weight ratio of 10:1. After 18-24 h of shaking, the cholate and lipid concentrations in all samples were adjusted to 2% and 25 mg/ml, respectively. After an additional incubation period of 30 min of slow shaking, the samples were centrifuged in an Eppendorf microfuge as before; the supernatants were collected, assayed for [^{125}I]-α-BGT binding activity, and dialyzed in order to form reconstituted vesicles. The resulting vesicles were then assayed for CCh-dependent uptake of $^{22}Na^{+}$ at 10^{-4} M CCh. Data were obtained from three sets of triplicate measurements (70).

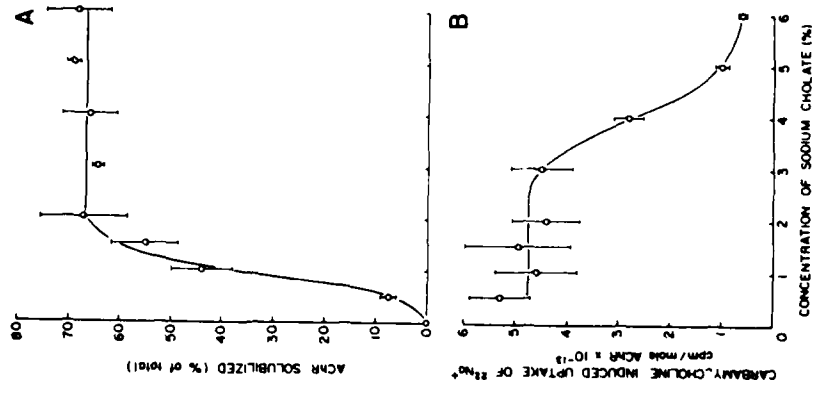

FIGURE 5. Schematic representation of AChR-lipid interactions during the solubilization and reconstitution processes (70).

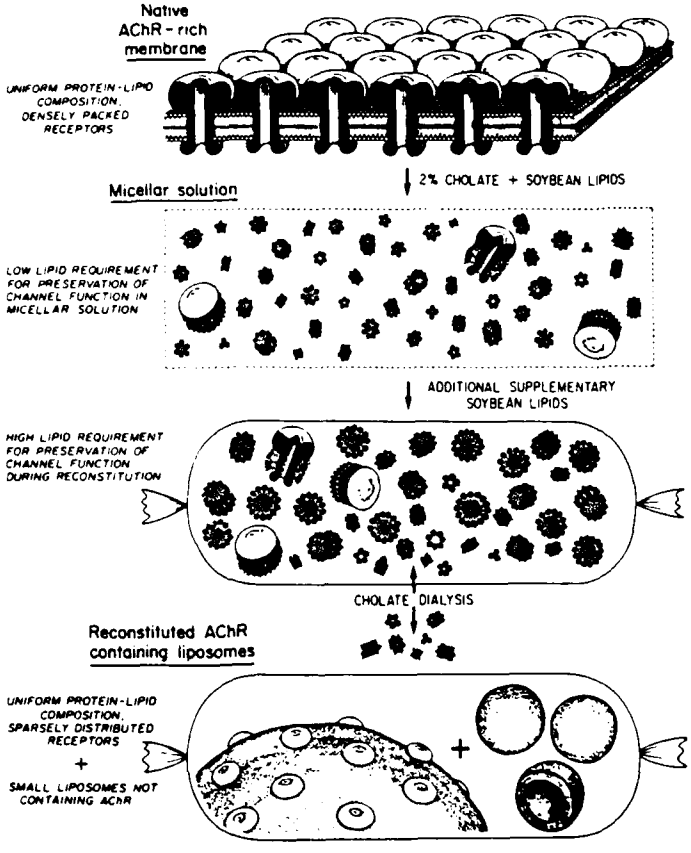

Figure 6. **Steroscopic electron micrographs of freeze-fracture replicas of native electric organ membranes and reconstituted vesicles. A.** - Native electric organ membrane: **B**- Regular reconstituted vesicles after a freeze-thaw cycle: **C**- Cholesterol (20% w/w)-supplemented reconstituted vesicles after a freeze-thaw cycle. In panel A, a native membrane vesicle containing densely packed AChRs is presented. The AChRs appear as 90 A particles which protrude at least 15 A from the plane of the membrane, as measured from the projected shadow of particles at the top of the vesicle. In panel B, a reconstituted vesicle containing sparsely distributed 90 A particles can be seen surrounded by a homogeneous population of smaller vesicles devoid of particles. In panel C, a similar size vesicle containing particles is surrounded by particle-free liposomes, which appear larger than their counterparts in panel B. The large vesicles in panels B and C contain about 40 and 26 particles, respectively, on their visible areas (about half of the vesicle surface). The stereo pairs can be viewed with a conventional three-dimensional viewer (Ted Pella, Inc.). Magnification: 65,000 x. The bar indicated 500 nm (44).

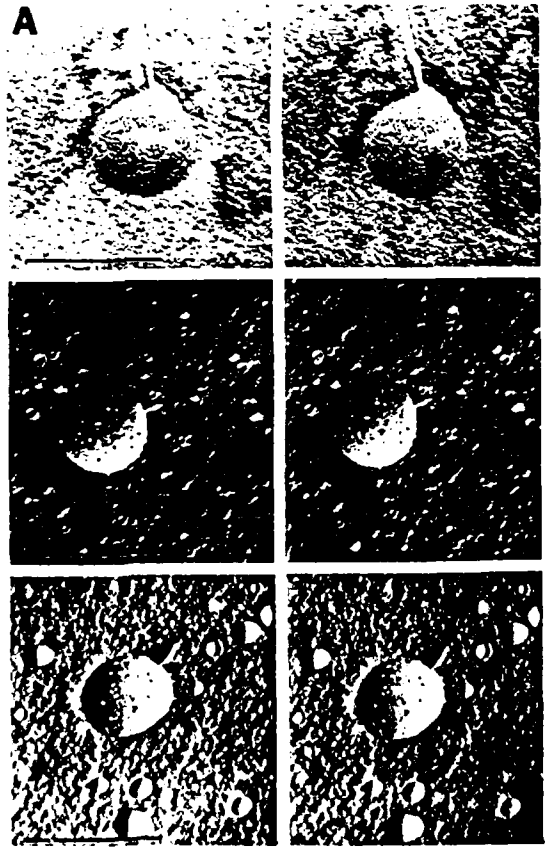

FIGURE 7. **Size distribution of reconstituted vesicles.** Electron micrographs of negatively stained vesicles were prepared. Vesicles were measured according to their longest diameter within the nearest 40 Å. Occasional structures appearing smaller than 240 Å (the approximate limiting diameter for a minimal size liposome, according to Chang and Bock (215) were discarded from the analysis. Sampling was continued until the histogram appeared to build up stably without significantly changing in terms of distribution. All liposomes in a given field were measured. Open arrows indicate the mean diameter of liposomes formed in the absence of AChR. Closed arrows indicate the mean diameter of liposomes formed in the presence of AChR. The number of vesicles with diameter larger than 1,000 Å is given as an arbitrary indicator of shifts in size distribution as a result of vesicle fusion (44).

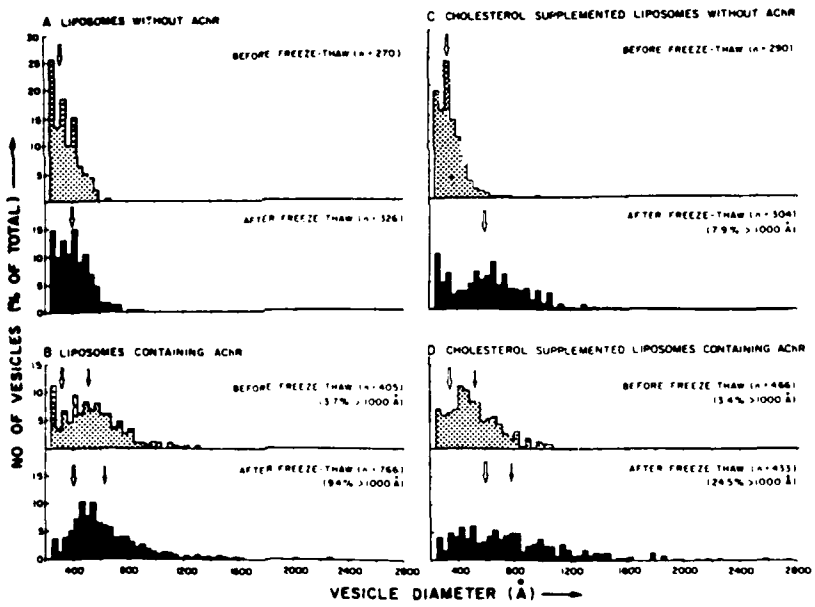

FIGURE 8. **Schematic representation of the major conformational transitions that underlie AChR function.** K and K' indicate the intrinsic equilibrium dissociation constants for the agonist of the resting and desensitized states of the AChR, respectively. M is the allosteric constant describing the isomerization equilibrium of the interconversion between unliganded activatable, and desensitized AChRs. The scheme indicates that the doubly liganded AChR is able to open a cation-selective channel. Desensitization of the AChR is accompanied by the closing of the channel and an increase in binding affinity for the agonist (indicated in the figure by thickening and shortening of the bars connecting ACh with the AChR). Desensitization is a two-step process which may involve a transient intermediate state in which ACh binds to a low affinity site, as indicated in the figure (216,91,92). The figure is merely illustrative with regard to the nature of the various closed states of the channel, which is, in reality, unknown. For precise values for *Torpedo californica* of the constants K, K' and M, see (84) or (86) from (3).

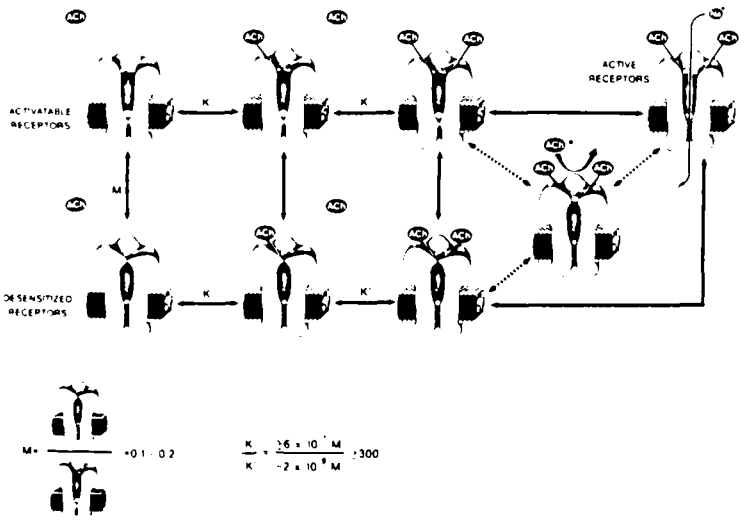

FIGURE 9. **Dose dependence for activation and desensitization of reconstituted AChRs.** Equilibrium measurements were made using a $^{22}Na^{+}$ uptake assay. Counts at the maximal response were approximately 10-fold higher than the background control. The dose dependence for AChR desensitization was assayed by addition of 10^{-4} M CCh after a preincubation period of at least 30 min with the indicated concentration of agonist in the absence of radioisotope. Assays were performed at 48 nM (●) and 800 nM (○) ligand binding sites. The dose reponse characteristics for activation and desensitization will depend on the AChR concentration when it is high with respect to the dissociation constant for the agonist, since the AChR will, under these conditions, deplete the concentration of free ligand by binding a significant fraction of the total agonist. As a result, the dose response curve will be displaced depending on the affinity of the receptor for the agonist. The larger displacement of the dose response curves for ACh as compared to those for CCh reflects the expected higher affinity for ACh. The fact that the dose response curves for desensitization for each agonist are more sensitive to the receptor concentration than the corresponding dose response curves for activation indicates that desensitization of the receptor is accompanied by an increase in binding affinity for the receptor. It should be noted that the midpoint of the dose response curve for receptor activation at low receptor concentrations is at least an order of magnitude lower when cumulative responses are measured at equilibrium than when initial flux rates are measured (adapted from (3)).

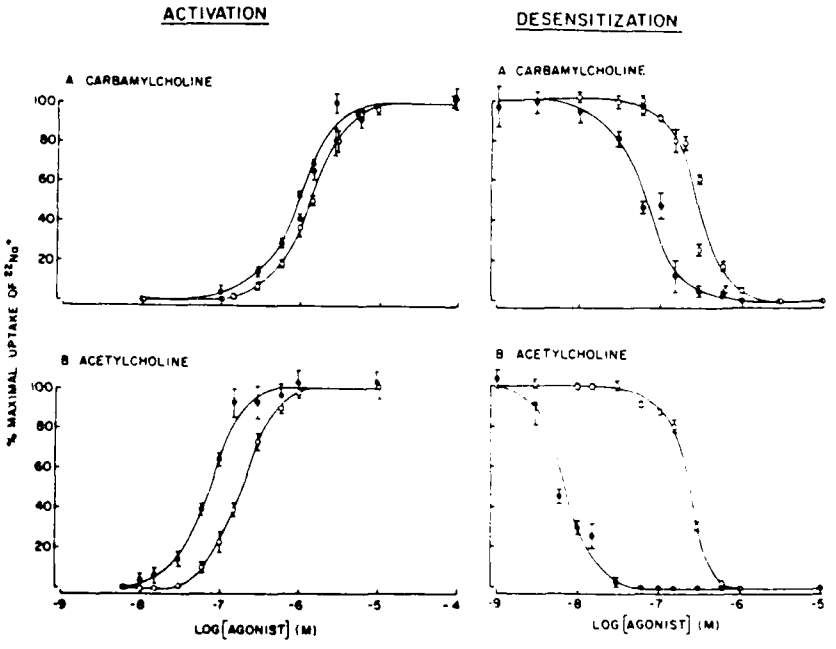

FIGURE 10. **Titration of the CCh-induced cation uptake response by inhibition with cobra-toxin.** Native electric organ membranes or reconstituted vesicles were incubated for 2 h at room temperature with increasing amounts of *Naja naja siamensis* toxins III (38) and assayed for uptake of $^{22}Na^{+}$ at 10^{-4} (●) or 2×10^{-6} M (O) CCh. Data are compiled from triplicate measurements. The dotted line in each panel indicates the predicted parabolic decline according to the equation $(F(y) = (1 - y)^2$ for a model of double liganded control of channel gating in the absence of volume limitations, in which f(y) is the fractionof AChRs which remain active, having both ligand binding sites unoccupied by cobratoxin, and y represents the fraction of all binding sites occupied by cobratoxin. A- Native electric organ membranes: B- A theoretical qualitative description of the effect of limited internal volume on the cobratoxin titration curve. The curves are described by the equation $f(y) = 1-\exp[-\gamma (1-y)^2]/1-\exp.-\gamma$, in which f(y) is the remaining fraction of AChR mediated $^{22}Na^{+}$ uptake, y the fractional occupany of [125I]-1α-BGT binding sites by cobratoxin and γ a parameter which relates the integrated $^{22}Na^{+}$ uptake per AChR channel to the available internal volume per AChR. Volume restrictions become more severe as the value of γ increases. When $\gamma \rightarrow 0$, the above equation obtains the forms $f(y) = (1 - y)^2$ (for derivation, see (44)). C-, D-, and E- Variable behavior of the regular reconstituted vesicles aafter a freeze-thaw cycle. F- Typical behavior of cholesterol-supplemented reconstituted vesicles after a freeze-thaw cycle (from (44).

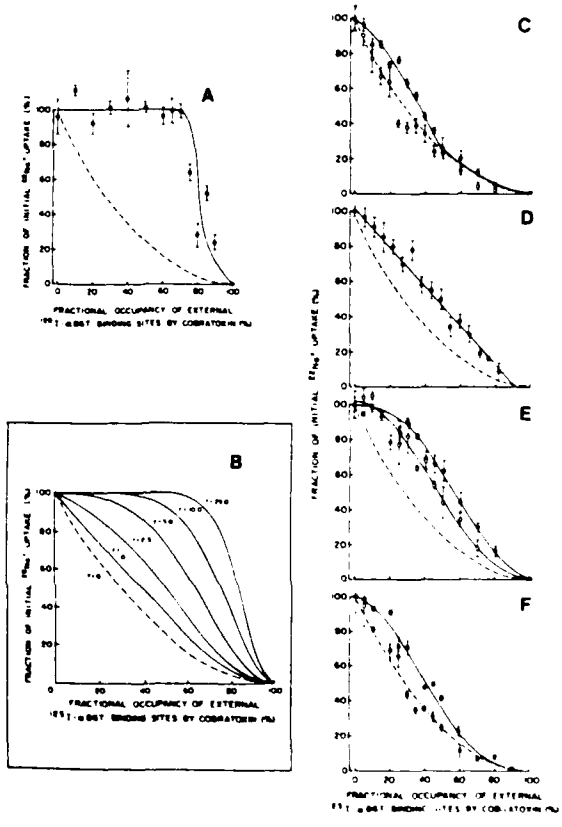

FIGURE 11. Time course of the change in surface pressure caused by the formation of vesicle-derived monolayers at an air–water interface (from 58).

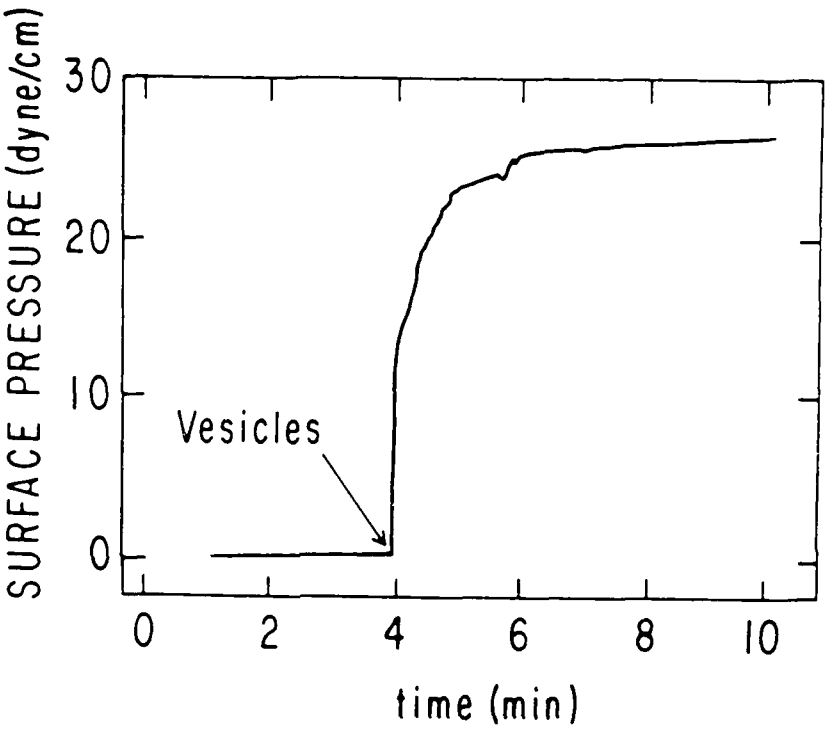

FIGURE 12. **Single AChR channel currents activated by suberyldicholine (0.1 μM, left-hand panel and acetylcholine (1 μM, right-hand panel) at an applied voltage of 100 mV.** The recordings were obtained from a bilayer formed either across a Teflon aperture (left record) or at the tip of a patch pipet (right record). The records were low-pass-filtered at 2 kHz (8 pole Bessel filter). As indicated, an upward deflection corresponcs to a channel opening event. Bilayers were formed in 0.44 M NaCl (left) or 0.5 M NaCl (right), 0.5 mM $CaCl_2$, 2.5 mM tricine, pH 7.4. The single-channel conductance was 42 pS for suberyldicholine and 47 pS for acetylcholine.

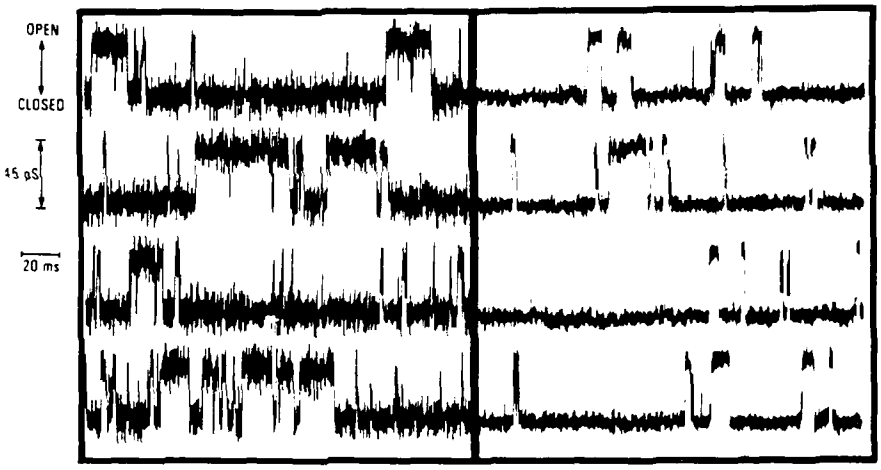

FIGURE 13. **Single-channel conductance histograms of the recordings illustrated in Figure 12.** Two Gaussian distributions are clearly discerned corresponding to the channel closed state (peaks at zero current) and the open state (peaks at 4.2 and 4.7 pA). At the applied voltage of 100 mV, γ = 42 pS and 47 pS. The relative areas under the closed and open curves reflect the probability of each state at 100 mV, indicating that the channel is preferentially closed. The width parameter or standard deviation of the Gaussian distribution is significantly larger for the open state (>10%).

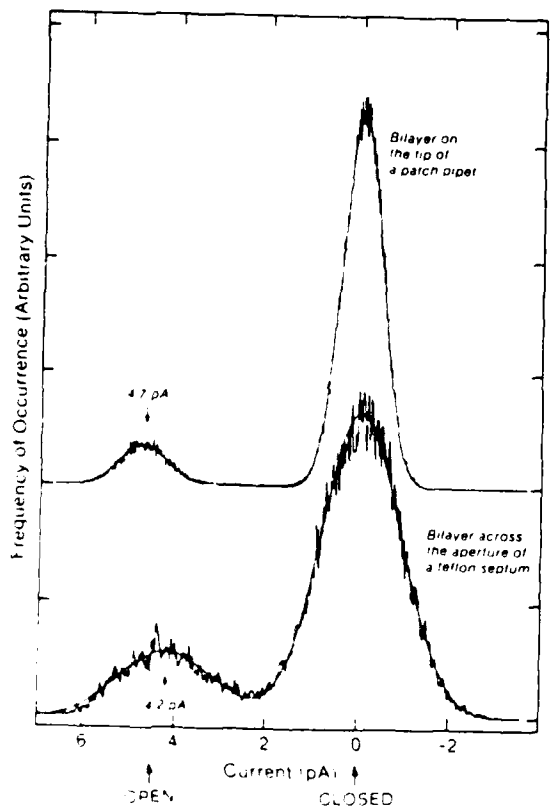

FIGURE 14. **Prabability density analysis of dwell times in the open state of the AChR channel activated by 0.1 μM ACh and recorded at 100 mV.** The data are well fitted with a sum of two exponentials, with p = 0.99. The fitted curve (smooth curve) is superimposed on the histogram of the actual data (noisy curve). The parameters of the fitted curve are: A_S = 0.92, τ_S = 0.42 ms: A_L = 0.08, τ_L = 4.3 ms. The total number of openings, analyzed in this histogram 967 (n = 967).

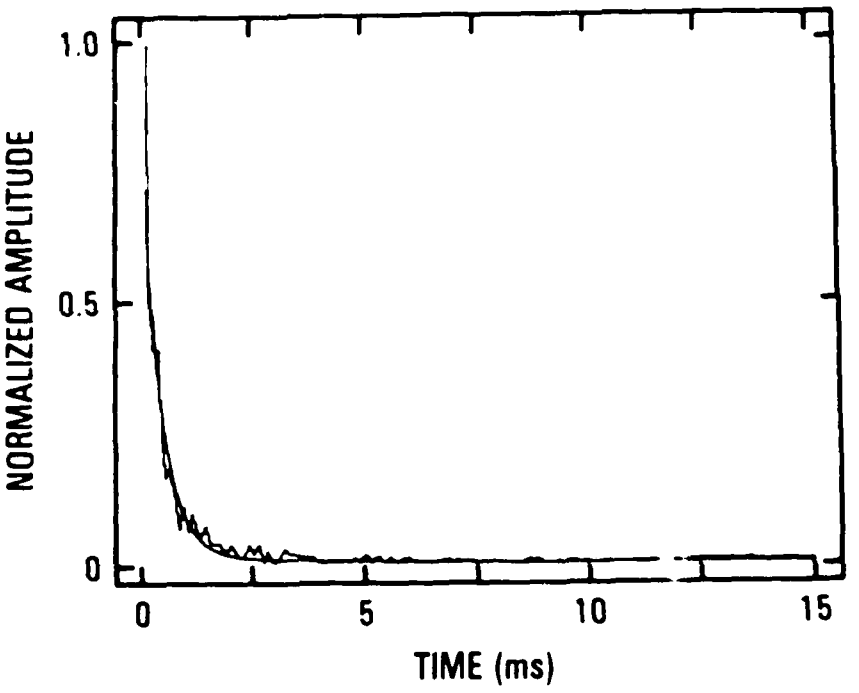

Figure 15. **Autocorrelation function for the open state of the reconstituted AChR channel.** The analysis considers a sequence of open dwell times T_i, T_{i+1}, ... and computes the covariance function:

$$\hat{\Gamma}(k) = \frac{1}{n-k} \sum_{i=1}^{n-k} (T_i - \bar{T})(T_{i+k} - \bar{T}),$$

where

$$\bar{T} = \frac{1}{n} \sum_{i=1}^{n} T_i \text{ and } k = 0,1,2,\ldots$$

the correlation function:

$$\hat{\rho}(k) = \frac{\hat{\Gamma}(k)}{\hat{\Gamma}(o)}$$

is illustrated. The dashed horizontal lines are at plus and minus twice the approximate standard error of the estimate in the case of white noise. The recordings were obtained from bilayers formed at the tip of patch pipets. ACh was ~50 μM and the applied voltage was 100 mV. The total number of openings analyzed was 1,600 (from 59).

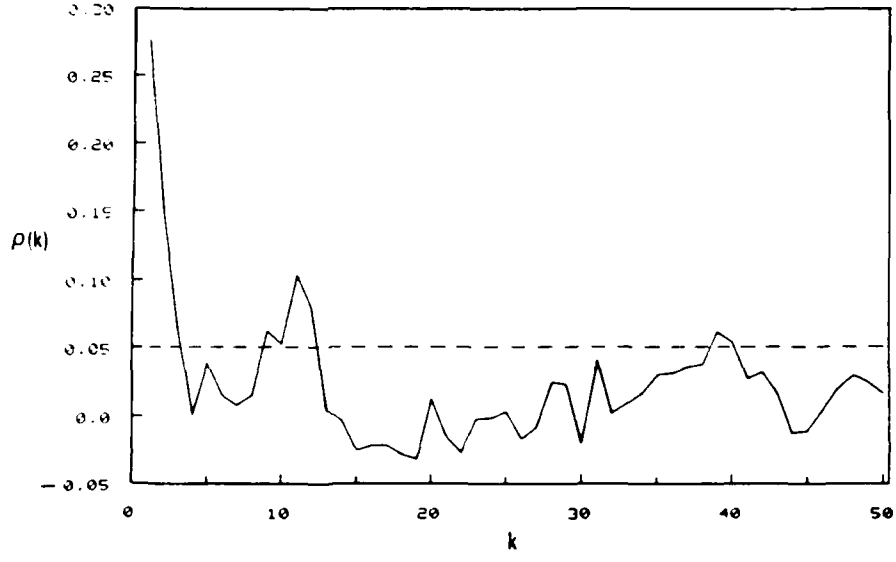

FIGURE 16A-D **A. Single AChR channel currents activated by desensitizing concentrations of agonist.** This record, displayed at low time resolution, shows paroxysms of single AChR channels separated by quiescent periods. The channels were activated by 1 μM SubCh and recorded at V = 100 mV. **B–D** Frequency of channel openings in the presence of desensitizing concentrations of CCh. Records of single AChR channel currents were activated with 1 mM CCh and recorded at 70 mV. **B**-Experimental data ; **C**-Monte Carlo simulation with the four-state model:

$$\begin{array}{ccccc} C & \rightleftharpoons & CL & \rightleftharpoons & OL \\ & & \updownarrow & & \\ & & DL & & \end{array}$$

which includes a desensitized state (DL); **D**-Monte Carlo simuation with the three-state model:

$$C \rightleftharpoons CL \rightleftharpoons OL$$

(from (122)).

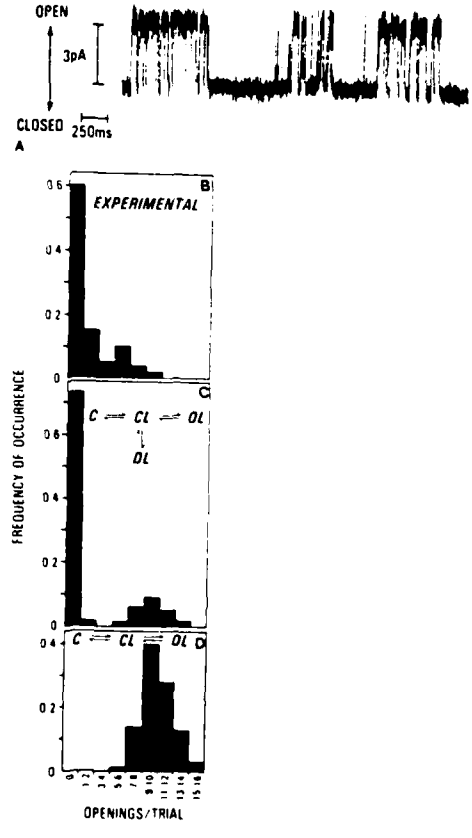

FIGURE 17. **Monoclonal antibodies specific to the β and γ subunits block the channel activity of the reconstituted AChR.** Single AChR channel currents were activated by 10 μM ACh and recorded at 100 mV. The concentration of AChR was 0.05 μM. The recordings were obtained from bilayers formed at the tip of patch pipets. **A**- Ab 10 inhibits single AChR channel activity. At the arrow, mAb 10(0.1 μM) was added to the *cis*-chamber. The seal resistance was 5 GΩ. **B**-Ab 148 inhibits single AChR channel activity At the arrow, 3.8 ∂ mAb 148 was added to the *trans*-chamber. The seal resistance was 6 GΩ. **C**-Ab 168 inhibits single AChR channel activity. At the arrow, 1.3 μM mAb 168 was added to the *trans*-chamber. The seal resistance was 7 GΩ. In A,B and C, the lower panel shows the section of the record indicated by the arrow at higher time resolution (note the change in time calibration) (from (150)).

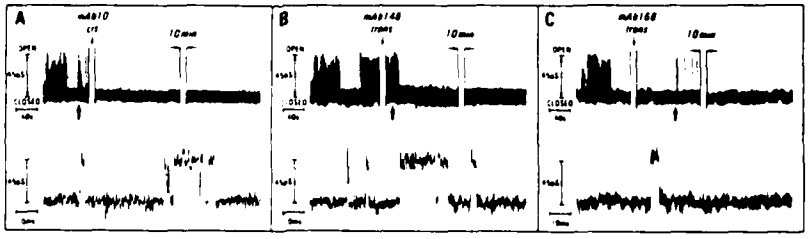

Figure 18. **Subunit composition of purified sodium channels from rat brain.** Purified sodium channel were dissociated by boiling in 2% SDS and 20 mM 2-mercaptoethanol and then analyzed by electrophoresis in polyacrylamide gel (183). Silver staining (39) shows the three subunits of the purified protein, α, β1 and β2.

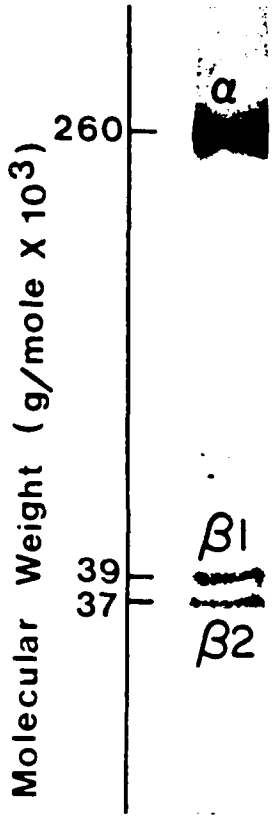

FIGURE 19. **Electron micrographs of freeze-fracture replicas of purified sodium channels reconstituted in egg PC vesicles.** The bar indicates 1,000 A. The arrow indicates a vesicle containing an intramembranous particle likely to be a sodium channel.

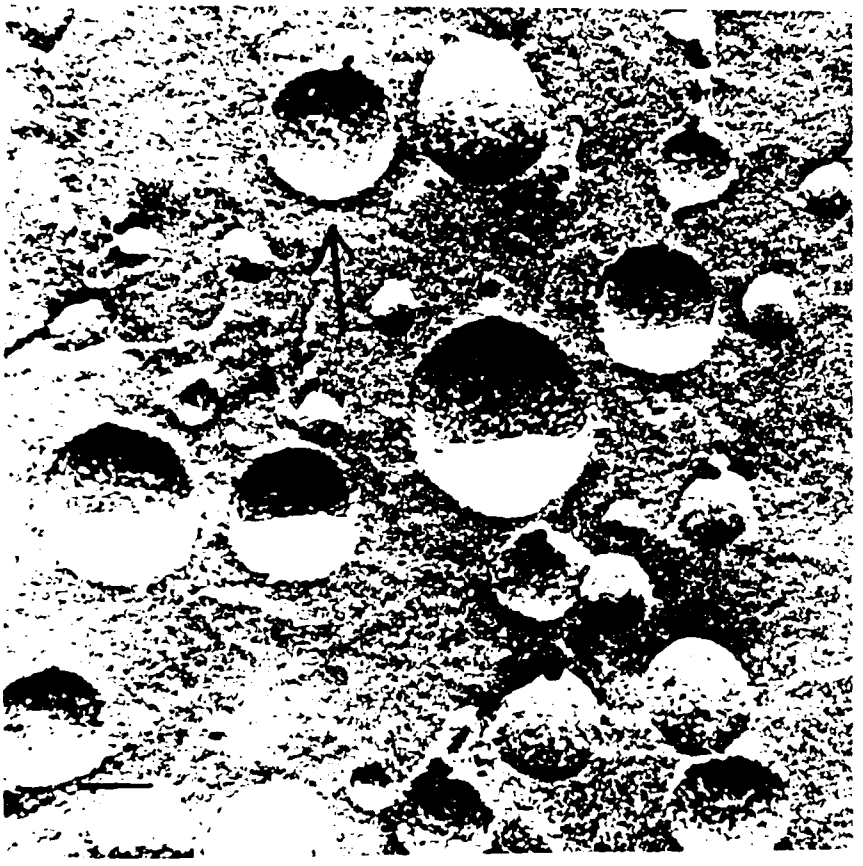

FIGURE 20. **Specific and nonspecific binding of ^{125}I-LqTX to reconstituted vesicles.** Purified sodium channels were reconstituted in vesicles composed of PC and purified rat brain lipids. Prior to reconstitution, sodium channels were either incubated at 36°C for 15 min (●) or untreated (Δ). Binding was measured in the presence of 0.1 nM ^{125}I-LqTX and increasing concentrations of unlabeled LqTX as indicated. Specific binding is defined as the difference between binding to vesicles containing untreated sodium channels and binding to comparable vesicles containing heat-denatured channels (from Publication #16).

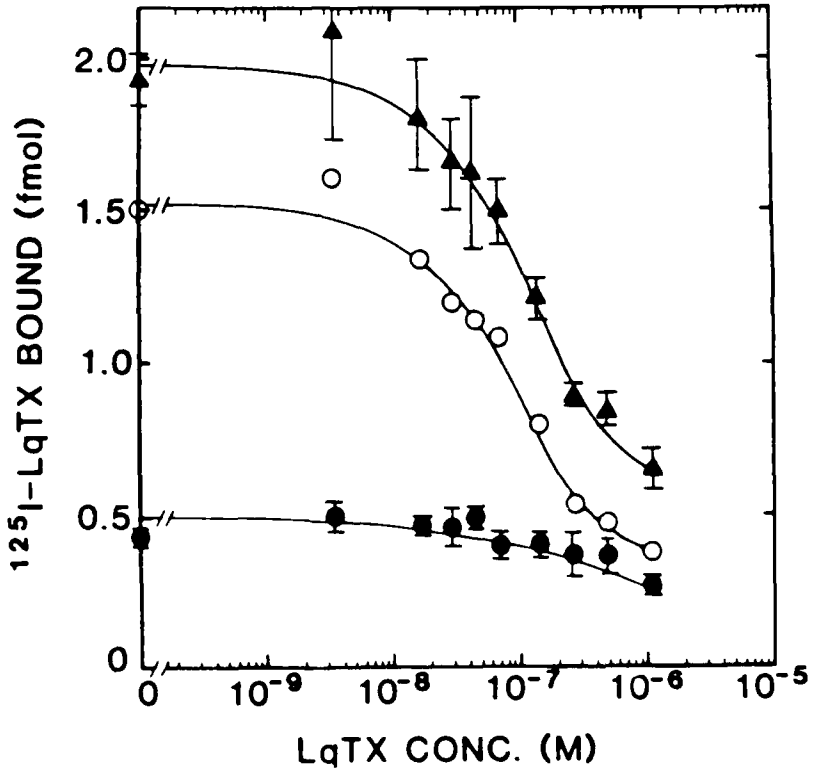

FIGURE 21. **Thermal inactivation of the [^{3}H]-STX and ^{125}I-LqTX binding activities of the purified sodium channel.** Sodium channels were incubated at 36°C for the indicated times. Channels were reconstituted in vesicles composed of PC and purified rat brain lipid, and [^{3}H]-STX (●) and ^{125}I-LqTX (Δ) binding activities were measured. [^{3}H]-STX binding was determined inthe presence of 10 nM [^{3}H]-STX incubated for 15 min atr 4°C. ^{125}I-LqTX binding was measured in the presence of 0.1 nM ^{125}I-LqTX for 15 min at 36°C. (From Publication #16).

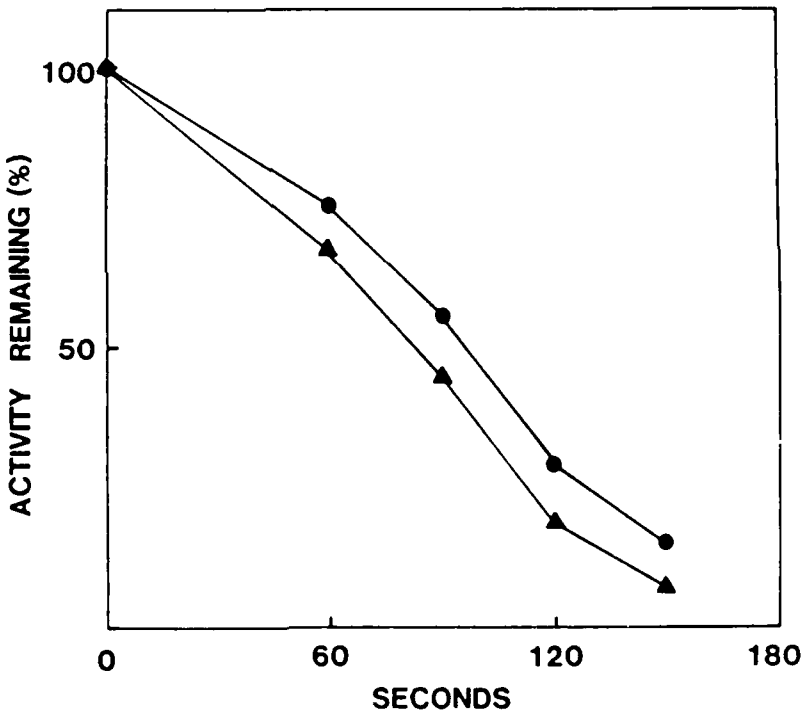

FIGURE 22. **Time course for $^{22}Na^{+}$ uptake by purified sodium channels reconstituted in PC vesicles.** The uptake measured in the presence of 100 μM Ver (●), 100 μM Ver together with 1 μM TTX (Δ), and no added toxins (O) is illustrated. (From Publication #16).

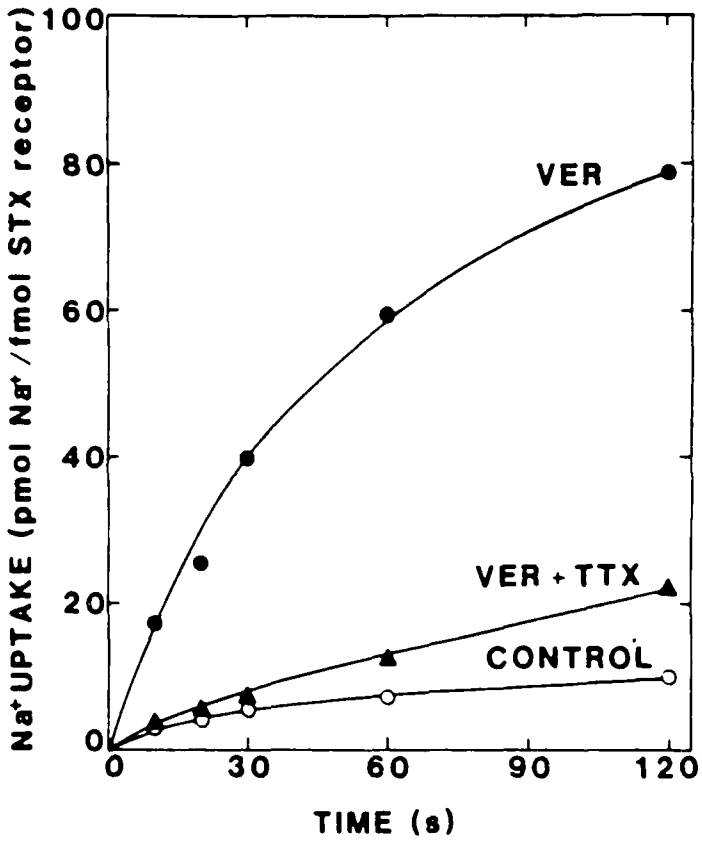

FIGURE 23. **Concentration dependence of tetrodotoxin inhibition of veratridine-activated $^{22}Na^{+}$ uptake by purified sodium channels reconstituted in PC vesicles.** Vesicles were incubated with 100 μM Ver and the indicated concentration of TTX for 2 min at 37°C prior to dilution into Tris-SO_4 medium containing the same toxin concentration. Each point is the mean ± S.D. (n=6). (From Publication #16).

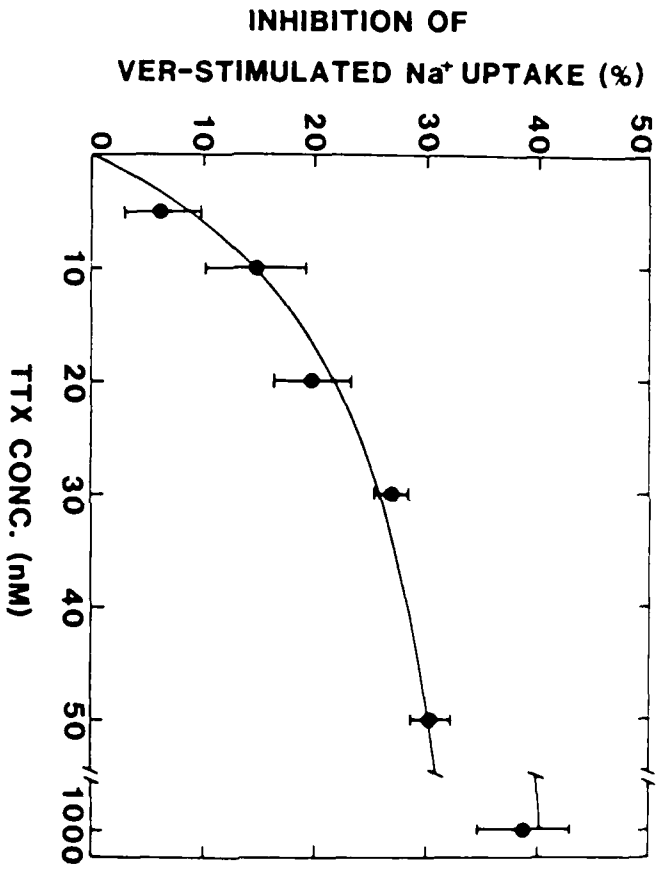

FIGURE 24. **TTX block of reconstituted sodium channels in planar lipid bilayers** This POPE/POPC membrane contained one *trans*-facing and three *cis*-facing sodium channels in symmetric 0.5 M NaCl medium A with 1 μM BTX *trans*. V was -50 mV for the *cis*-facing channels and +50 mV for the *trans*-facing channel. The records were filtered at 500 Hz.

A- Orientation dependence of TTX block. The initial current record shows four open channels interrupted by occasional brief closures. At the arrow, 40 μM TTX (final concentration) was added to the *trans*-chamber. The 25 s delay between the addition of TTX and channel block was the result of slow mixing of TTX with the solution. This was intentionally done to allow the channel blocking event to be recorded.

B- Continuation of current record in A 3 min later following complete mixing of the *trans*-chamber. Addition of 2 μM TTX to the *cis*-chamber blocks the remaining channels.

C- Reversibility of TTX block. With TTX on both sides, all channels remain blocked with occasioinal brief openings. Upon removal of TTX from the *trans*-chamber by perfusion (exchange of 14 volumes with stirring), the membrane current returns to the pre-TTX value. The *trans*-facing channel remains blocked.

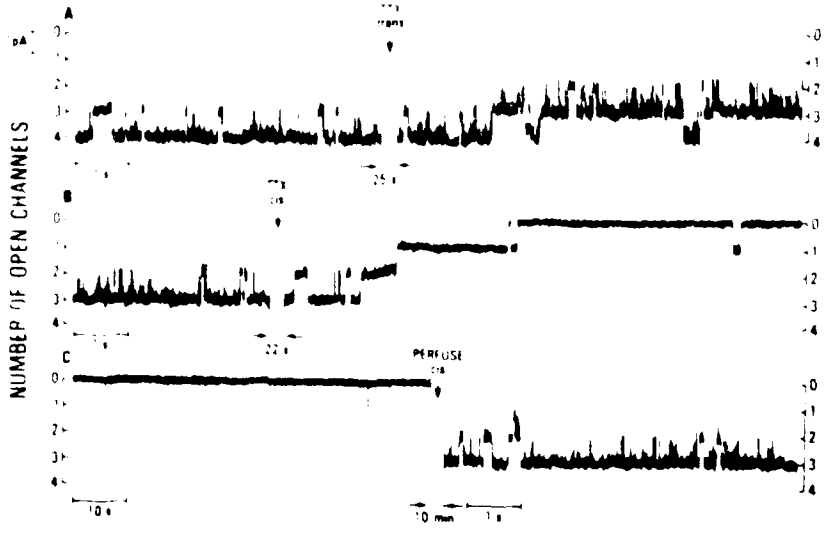

FIGURE 25. **Single sodium channel current records.** A *trans*-facing sodium channel was incorporated into a diphytanoyl PC bilayer in a 70 μm aperture bathed by 0.5 M NaCl medium A *cis* and 0.2 M NaCl medium A plus 1 μM BTX *trans*. The voltages indicated were applied to the channel for 1 min intervals. Representative current records, filtered at 1 kHz, are shown.

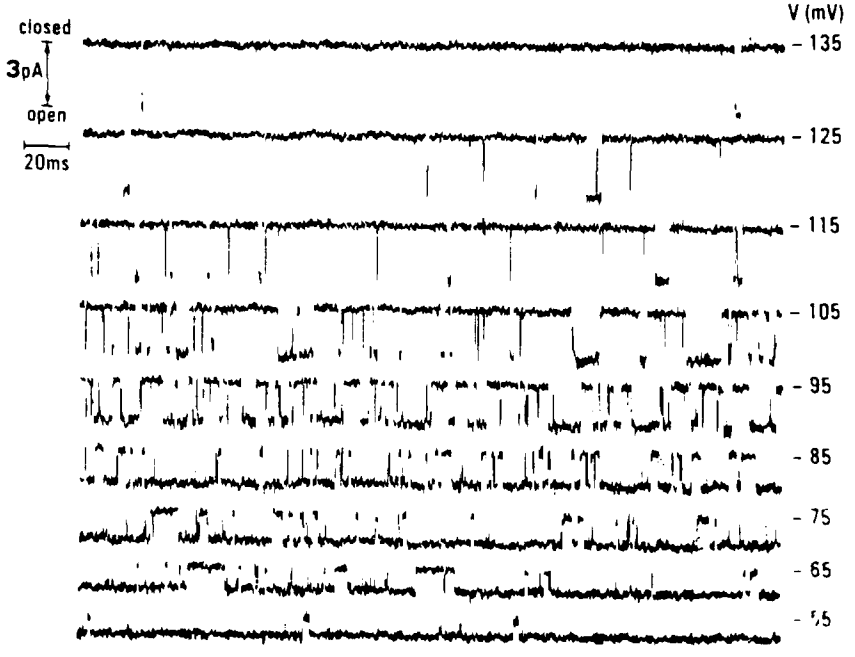

AD-A187 784 ACETYLCHOLINE RECEPTORS IN MODEL MEMBRANES: STRUCTURE/FUNCTION CORRELATES(U) CALIFORNIA UNIV SAN DIEGO LA JOLLA M MONTAL DEC 85 DAMD17-82-C-2221 2/2

UNCLASSIFIED F/G 6/4 NL

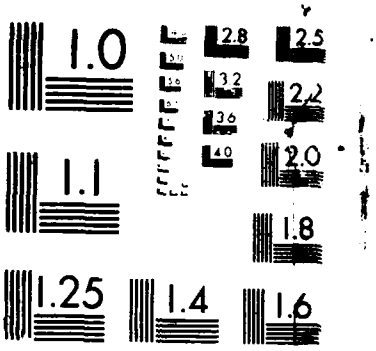

FIGURE 26A-B **A Voltage dependence of sodium channel opening.** The fraction of time a channel was open was determined by integrating conductance histograms derived from 25 s of current record at each voltage as described in (171). The voltage dependence for three different channels, selected because of their widely differing V_{50} values, are illustrated. The channels are POPE/POPC bilayers bathed in symmetric 0.5 M NaCl medium A plus 1 μM BTX *trans*. B Apparent gating charge. For each of the channels in Fig. 26A, the fraction of time it is open (f_o) is transformed to a linear function of voltage by plotting ln ($f_o/1-f_o$). The lines are least squares fit to a linearized form of the Boltzmann equation where the slope is proportional to the apparent gating charge.

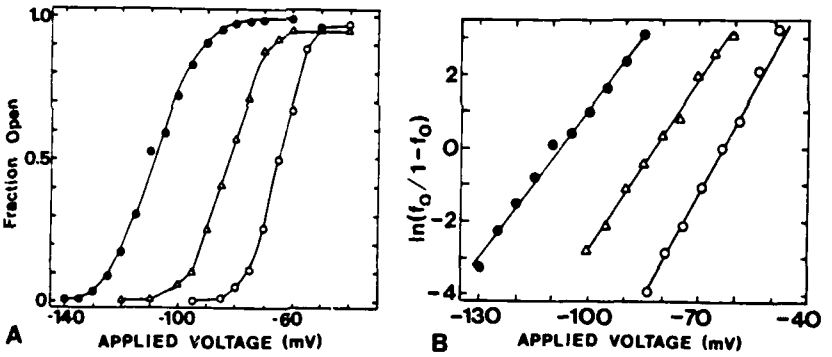

FIGURE 27. **Current-voltage relationship of single sodium channels for Na^+, K^+ and Rb^+.** The amplitude of single-channel currents was determined in 0.5 M symmetric solutions of NaCl (Δ), KCl (O) and RbCl (O) in 10 mM HEPES/Tris pH 7.4, 0.15 mM $CaCl_2$. 0.1 mM $MgCl_2$ and 0.05 mM EGTA with 1 μM BTX *trans*. To accurately determine the small single-channel current in RbCl, 200 nM TTX was added to the *cis*-chamber to produce long closed periods and the current records were filtered at 50 Hz to resolve the open and blocked channels from the noise. For this reason, only the positive branch of the curve for Rb^+ is shown. The continuous lines are the least square fits to the data points. The slope of a line is the single-channel conductance for the ion: γ_{Na^+} = 25 pS, γ_{K^+} = 3.2 pS and γ_{Rb^+} = 1.1 pS in this experiment. The uncorrected zero-current potentials were 1.4 mV and 1.5 mV for Na^+ and K^+, respectively.

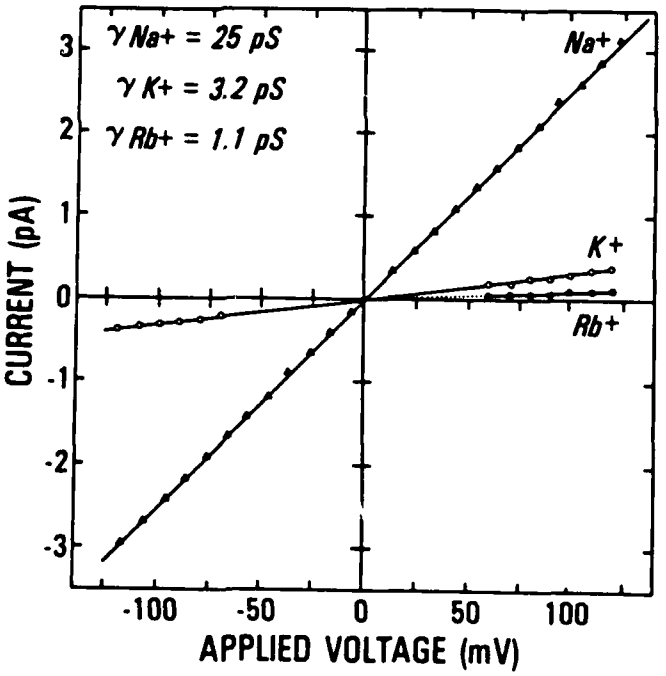

TABLE I

STX receptor purification.

	STX Receptor pmoles	%	Protein mg	%	Sp.Act. pmoles/mg	Fold Purified
Membrane Extract	6608 ± 726	100.0	1145.0 ± 62.9	100	5.8	1.0
DEAE-Sephadex	3857 ± 398	58.3	42.8 ± 8.6	3.7	90.1	15.6
Hydroxylapatite	1486 ± 276	22.4	6.8 ± 0.3	0.59	218.0	37.8
WGA Sepharose	926 ± 194	14.0	0.97 ± 0.2	0.085	955.0	165.0
Sucrose Gradient	513 ± 90	7.8	0.17 ± 0.03	0.015	2910.0	505.0

(± S.E.M. n=3)

TABLE II

Comparison of functional properties of purified and native sodium channels from rat brain

Property	Purified	Native
BTX $K_{0.5}$	2 μM[a]	0.5 μM[b]
Ver $K_{0.5}$	30 μM[a]	14 μM[b]
LqTX K_O	57 nM[a]	2 nM[b]
STX K_D	0.4 nM[a]	0.2 nM[c]
TTX K_I at V = -50 mV	8.3 nM[d]	7-16 nM[e]
mV/e-fold shift in K_I (TTX)	4.3 mV[d]	35-41 mV[e]
V_{50} for channel opening	-91 mV[d]	-93 mV[f]
Apparent gating charge (q)	3.8[d]	4-6[f]
γ (0.5 M NaCl)	25 pS[d]	30 pS[g]
Permeability relative to Na^+:		
P_{K^+}	0.14[d]	0.07[g],0.17[h]
P_{Rb^+}	0.05[d]	0.08[h]

a - (170)

b - (194)

c - (173)

d - (171)

e - R.J. French and B.K. Krueger, personal communication.

f - (203)

g - (201)

h - Data from N18 neuroblastoma cells (205).

GLOSSARY

αBGT - α-bungarotoxin.

Acetylcholine Receptor (AChR) - the receptor for acetylcholine that transuces the binding of this neurotransmitter into the opening of an ion channel, an event which brings about a change in the voltage difference across the membrane and causes the muscle cell to contract.

ACh- acetylcholine.

AChR(s) - acetylcholine receptor(s).

Activation of acetylcholine receptors - opening of channels in the presence of acetylcholine.

Amphipatic - molecules, such as lipids and detergents, that have spatially separated hydrophilic and hydrophobic regions.

BTX- bactrachotoxin.

Cell Membrane - the lipoprotein structure that encloses the cytoplasm of a cell and is its boundary

ConA-agarose - concanavalin A conjugated to Sepharose Cl4B.

Curare - d-tubocurarine

Desensitization of acetylcholine receptors - a state of acetyl- choline receptors characterized with a high affinity for acetylcholine and a closed channel.

DIINS - 4-4'-di-isothiocyanatostilbene-2-2'-disulfonic acid.

EDTA - ethylenediaminetetracetic acid.

Electrical Excitability - transient change in membrane conductance in response to changes in membrane potential.

γ- single channel conductance.

Hydrophilic - molecules or part of molecules that readily interact with water.

Hydrophobic - molecules or part of molecules that do not readily interact with water.

Ion Channels - membrane proteins that form aqueous pores through which ions cross the low dielectric constant core of the lipid bilayer. The state of the channel (open or closed) can be controlled, i.e. gated, by voltage, ligands and other regulators.

Lipid Bilayers - the fundamental structural element of cell membranes. In the bilayer, the hydrocarbon tails of the two apposed monolayers are repelled from the aqueous environment but interact with each other while their respective polar heads interact with water. This gives rise to a thin film (~ 40 A) of hydrocarbon bounded on both sides by aqueous solutions.

Lipid Monolayers - oriented monomolecular films of lipid at an air-water interface.

Lipids - fatty acid esters that are insoluble in water but soluble in non-aqueous solvents. These amphipatic molecules contain long hydrocarbon chains, the tail, that are hydrophobic (do not interact with water) and a polar end, the head, often consisting of phosphate ester.

LqTX - *Leiurus quinquestriatus* scorpion toxin.

MBTA - 4-(N-maleimido)benzyltrimethylammoniumioside.

Membrane Proteins - macromolecules, composed of amino acids, which are embedded within the hydrocarbon regions of the bilayer and expose sections to both aqeuous environments. These entities confer the biological function and the specificity characterisic of living systems.

Membrane Reconstitution or Reconstruction - reassembly of a membrane from defined lipids and specific membrane protein components that exhibit functional activity. They can be in the foirm of either small vesicles (~ 1000 A diameter) or planar bilayers that separate two aqueous phases large enough to allow direct electrical measurments.

Membrane Resolution - isolation and purification of individual specific membrane proteins.

Micelle - a spherical structure formed by amphiphatic molecules in water. The apolar part of the molecular is on the side of the sphere.

Neuron - a nerve. cell. The excitable cell on which the nervous system is based.

Neutransmitter - a chemical that transmits the nerve impulse from a neuron to another excitable cell.

PC - phosphatidylcholine.

PE - phosphatidylethanolamine.

POPC78 1-palmitoyl-2-oleoyl-PC.

POPE - 1-palmmitoyl-2-oleoyl-PE.

Receptors - light, or chemical, (e.g. a neurotransmitter) and transform the recognition process into a transmembrane event, that may effect the activity of the cell.

SDS - sodium dodenyl sulfate.

STX - saxitoxin.

Synapse - specialized connection between one nerve cell and another excitable cell.

Toxin Agarose - *Naja naja siamensis* toxin III conjugated to Sepharose Cl4B.

Trizma - 2-amino-2-hydroxymethyl-1-,2-propaneidiol.

TTX - tetrodotoxin.

Ver - veratridine.

WGA - wheat germ hemaglutinin.

δ - single channel conductance.

DISTRIBUTION LIST

1 copy	Commander US Army Medical Research and Development Command ATT: SGRD-RMI-S Fort Detrick Frederick, Maryland 21701-5012
5 copies	Commander US Army Medical Research and Development Command ATTN: SGRD-PLE Fort Detrick Frederick, Maryland 21701-5012
12 copies	Defense Technical Information Center (DTIC) ATTN: DTIC-DDAC Cameron Station Alexandria, VA 22304-6145
1 copy	Dean School of Medicine Uniformed Services University of the Health Sciences 4301 Jones Bridge Road Bethesda, MD 20814-4799
1 copy	Commandant Academy of Health Sciences, US Army ATTN: AHS-CDM Fort Sam Houston, TX 78234-6100

END

FEB.

1988

DTIC